INFORMATION TO USERS

This manuscript has been reproduced from the microfilm master. UMI films the text directly from the original or copy submitted. Thus, some thesis and dissertation copies are in typewriter face, while others may be from any type of computer printer.

The quality of this reproduction is dependent upon the quality of the copy submitted. Broken or indistinct print, colored or poor quality illustrations and photographs, print bleedthrough, substandard margins, and improper alignment can adversely affect reproduction.

In the unlikely event that the author did not send UMI a complete manuscript and there are missing pages, these will be noted. Also, if unauthorized copyright material had to be removed, a note will indicate the deletion.

Oversize materials (e.g., maps, drawings, charts) are reproduced by sectioning the original, beginning at the upper left-hand corner and continuing from left to right in equal sections with small overlaps.

Photographs included in the original manuscript have been reproduced xerographically in this copy. Higher quality 6" x 9" black and white photographic prints are available for any photographs or illustrations appearing in this copy for an additional charge. Contact UMI directly to order.

ProQuest Information and Learning
300 North Zeeb Road, Ann Arbor, MI 48106-1346 USA
800-521-0600

UMI®

TEMPERATURE DEPENDENCE OF ELECTRON TRANSFER IN PHOTOSYNTHETIC REACTION CENTERS FROM *RHODOBACTER SPHAEROIDES*: TRAPPING AND CHARACTERIZATION OF CONFORMATIONAL SUBSTATES

by

Qiang Xu

A dissertation submitted to the Graduate Faculty in Physics in partial fulfillment of the requirements for the degree of Doctor of Philosophy, The City University of New York

2001

This manuscript has been read and accepted for the Graduate Faculty in Physics in the satisfaction of the dissertation requirement for the degree of Doctor of Philosophy.

9/6/01
Date

Chair of Examining Committee

9/20/01
Date

Executive Officer

T. Boyer

R. Callender

T. Lazaridis

F. Smith
Supervisory Committee

THE CITY UNIVERSITY OF NEW YORK

Abstract

TEMPERATURE DEPENDENCE OF ELECTRON TRANSFER IN PHOTOSYNTHETIC REACTION CENTERS FROM *RHODOBACTER SPHAEROIDES*: TRAPPING AND CHARACTERIZATION OF CONFORMATIONAL SUBSTATES

by

Qiang Xu

Advisor: Professor Marilyn R. Gunner

The photosynthetic reaction center protein (RC) provides an excellent model system for study of electron transfer process. The influence of conformational changes on the electron transfer energetics and kinetics was investigated in this study.

By measuring the temperature dependence of $P^+Q_A^-$ charge recombination for RCs with low potential quinones as Q_A, we established that at room temperature, the entropy change between the $P^+Q_A^-$ state and P^+H^- state is quite small on the time scale of the measurement. When temperature is lowered, a break in the temperature dependence was observed at ~210 K. Analysis of the data suggests that at low temperature, the product is trapped in an unrelaxed state which is higher in energy. Such relaxation could help explain why different values of ΔS are found in previous measurements done on different time scale.

It was proposed previously that a conformational change is the rate limiting step in the Q_A^- to Q_B electron transfer. We confirmed that by freezing the sample under illumination, RCs can be trapped in the active, light adapted conformation. Q_A^- to Q_B electron transfer proceeds with high quantum efficiency at low temperature in light adapted RCs, while it stops in dark adapted proteins. Direct electron tunneling from Q_B^- to P^+ was measured in the light adapted sample and found to be temperature independent. The relaxation of RCs in the active conformation to a new inactive conformation was observed in the temperature range of 120-200 K.

The freeze out of the Q_A^- to Q_B electron transfer can be influenced by many factors such as pH, substrate and residues near the Q_B site. By measuring how these factors change the temperature dependence of the quantum efficiency of the electron transfer, we conclude that the proper protonation state for residues near the Q_B site is required for the electron transfer. The energy barriers between the protonated and unprotonated reactant substate and product state is characterized. L209 Proline mutation and change of the quinone hydrocarbon tail length indicate that a simple shift of the quinone position is unlikely to be the only conformational change required for the electron transfer.

Acknowledgments

The work presented here would not be possible without the support of my advisor Marilyn Gunner. I benefited a lot from her insight into the electron transfer problem and her quick grasp of the essential meaning of the experimental observations. Her insistence for deeper understanding of the electron transfer process in reaction centers is the main driving force behind this study.

I would like to thank members of my exam committee, Professor Robert Callender, Themis Lazaridis, Timothy Boyer and Fredrick Smith for their time and support.

Many colleagues at various institutions kindly provided their precious time and sample for this study. Drs. Laura Baciou, Pierre Sebban, Mark Paddock and Mel Okamura sent me their protein sample for the experiments. Professor David Mauzerall and Dr. Greg Edens collaborated with us on the photoacoustic measurement. Drs. Steven Boxer and Alex deWinter provided the His-tagged bacterial strain that greatly simplified the sample preparation for my experiment. I also benefited from discussions with Drs. David Tiede and Armen Mulkidjanian.

I also want to thank all the current and former members of the Gunner lab, especially Drs. Jiali Li, Emil Alexov, Roxana Georgescu and Samir Lipovaca. Friends and colleagues at City College, Min Xu, Ping Sun, Hu Cheng, Hua Deng, Ruel Dasamero, Yongwei Song, Kevin Mertes, Yicheng Zhong, Gang Zhang and many others also provided their support over the years.

Finally, I want to thank the persons that I am most in debt to: my parents. Their understanding and patience over all these years made everything possible.

TABLE OF CONTENTS

LIST OF TABLES

LIST OF FIGURES

LIST OF ABBREVATIONS

RC, reaction center

Q_A and Q_B, primary and secondary quinone electron acceptors

P, bacteriochlorophyll dimer which is the primary electron donor

BPh_L and BPh_M, bacteriopheophytin associated with the L and M subunits respectively

$BChl_L$ and $BChl_M$, bacteriochlorophyll monomer in the L and M subunits, LDAO, lauryldimethylamine N-oxide

UQ10, ubiquinone-10 (2,3-dimethoxy-5-methyl-6-decaisopropyl-1,4-benzoquinone)

UQ1, ubiquinone-1

MQ4, 2-methyl-3-phytyl-1,4-naphthoquinone

1-Cl-AQ, 1-chloroanthraquinone

2-Cl-AQ, 2-chloroanthraquinone

2-Am-NQ, 2-aminonaphthoquinone

AQ, anthraquinone

2-Me-AQ, 2-methylanthraquinone

1-Am-AQ, 1-aminoathraquinone

2,3-dM-AQ, 2,3-dimethylanthraquinone

2,7-dM-AQ, 2,7-dimethylanthraquinone

1,3-dM-AQ, 1,3-dimethylanthraquinone

CCD, charge-coupled device

Chapter 1
INTRODUCTION

Photosynthesis is arguably the most important biological process on earth. In the photosynthetic bacteria, the initial steps of the conversion of light energy to chemical energy takes place in an integral membrane protein called the photosynthetic reaction center (RC). This protein provides an ideal model system for the study of many subjects of importance to biology and chemistry, such as electron transfer,[1-5] proton transfer,[6-9] protein dynamics[10-12] and the coupling between these processes.

Several advantages exist for the study of this protein as a model system. First, research has been carried out on RCs since the isolation of this protein in the late sixties.[13] As a result, detailed structural, spectroscopic and kinetic information is available. The structure has been solved to atomic resolution by X-ray crystallography.[14-18] The electron transfer pathway has been elucidated and the kinetics of most of the reactions have been well characterized.[19-21] Second, a variety of factors controlling the electron and proton transfer can be easily manipulated. Various mutants have been made by different groups.[22-26] In addition, two of the cofactors, the primary and second electron acceptor, Q_A and Q_B, can be easily extracted and replaced by other quinones with different properties, such as electron affinity, size, tail length, etc.[27-31] Finally, because most of the electron transfer steps in RC occur by quantum tunneling, the reaction can be investigated over a quite wide temperature range.[10,11,32,33] And even when a

reaction stops at low temperature, the temperature at which the reaction fails and how the temperature of the failure can shift with conditions such as pH, ion binding, quinone tail length could provide important information about the mechanism of the reaction.

1. The reaction center of photosynthetic bacteria

The bacterial reaction center was successfully isolated and purified from the cell first by R. K. Clayton and colleagues in the late 60s.[13] In the 80s, the X-ray crystal structure of reaction centers are solved for *Rhodopseudomonas viridis*[14,34,35] and *Rhodobacter sphaeroides.*[15,16,36-38]

The reaction center of *Rhodobacter sphaeroides* as shown in Figure 1.1, contains three domains. The three subunits of the protein, namely L, M, H, have 5, 5 and 1 transmembrane helices respectively. There are a group of cofactors noncovalently bound to the protein. The cofactors include a special pair of bacteriochlorophyll called P870 (P), two bacteriochlorophyll monomers, two bacteriopheophytins (BPh) and two quinone molecules called Q_A and Q_B. These cofactors are arranged in an approximately twofold symmetry between the L and M branch. There is also a non-heme iron atom bound on the C_2 axis between the two quinones.

The special pair P870 donates an electron in the electron transfer process after excitation. The electron is then transferred sequentially to the BPh at the L branch, Q_A and then Q_B. Figure 1.2 illustrates the pathway and free energy level of the electron transfers in RC including the competing back reactions. In

forward electron transfer, the special pair is restored to its reduced form by electron from cytochrome and a second electron transfer can be initiated. For experiments with isolated RCs, when no external electron donor is present, the electron recombines with the special pair P^+ to return to ground state.

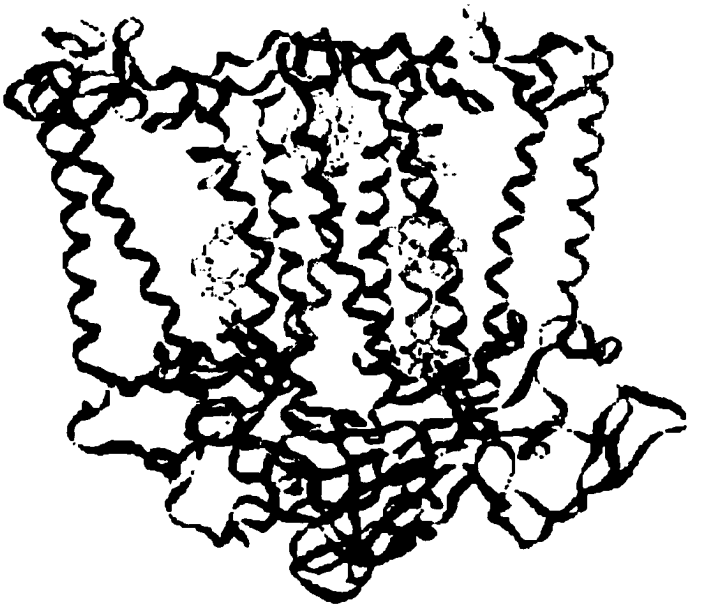

Figure 1.1 The structure of bacterial photosynthetic reaction center from *Rhodobacter sphaeroides.*

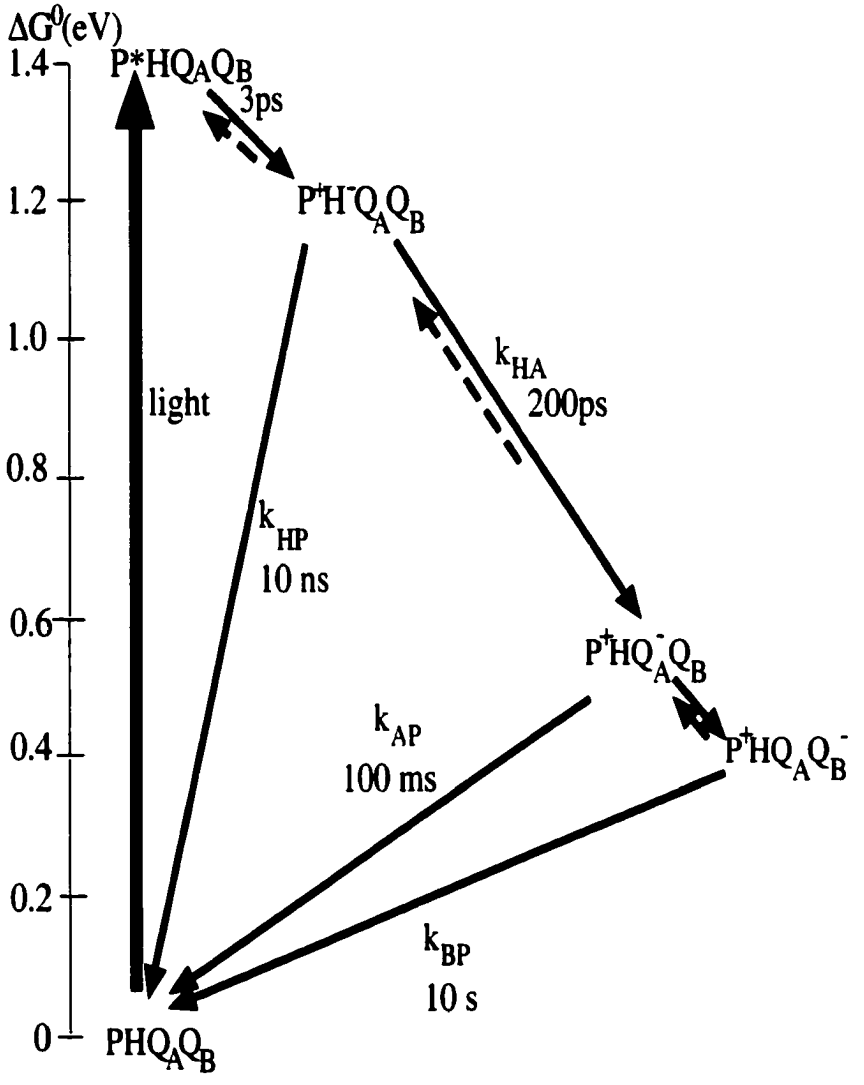

Figure 1.2. The relative free energy level for different states, electron transfer pathway and lifetime for reaction connecting the states for RCs from *Rb. Sphaeroides* RCs. The competing back reactions are also shown.

2. Conformational flexibility of protein

Proteins are not rigid. The protein energy landscape can be described as a rugged hyperspace with many minimum, each of which corresponds to a slightly different conformation with similar free energy level. At room temperature, protein can fluctuate amongst these conformations.[39-41] The conformational flexibility is important for the function of the protein, because the conformational change is often needed for processes such as the binding and dissociation of the substrate, movement of the substrate to the right position, change of residues in or near the active site to stabilize the product state. At low temperature, the protein is limited to harmonic vibration around the conformation that it is frozen into and those processes dependent on conformational change will stop. A change of protein flexibility with temperature has been demonstrated by inelastic neutron scattering[42-44] and Mössbauer spectroscopy[45,46], and is also seen in molecular dynamics simulation.[47] One major transition temperature is found to be about 200-220 K in all studies.

The structure of intermediate conformations along a reaction path can be studied by time resolved X-ray crystallography if the reaction can be triggered by light. High resolution, time resolved X-ray diffraction has been used in the study of the photosensitive yellow protein.[48] Intermediates can sometimes be trapped by varying parameters such as temperature, pH and by the use of various mutants. Intermediate states of cytochrome P450cam[49] and bacteriorhodopsin[50] and many others (for recent reviews, see reference 51 and

52) have been trapped and studied by electron microscopy and X-ray crystallography. The important conformational changes are also observed for several electron transfer steps in reaction centers.

3. Charge recombination of $P^+Q_A^-$ in RC: conformational relaxation

In reaction centers without the secondary quinone, the product of the charge separation is $P^+Q_A^-$. In the absence of external electron donors, the electron will go back to the special pair and return the system to the ground state.

The thermodynamics of the processes of $P^+Q_A^-$ charge separation and recombination have been investigated before. The free energy level for most of the states have been well characterized.[19-21](Figure 1.2) But there are still enough questions left to be answered.

It's often assumed in theoretical calculation that the entropy change for reaction involving Q_A is quite small. This assumption is supported by experimental evidence from several well established but indirect methods.[1,29,53] The indirect methods, which measures either the delayed fluorescence from the excited singlet state of the special pair or the $P^+Q_A^-$ charge recombination rate via the thermally activated route, monitor the equilibrium of the states on the time scale of the back reaction (10 μs or slower).

This assumption, however, is called into question recently by the direct measurement of enthalpy using an improved photoacoustic method.[54] The

photoacoustic method measures the heat released from the protein during the reaction, thus it measures the enthalpy changes directly and the known free energy value is used to calculate the entropy change. The entropic term ($-T\Delta S$) for the $P^+Q_A^-$ charge separation was found to be about half of the free energy change.

The discrepancy between the photoacoustic method and other methods could have several explanations. One of the possible reasons for the discrepancy is the different time scale of the measurement. The photoacoustic method measures the heat release during the forward electron transfer and the measurement is done on the time scale of 100 ns, much faster than the indirect methods. It is possible that relaxation after the electron transfer causes such a discrepancy.

To establish the entropy change for the formation of the $P^+Q_A^-$ state, we carried out a systematic study of the charge recombination kinetics using replacement low potential quinones as Q_A. The temperature region of the study was extended to 40 K. This part of the study will be discussed in detail in Chapter 3.

4. Electron transfer from Q_A^- to Q_B: conformational gating.

Most of the electron transfer steps in the RCs can proceed at cryogenic temperature at rates comparable to or faster than that at room temperature since these reactions occur by quantum tunneling with driving force, ΔG near the reorganization energy, λ.[32,55,56] But the first electron transfer from the reduced

primary quinone to the secondary quinone slows down and then stops when temperature is lowered.[10]

In isolated RCs with native ubiquinone as both Q_A and Q_B, the electron transfer rate was found to be 100 μs.[57-59] The driving force of the Q_A^- to Q_B electron transfer can be changed by replacing the native ubiquinone Q_A with low potential quinones.[28] The increased driving force is found to have no effect on the 100 μs rate, which suggests that the direct electron transfer is not the rate limiting step in RCs with native ubiquinone as both Q_A and Q_B.[30] Rather a conformational change is likely to be the kinetic gating step of this process and the freezing out of the electron transfer is due to the activation barrier of this conformational change. One interesting observation is that if the RCs are frozen in light, the Q_A^- to Q_B electron transfer can proceed with high quantum efficiency.[10] It was suggested that the RCs are trapped in the active conformation state while frozen under illumination. In RCs with low potential quinone as Q_A, another faster phase electron transfer was observed and found to be driving force dependent as predicted by Marcus theory.[31,60] These RCs appear to be prepared so that the conformational change is no longer rate determining. This can be attributed to the increased distribution of RCs in the activated state.

To further characterize this activated state, we studied in detail the absorption spectrum of the RCs trapped in the active conformation. The spectral shift is analyzed to reveal the change in the electrostatic environment of the cofactors. Also we studied the relaxation of the protein from this active conformation into an inactive form when the temperature is raised. When the

RCs are warmed to between 120 K to 200 K, the relaxation leads not to the dark conformation, but a new inactive intermediate state with higher free energy. This part of the study will described in detail in Chapter 4.

5. Coupling between the electron transfer, proton transfer and conformational change.

In the reaction center, both the singly reduced Q_A^- and Q_B^- exists in the anionic form.[57,61] But there is sub-stoichiometric proton uptake from the solution accompanying the first electron transfer to Q_B. At neutral pH, the proton uptake is small (<0.3), but it increases around pH 9 to about 0.8.[62,63] The proton picked up from the solution presumably goes to residues near the Q_B binding site, most likely Glu L212 or Asp L213. At neutral pH, computational work suggests that an internal proton shift between residues help stabilize the semiquinone.[9] At high pH when such internal proton buffer is exhausted, the proton uptake from the solution becomes necessary.

This proton uptake will have implication for the kinetics of electron transfer and indeed the Q_A^- to Q_B electron transfer is observed to decrease at high pH with an apparent pK of 9.5.[64] The pH dependence can be changed by mutation of residues near Q_B. When the Glu L212, which is only 4 Å away from Q_B, is changed to Gln, the pH dependence disappears.[22] In the Asp L213 -> Asn mutant, onset of the rate decrease has now shifted to below pH 5.[65] Apparent while proton uptake is not rate limiting in the native quinone at neutral pH, it

can become rate determining at high pH or in mutants where proton uptake is necessary.

Therefore the RCs provides an ideal model system to study the coupling between this proton and electron transfer. The temperature dependence of the electron transfer rate gives us the activation energy of the reaction. How the activation energy will change with pH will tell us how the protonation state of the residue nearby influence the activation barrier to the electron transfer.

As discussed previously, the activation barrier to the electron transfer is actually the barrier to the conformational gating process. From the crystallography study, it was proposed that the quinone movement between two possible binding sites is the rate limiting step.[18,66] If this suggestion is correct, changing the chemical identity of the quinone or mutating the residue close to the binding site might change the mobility of the quinone and thus influence the kinetics and/or its temperature dependence.

To gain more insight into the problem of the coupling between the proton, electron transfer and conformational change, we measured the temperature dependence of the kinetics at various pH, with different quinones as Q_B and with several mutants. This part of the study is discussed in chapters 5 and 6.

References

(1) Gunner, M. R. The temperature and ΔG dependence of long range electron transfer in reaction center protein from *Rhodobacter sphaeroides*. Ph.D., University of Pennsylvania, 1988.

(2) Friesner, R., A.; Won, Y. *Biochim. Biophys. Acta* **1989**, *977*, 99-122.

(3) Moser, C. C.; Keske, J. M.; Warncke, K.; Farid, R.; Dutton, P. L. *Nature* **1992**, *355*, 796-802.

(4) Gray, H. B.; Winkler, J. R. *Annu Rev Biochem* **1996**, *65*, 537-561.

(5) Page, C. C.; Moser, C. C.; Chen, X.; Dutton, P. L. *Nature* **1999**, *402*, 47-52.

(6) Maroti, P.; Hanson, D. K.; Baciou, L.; Marianne, S.; Sebban, P. *Proc. Natl. Acad. Sci.* **1994**, *91*, 5617-5621.

(7) Okamura, M. Y.; Feher, G. Proton-coupled electron transfer reactions of Q_B in reaction centers from photosynthetic bacteria. In *Anoxygenic Photosynthetic Bacteria*; Blankenship, R., Madigan, M., Bauer, C., Eds.; Kluwer Academic Publishers: Dordrecht, 1995; Vol. 2; pp 577-593.

(8) Tiede, D. M.; Utschig, L.; Hanson, D. K.; Gallo, D. M. *Photosynth. Res* **1998**, *55*, 267-273.

(9) Alexov, E.; Gunner, M. *Biochemistry* **1999**, *38*, 8253-8270.

(10) Kleinfeld, D.; Okamura, M. Y.; Feher, G. *Biochemistry* **1984**, *23*, 5780-5786.

(11) McMahon, B. H.; Muller, J. D.; Wraight, C. A.; Nienhaus, G. U. *Biophysical Journal* **1998**, *74*, 2567-2587.

(12) Goushcha, A. O.; Kapoustina, M. T.; Kharkyanen, V. N.; Holzwarth, A. R. *J.Phys.Chem.B* **1997**, *101*, 7612-7619.

(13) Clayton, R. K.; Wang, R. T. *Methods Enzymol* **1971**, *23*, 696-704.

(14) Deisenhofer, J.; Michel, H. *The EMBO Journal* **1989**, *8*, 2149-2170.

(15) Allen, J. P.; Feher, G.; Yeates, T. O.; Komiya, H.; Rees, D. C. *Proc. Natl. Acad. Sci. USA* **1987**, *84*, 5730-5734.

(16) Allen, J. P.; Feher, G.; Yeates, T. O.; Komiya, H.; Rees, D. C. *Proc. Natl. Acad. Sci. USA* **1987**, *84*, 6162-6166.

(17) Chang, C.-H.; El-Kabbani, O.; Tiede, D.; Norris, J.; Schiffer, M. *Biochemistry* **1991**, *30*, 5352-5360.

(18) Stowell, M. H. B.; McPhillips, T. M.; Rees, D. C.; Soltis, S. M.; Abresch, E.; Feher, G. *Science* **1997**, *276*, 812-816.

(19) Feher, G.; Allen, J. P.; Okamura, M. Y.; Rees, D. C. *Nature* **1989**, *339*, 111-116.

(20) Gunner, M. R. *Current Topics in Bioenergetics* **1991**, *16*, 319-367.

(21) Blankenship, R. E.; Madigan, M. T.; Bauer, C. E. *Anoxygenic Photosynthetic Bacteria*; Kluwer Academic Publishers:, 1995; Vol. 2.

(22) Paddock, M. L.; Rongey, S. H.; Feher, G.; Okamura, M. Y. *Proc. Natl. Acad. Sci. USA* **1989**, *86*, 6602-6606.

(23) Takahashi, E.; Wraight, C. A. *Biochemistry* **1992**, *31*, 855-866.

(24) Lin, X.; Murchison, H. A.; Nagarajan, V.; Parson, W. W.; Allen, J. P.; Williams, J. C. *Proc. Natl. Acad. Sci. USA* **1994**, *91*, 10265-10269.

(25) Alexov, E.; Miksovska, J.; Baciou, L.; Schifer, M.; Hanson, D.; Sebban, P.; Gunner, M. R. *Biochemistry* **2000**, *39*, 5940-5952.

(26) McAuley-Hecht, K. E.; Fyfe, P. K.; Ridge, J. P.; Prince, S. M.; Hunter, C. N.; Issac, N. W.; Cogdell, R. J.; Jones, M. R. *Biochemistry* **1998**, *37*, 4740-4750.

(27) Okamura, M. Y.; Isaacson, R. A.; Feher, G. *Proc. Natl. Acad. Sci. USA* **1975**, *72*, 3492-3496.

(28) Gunner, M. R.; Tiede, D. M.; Prince, R. C.; Dutton, P. L. Quinones as prosthetic groups in membrane electron-transfer proteins I: Systematic replacement of the primary ubiquinone of photochemical reaction centers with other quinones. In *Function of Quinones in Energy Conserving Systems*; Trumpower, B. L., Ed.; Academic Press: New York, 1982; pp 265-269.

(29) Woodbury, N. W.; Parson, W. W.; Gunner, M. R.; Prince, R. C.; Dutton, P. L. *Biochim. Biophys. Acta.* **1986**, *851*, 6-22.

(30) Graige, M. S.; Feher, G.; Okamura, M. Y. *Proc. Natl. Acad. Sci. USA* **1998**, *95*, 11679-11684.

(31) Li, J.; Takahashi, E.; Gunner, M. R. *Biochemistry* **2000**, *39*, 7445-7454.

(32) Gunner, M. R.; Robertson, D. E.; Dutton, P. L. *J. Phys. Chem.* **1986**, *90*, 3783-3795.

(33) Gunner, M. R.; Dutton, P. L. *J. Am. Chem. Soc.* **1989**, *111*, 3400-3412.

(34) Deisenhofer, J.; Epp, O.; Miki, K.; Huber, R.; Michel, H. *J. Mol. Biol.* **1984**, *385*, 385.

(35) Deisenhofer, J.; Epp, O.; Miki, R.; Michel, H. *Nature* **1985**, *318*, 618-624.

(36) Chang, C. H.; Tiede, D.; Tang, J.; Smith, U.; Norris, J.; Schiffer, M. *FEBS Lett.* **1986**, *205*, 82-86.

(37) Allen, J. P.; Feher, G.; Yeates, T. O.; Komiya, H.; Rees, D. C. *Proc. Natl. Acad. Sci. USA* **1988**, *85*, 8487-8491.

(38) Allen, J. P.; Feher, G.; Yeates, T. O.; Komiya, H.; Rees, D. C. **1988**, 5-11.

(39) Austin, R. H.; Beeson, K. W.; Eisenstein, D. L.; Frauenfelder, E. H.; Gunsalus, I. C. *Biochem.* **1975**, *24*, 5355-5373.

(40) Frauenfelder, H.; Sligar, S. G.; Wolynes, P. G. *Science* **1991**, *254*, 1598-1603.

(41) Zaccai, G. *Science* **2000**, *288*, 1604-7.

(42) Doster, W.; Cusack, S.; Petry, W. *Nature* **1989**, *337*, 754-756.

(43) Reat, V.; Patzelt, H.; Ferrand, M.; Pfister, C.; Oesterhelt, D.; Zaccai, G. *Proc Natl Acad Sci U S A* **1998**, *95*, 4970-5.

(44) Daniel, R. M.; Smith, J. C.; Ferrand, M.; Héry, S.; Dunn, R.; Finney, J. L. *Biophys. J.* **1998**, *75*, 2504-2507.

(45) Parak, F. *Methods Enzymol* **1986**, *127*, 196-206.

(46) Garbers, A.; Reifarth, F.; Kurreck, J.; Renger, G.; Parak, F. *Biochemistry* **1998**, *37*, 11399-11404.

(47) Vitcup, D.; Ringe, D.; Petsko, G. A.; Karplus, M. *Nature structural biology* **2000**, *7*, 34-38.

(48) Genick, U. K.; Borgstahl, G. E. O.; Ng, K.; Ren, Z.; Pradervand, C.; Burke, P. M.; Srajer, V.; Teng, T.; Schildkamp, W.; McRee, D. E.; Moffat, K.; Getzoff, E. D. *Science* **1997**, *275*, 1471-1475.

(49) Schlichting, I.; Berendzen, J.; Chu, K.; Stock, A. M.; Maves, S. A.; Benson, D. E.; Sweet, R. M.; Ringe, D.; Petsko, G. A.; Sligar, S. G. *Science* **2000**, *287*, 1615-22.

(50) Luecke, H.; Schobert, B.; Richter, H. T.; Cartailler, J. P.; Lanyi, J. K. *Science* **1999**, *286*, 255-261.

(51) Schlichting, I.; Chu, K. *Curr Opin Struct Biol* **2000**, *10*, 744-52.

(52) Petsko, G. A.; Ringe, D. *Curr Opin Chem Biol* **2000**, *4*, 89-94.

(53) Arata, H.; Parson, W. W. *Biochim. Biophys. Acta* **1981**, *638*, 201-209.

(54) Edens, G. J.; Gunner, M. R.; Xu, Q.; Mauzerall, D. *J. Am. Chem. Soc.* **2000**, *122*, 1479-1485.

(55) DeVault, D.; Chance, B. *Biophys. J.* **1966**, *6*, 825-847.

(56) McElroy, J. D.; Mauzerall, D. C.; Feher, G. *Biochim. Biophys. Acta* **1974**, *333*, 261-277.

(57) Vermeglio, A.; Clayton, R. K. *Biochim. Biophys. Acta* **1977**, *461*, 159-165.

(58) Wraight, C. A. *Biochim. Biophys. Acta* **1979**, *548*, 309-327.

(59) Kleinfeld, D.; Okamura, M. Y.; Feher, G. *Biochim. Biophys. Acta* **1985**, *809*, 291-310.

(60) Li, J.; Gilroy, D.; Tiede, D. M.; Gunner, M. R. *Biochemistry* **1998**, *37*, 2818-2829.

(61) Wraight, C. A. *Biochim. Biophys. Acta* **1977**, *459*, 525-531.

(62) Maroti, P.; Wraight, C. A. *Biochim. Biophys. Acta* **1988**, *934*, 329-347.

(63) McPherson, P. H.; Okamura, M. Y.; Feher, G. *Biochim. Biophys. Acta* **1988**, *934*, 348-368.

(64) Kleinfeld, D.; Okamura, M. Y.; Feher, G. *Biochim. Biophys. Acta* **1984**, *766*, 126-140.

(65) Takahashi, E.; Wraight, C. A. *Biochim. Biophys. Acta* **1990**, *1020*, 107-111.

(66) Lancaster, R.; Michel, H. *Structure* **1997**, *5*, 1339-1359.

Chapter 2
Material and methods

1. Sample preparation

Two strains of the purple non-sulfur photosynthetic bacteria *Rhodobactor sphaeroides* were used in this study. One is the carotenoidless mutant R-26; the other is an engineered poly-histidine tagged, carotenoid containing strain provided by Professor Steven Boxer at Stanford, which can be isolated rapidly. The protocols for growing both strains and for reaction center isolation are well studied and documented.[1-3]

His-tagged reaction centers were purified using affinity chromatography, utilizing the high affinity interaction between the poly-Histidine tag and Ni-NTA (nitrilo-Tri-Acetic acid) resin (from Qiagen).[3] For the strain R-26, reaction centers were isolated following established procedures using lauryldimethylamine-N-oxide (LDAO) extraction and purified using ammonium sulfate and DEAE(diethylaminoethyl) chromatography.[1] The native ubiquinones in Q_A and Q_B sites were extracted with 4% LDAO and 10 mM orthophenathroline using the method of Okamura[4] with minor modification.[5]

In order to probe the factors that control the electron transfer, quinones with different redox potential, tail length, size, ionization state were substituted into the quinone binding sites of RC. Small quinones were usually first dissolved in alcohol, then added to the sample at the desired concentration. Quinones with a long hydrocarbon tail were dissolved in 2% Triton X-100. The relatively insoluble

UQ-10 stock solution was heated for 5 seconds in a microwave oven before being added to the RCs.

2. Spectroscopy

Flash induced absorbance transient at single wavelength were measured using a flash spectrophotometer designed by the University of Pennsylvania Biomedical Instrumentation Group shown in Figure 2.1. The sample is excited by either 10μs flash from a xenon flash lamp or 5ns, 532nm pulsed YAG laser (Continuum Surelite 2) pumping a fluorescent dye (LDS 751 or Rhodamine 640 from Exciton) . The transmitted light is detected by a Thorn EMI 9798QB photomultiplier. The signal is monitored using a LeCroy 9310M (300MHz) or 9310A (400MHz) oscilloscope after it is amplified and filtered.

The flash induced absorbance transient was also measured in a large spectral range (For example, 700nm to 950nm) simultaneously using the setup shown in Figure 2.2. The probing light was provide by a weak, non-actinic submicrosecond xenon flash lamp (IBH Consultants, 5000XeF). The actinic light is the same as in the single wavelength experiment. The transmitted light was focused onto an optical fiber and into the spectrometer (Jobin-Yvon, HR460). The spectrum was recorded using a liquid nitrogen cooled CCD detector (Princeton Instrument, LN/CCD-1024-EHRB/1) with a ST-138 controller.

The delay between the pump and probe flash was varied with a delay generator (Stanford Research DG535) to follow the time dependence of the reaction. The time sequence of the triggering signal is shown in Figure 2.3. The laser was set at Q switch external trigger mode. In this mode, a 10 Hz TTL signal is used for the flash lamp of laser and another TTL signal with proper delay was

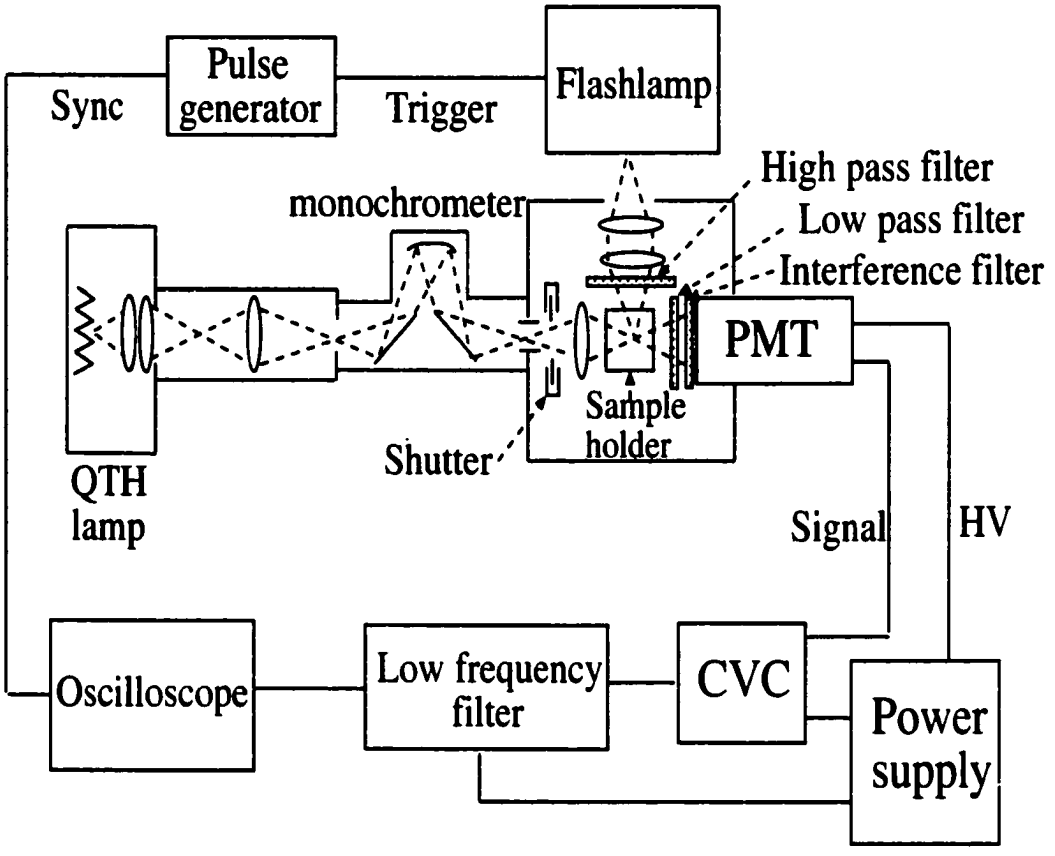

Figure 2.1. Setup for measurement of absorption change at single wavelength. The Flashlamp can be replaced by laser for faster measurement.

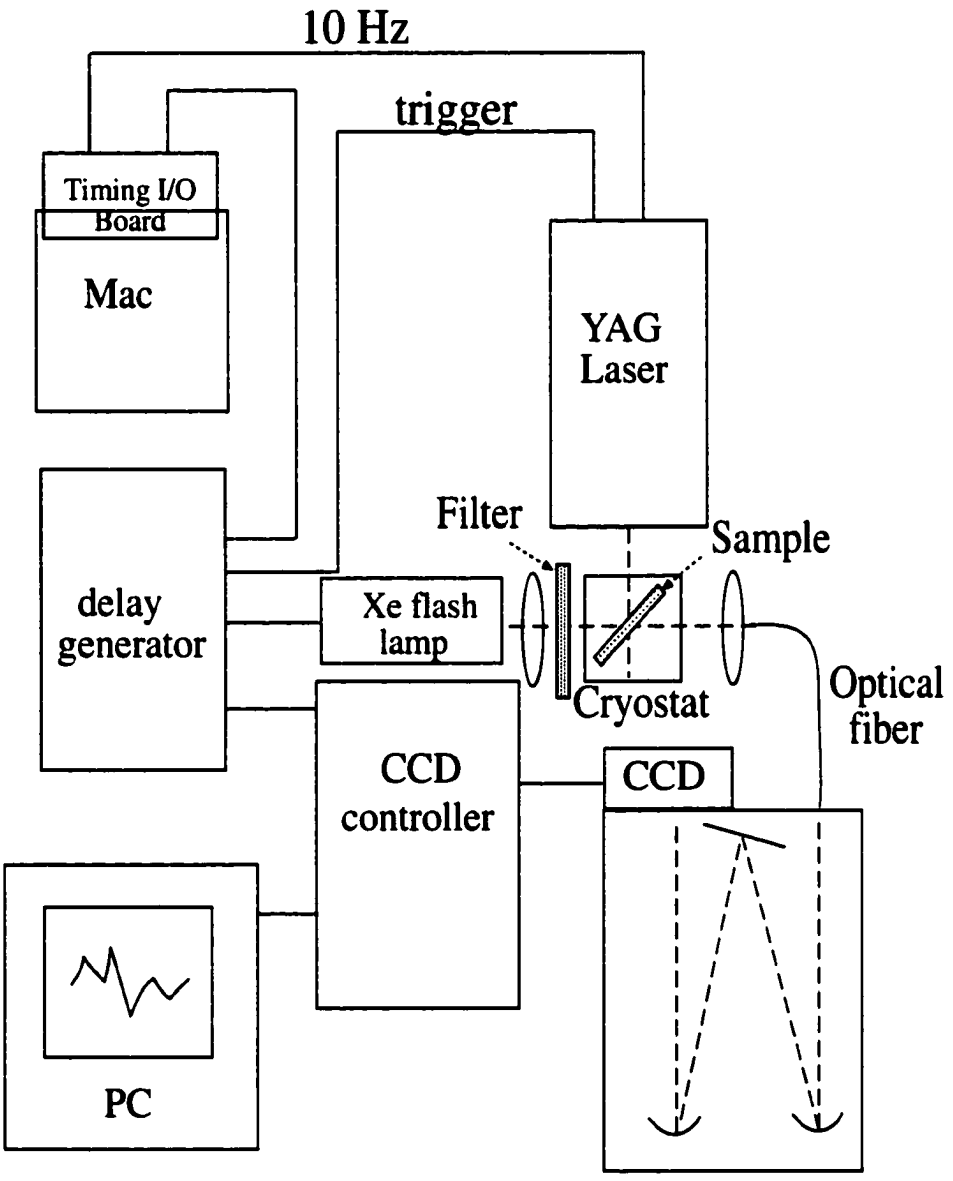

Figure 2.2. Setup for time resolved absorption change measurement in a large spectral range. Dashed lines represent the path of the light.

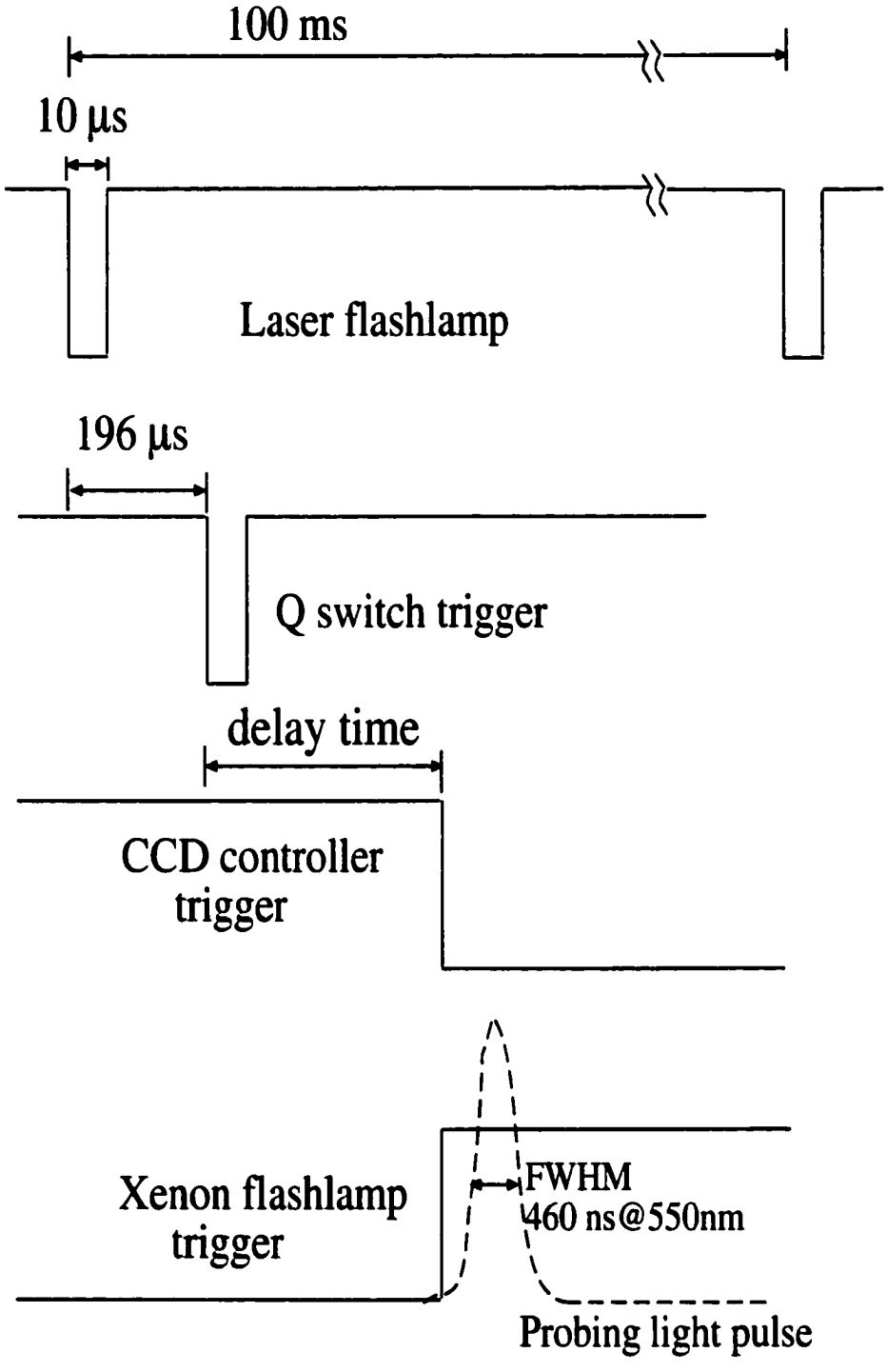

Figure 2.3. Pulse sequence for the time resolved absorption study using the CCD detector.

sent to trigger the Q switch. The time jitter for this mode is 10ns. The CCD detector and the probing light were triggered simultaneously. The time jitter is ~0.1 μS for the probe light. The CCD detector was set at external trigger and continuous clean mode. When the actinic and measuring light are close in wavelength, the scattering and fluorescent effect from the sample and glass sample holder limits the time resolution of the measurement to ~10 ms. But when the wavelengths are shifted apart far enough (>100 nm in the current setup), the time resolution should only be limited by the pulse width of the measuring light.

References

(1) Clayton, R. K.; Wang, R. T. *Methods Enzymol* **1971**, *23*, 696-704.

(2) Clayton, R. K.; Sistrom, W. R. *The Photosynthetic Bacteria*; Plenum Press: New York, 1978.

(3) Goldsmith, J. O.; Boxer, S. G. *Biochim Biophys Acta* **1996**, *1276*, 171-175.

(4) Okamura, M. Y.; Isaacson, R. A.; Feher, G. *Proc. Natl. Acad. Sci. USA* **1975**, *72*, 3492-3496.

(5) Woodbury, N. W.; Parson, W. W.; Gunner, M. R.; Prince, R. C.; Dutton, P. L. *Biochim. Biophys. Acta.* **1986**, *851*, 6-22.

Chapter 3

Temperature dependence of the free energy, enthalpy and entropy of $P^+Q_A^-$ charge recombination in *Rhodobacter sphaeroides* R26 reaction centers

Abstract

For reaction centers of photosynthetic bacteria reconstituted with low potential quinones in the Q_A site, the state $P^+Q_A^-$ formed by light activation, decays to the ground state via a thermally activated route through the P^+H^- state. The rate of charge recombination by this thermal pathway is proportional to the equilibrium constant between $P^+Q_A^-$ and P^+H^-. Thus the free energy difference between $P^+Q_A^-$ and P^+H^- can be determined by measuring the charge recombination rate via the uphill route. The enthalpy and entropy change of the reaction can then be deduced from the temperature dependence of the charge recombination kinetics. The free energy, entropy and enthalpy changes between $P^+Q_A^-$ and P^+H^- were determined from 40 to 318 K for nine low potential quinones. $\Delta H^0 \approx \Delta G^0$ from 200 K to room temperature, so the entropy changes are small. However, in the temperature region 80-200 K, a significant entropy change is observed and the free energy becomes strongly temperature dependent. The newly formed $P^+Q_A^-$ state lives for milliseconds. On this time

scale at low temperature, the $P^+Q_A^-$ state appears to be trapped prior to charge recombination in a state ≈200 meV (10 K) higher than the relaxed form found at room temperature.

Introduction

The bacterial photosynthetic reaction center (RC) is the intrinsic membrane protein that facilitates the conversion of light energy to chemical energy. Upon absorption of a photon, charge separation is achieved by a series of electron transfers between the cofactors bound to the protein. The crystal structure and the electron transfer sequence of RCs from several species of bacteria have been well characterized. (For reviews, see references 1-3) Electron transfers in this protein proceed through a quantum tunneling mechanism. This protein has proved to be an ideal model system for study of the basic chemistry of electron transfer in biology and chemistry.[4,5] In addition to the advantages of having a well defined configuration of electron donors and acceptors, sophisticated methods are available to change the driving force of the reaction and to manipulate the local protein environment of the cofactors.[6-9] In addition, most of the electron transfer steps in this protein are able to proceed at cryogenic temperature, providing unique advantages for the study of protein dynamics.[10-14]

The charge separation in reaction centers starts with a very fast picosecond electron transfer from the primary electron donor P, a dimer of bacteriochlorophyll, to the bacteriopheophytin H in the active L branch of the protein, followed by a slower reduction (~200 ps) of the primary quinone Q_A. When the secondary quinone Q_B is absent, the resultant charges on P^+ and Q_A^- recombine to return the system to the ground state (Figure 3.1). Following the

electron transfer from P* to H the system can return to the ground state in a reaction that competes with the forward electron transfer to Q_A. Because of spin rephasing in the P^+H^- state, charge recombination yields the triplet ^3P as well as the singlet P. ^3P returns to ground state through relatively slow intersystem crossing.[15,16]

Several different methods have been applied to reaction centers from *Rhodobacter sphaeroides* strain R-26 to measure the free energy, enthalpy and entropy of different reactions. The energy level of $P^+Q_A^-$ relative to other state has been determined in several ways. During the slow charge recombination process of $P^+Q_A^-$, $P^+Q_A^-$ and P* are in pseudo-equilibrium. The fraction of the population where electrons return to the donor reforming the P* state can be determined from the integrated amplitude of delayed fluorescence from P*. The ratio of P* and $P^+Q_A^-$ in pseudo-equilibrium provides the free energy difference between the two redox states. The enthalpy and entropy change of the reaction can then be deduced from the temperature dependence of the delayed fluorescence.[17,18] A second, photoacoustic, method measures the enthalpy change of the reaction directly from the heat released during the electron transfer from P* to $P^+Q_A^-$. Given the reaction free energy obtained by other methods, the entropy change can be found.[19-21]

A third method of determining *in situ* thermodynamic parameters utilizes the fact that the $P^+Q_A^-$ charge recombination can proceed through two pathways. One is by direct electron tunneling from Q_A^- to P^+. In the other, $P^+Q_A^-$

equilibrates with a higher energy state, most likely P^+H^-, which then decays to the ground state.[18,22-24] The rate of charge recombination by this thermal pathway is proportional to the equilibrium constant between $P^+Q_A^-$ and P^+H^- and to the rate of charge recombination from P^+H^-. Thus by measuring the charge recombination rate via this uphill route, the free energy difference between $P^+Q_A^-$ and P^+H^- can be determined using the known P^+H^- decay rate. With the native ubiquinone-10 as Q_A, the activated state is 520 meV higher than the $P^+Q_A^-$ state, so the contribution of the uphill route to charge recombination is negligible compared to the direct route in the ambient temperature range. However, the ubiquinone in the Q_A site can be replaced with other quinones, a technique that allows the reaction ΔG^0 of states involving Q_A to be changed.[18,22-24] With substituted quinones with *in situ* redox potentials more than 100 meV lower than ubiquinone, the rate via this thermal route is comparable to or even much faster than the direct route.

The energy of $P^+Q_A^-$ with different quinones as Q_A measured by the rate of the thermal back reaction is consistent with that determined by the delayed fluorescence measurement[18] (Fig. 3.2) and with values measured by $P^+Q_B^-$ charge recombination through $P^+Q_A^-$ as an intermediate state. [9,25] Thermal back reaction measurements have been applied to reaction centers with a series of low potential quinones[11,18] and several non-quinone compounds[26] as Q_A. This

activated reaction has been used to measure the effects of pH,[27,28] external electrical field[6,13] and mutation[25] on the *in-situ* quinone redox potential.

Measurement of the temperature dependence of the up-hill charge recombination rate provides the enthalpy change of this reaction.[18,26,28] The reaction free energy, entropy and enthalpy influence the electron transfer rate and the portion of the photon's energy that is stored. A significant entropy change could indicate that conformational changes or binding or release of waters or ions are coupled to the electron transfer reaction. In the absence of direct measurements, most theoretical treatments of electron transfer in reaction centers assume the entropy change is negligible.[4,5,29]

The changes in entropy and enthalpy of several reactions involving Q_A have been investigated near room temperature. There are indications from delayed fluorescence that the change in entropy for the charge separation forming $P^+Q_A^-$ from P^*Q_A is small.[17,18]. Several photoacoustic measurements also found that ΔH^0 is close to ΔG^0 for this reaction.[19,20] However, recent photoacoustic measurements, indicate instead that there may be a significant entropy change for the same process. A $T\Delta S^0$ value of 420 meV (298 K) was found for native RCs where the ΔG^0 is -860 meV.[21]

The temperature dependence of the $P^+Q_A^-$ thermal charge recombination rate has been measured with several different quinones as Q_A.[12,28] With anthraquinone as Q_A, ΔH^0 changes between $P^+Q_A^-$ and P^+H^- by ≈400 meV while $T\Delta S^0$ is ≈120 meV. The temperature dependence of the charge recombination

kinetics for several non-quinone compounds that are functional in the Q_A site also showed enthalpy changes close to the reaction free energy change.[26] Measurements in reaction centers from *Rhodopseudomonas viridis* also showed also showed small values for ΔS^0.[23,30]

The ability to measure thermodynamic parameters over a wide temperature range allows the comparison of the protein above and below the solvent freezing and glass transition temperature. This can provide additional information on the protein dynamics. The region around 200 K is of particular interest.[31] Temperature dependent transitions of the equilibrium dynamical fluctuations in several proteins at have been observed at 200-220 K.[32] The solvent glass transition (Tg) is also found in this region. Tg is about 180 K for 3:1 glycerol-water mixtures which is often the solvent for low temperature measurements with protein, which may influence the measured protein reaction kinetics.[33] Previous studies of the thermal back reaction kinetics with non-quinone compounds and in RCs from *Rps. viridis* have been extended to cryogenic temperature. However, the temperature range for these earlier measurements was still quite restricted. Either the indirect route of $P^+Q_A^-$ charge recombination was frozen out above 200 K[23,26,30] or measurements were only made at temperatures well below 200 K.[26]

Previous studies of reaction centers with the native ubiquinone-10 as Q_A showed the exothermic, direct tunneling $P^+Q_A^-$ charge recombination rate undergoes an increase of about 4 fold over a relatively narrow temperature

range around 200 K.[14] It has been suggested that this arises from changes in the $P^+Q_A^-$ energy level due to changes of the distribution of accessible protein conformations with temperature. Further evidence for changes in the temperature region was also found in studies of the same reaction in mutants with a modified P/P^+ midpoint potential. It was showed that the sum of the electron transfer reorganization energy and the reaction free energy decreases by about 280 meV from 293 k to 10 k, with the sharpest decline near 200 K.[34]

The work presented here reports a systematic study of the temperature dependence for the $P^+Q_A^-$ thermal charge recombination kinetics from 40 K to 318 K. Eight low potential anthraquinones and one naphthoquinone were substituted into the Q_A site. These quinones vary the ΔG^0 of the reaction by about 200 meV. The results clarify some of the discrepancies between different previous measurements and extend the measurement to cover a wider temperature range. Additional evidence is found for change in protein relaxation for formation of the $P^+Q_A^-$ state in the temperature region near 200 K.

Experimental Section

Reaction centers of *Rb. sphaeroides* strain R-26 were isolated following established procedures using lauryldimethylamine-N-oxide (LDAO) extraction and purified using ammonium sulfate and DEAE(diethylaminoethyl) chromatography.[35] The native ubiquinones in Q_A and Q_B sites were extracted

with 4% LDAO and 10 mM orthophenathroline using the method of Okamura[36] with minor modification[18]. The typical residual quinone after the treatment is: $Q_A \leq 5\%$ and $Q_B=0\%$. In the final assay mixture the residual LDAO concentration from the RC stock solution is less than 0.025%. For Q_A reconstitution, quinones were first dissolved in alcohol, then added to the sample at the desired concentration. 10 mM Tris with 2.5 mM KCl (pH=8.0) was used as buffer. Eight anthraquinone and one naphthoqinone were used: 1-chloroanthraquinone (1-Cl-AQ), 2-chloroanthraquinone (2-Cl-AQ), 2-aminonaphthoquinone (2-Am-NQ), anthraquinone (AQ), 2-methylanthraquinone (2-Me-AQ), 1-aminoathraquinone (1-Am-AQ), 2,3-dimethylanthraquinone (2,3-dM-AQ), 2,7-dimethylanthraquinone (2,7-dM-AQ), 1,3-dimethylanthraquinone (1,3-dM-AQ). 2,7-dM-AQ was synthesized in the laboratory of Dr. J. Malcolm Bruce (University of Manchester), the other quinones were purchased from Fluka (AQ and 2-Am-AQ) and Aldrich (all other).

Charge recombination kinetics was observed in a flash spectrometer of local design. The electron transfer reaction was initiated by a 10 μs xenon flash. The changing redox state of the electron donor P was followed by monitoring the absorption change at 430 nm. The transmitted light was collected by a photomultiplier tube (Thorn EMI9798QB). The signal was filtered and amplified before being sent to a LeCroy digital oscilloscope (model 9310M 300 MHz).

The temperature dependence of the charge recombination reaction was measured in the range of 5-45°C for all 9 quinones substituted into the Q_A site. The reaction center concentration was 300-400 nM. The temperature was controlled by using a jacketed cuvette with a circulating waterbath (Fisher Model

9101). A thermal-couple monitors the temperature change with an accuracy of 0.1°C. Measurement starts ≈5 minutes after the sample reaches the preset temperature. 10 to 15 traces were averaged for each measurement.

For reaction centers with 2-Cl-AQ, 2-Me-AQ and 2,3-dM-AQ as Q_A the $P^+Q_A^-$ charge recombination reaction was monitored from 40K to 300K. The temperature was controlled by a closed cycle helium cryostat system (APD cryogenics Inc., Model CSW202A) with a programmable temperature controller. The temperature resolution is 0.1 K and controllability is ± 0.4 K. The samples used for the low temperature experiment were obtained by mixing the reaction centers in Tris buffer with two volumes of glycerol. The final reaction center concentration is 3-4 μM. The optical cell has a light path of 1 mm. The actinic and measuring light, which are perpendicular to each other, meet with an incident angle of 45 degrees at the sample.

The observed kinetics were analyzed by both one and two exponential decays plus a constant using a nonlinear least square fitting program of Levenberg-Marquardt algorithm (Igor Pro from WaveMetrics). For 2-Me-AQ and 2,3-dM-AQ at low temperature, an extra exponential function is needed to fit a fast phase that decays at about 5000 s^{-1}. This phase can be attributed to the formation of the triplet state of the bacteriochlorophyll dimer (^3P).[37]

The observed reaction kinetics monitor the charge recombination in the $P^+Q_A^-$ state, which proceeds through a thermally activated pathway via P^+H^- in addition to the direct tunneling rate (Fig. 3.1). Since the uphill rate monitors the equilibrium constant, the temperature dependence of the kinetics can provide

the enthalpy and entropy difference between $P^+Q_A^-$ and P^+H^-. The charge recombination rate can be written as

$$k = k_0 + k_1 \exp\left(-\Delta G^0 / k_B T\right)$$
$$= k_0 + k_1 \exp(\Delta S^0 / k_B) \exp\left(-\Delta H^0 / k_B T\right) \quad (3.1)$$

where k_0 is the rate by the direct electron tunneling route, which is relatively temperature independent.[10,11] k_1 is the quinone independent decay rate from P^+H^- to reform the ground state, k_B is the Boltzman constant, and T is temperature. ΔG^0, ΔH^0 and ΔS^0 are the standard free energy, enthalpy and entropy change between $P^+Q_A^-$ and P^+H^-. The thermodynamic parameters are obtained from the Van't Hoff plot of Log(k-k_0) vs. 1/temperature,

$$\log(k - k_0) = \log k_1 + \left(\Delta S^0 / 2.3 k_B\right) - \left(\Delta H^0 / 2.3 k_B T\right) \quad (3.2)$$

Results

Analysis of the charge recombination kinetics. The temperature dependence of the $P^+Q_A^-$ charge recombination kinetics was measured from 40 to 318 K in reaction centers substituted with different low potential quinones. The exact

value of the rate is sensitive to the fitting procedure. The charge recombination kinetics were fit using single, double and distributed rate functions. With a double exponential, the fast rate (k_f) is two to three times the slower rate (k_s) in the ambient temperature range, for all Q_A's with *in situ* midpoint potentials more positive than 1-Am-AQ (-285 meV relative to UQ_{10}). As the Q_A midpoint is lowered the rate becomes substantially faster (Fig. 3.2). The limited resolution of the measurements provides enough data for only single exponential fit. For the higher potential Q_A's, the double exponential fits the kinetic data with no systematic error while the single exponential fit underestimates the amplitude at early times (See Fig. 3.3). This has been observed previously.[28,30,38] The different rates have been attributed to two populations of reaction centers with different protonation states of residues close to the Q_A binding site.[28] Because the fast and slow phases are not very different, the parameters obtained for the two rates have larger uncertainty than the single exponential fit. The rates of charge recombination in RCs with 2-Me-AQ in aqueous solution are plotted in Figure 3.4. As will be shown later, the values of ΔG^0 and ΔH^0 are only weakly dependent on the fitting procedure. Therefore the simplest single exponential analysis will be used.

More complicated fitting schemes using distributed rates have been suggested by Kleinfeld et al.[10] and McMahon et al.[14] for analysis of low temperature kinetics which assumes a distribution of conformational states. The result from the single rate method can be regarded as the weighed average value of the distribution.[39] The data obtained here can be fit as well by two

exponential functions as by a model with a distribution of rate constants (not shown).

An additional complication is found at low temperature for the low potential Q_A's. In RCs with 2-Me-AQ and 2,3-dM-AQ as Q_A, an extra, fast phase with a rate of approximately 5000 s^{-1} was observed below 200 K and 220 K respectively. This phase can be attributed to the decay of the triplet state ^3P.[37,40] As expected, a phase with the same rate constant but larger amplitude is seen in reaction centers with no Q_A but not seen in reaction centers containing the native ubiquinone-10. The rate of this phase is fixed in the analysis of the reaction kinetics using the value measured in reaction centers with no Q_A.

The rates obtained by a single exponential fit for reaction centers with several different low potential quinones as Q_A in the temperature range 220-318 K are shown in Figure 3.5. The rate varies with *in situ* E_m as discussed in the methods section. It accelerates with increasing temperature as expected if ΔH^0 is significant. Figure 3.6 shows the temperature dependence of the reaction between 40 and 300 K for reaction centers with 2-Me-AQ , 2,3-dM-AQ and 2-Cl-AQ as Q_A.

Aqueous buffer was used for measurement in the ambient temperature range, while in the low temperature experiments, 67% glycerol solution was used. The $P^+Q_A^-$ charge recombination rate in glycerol solution is very close to the rate in aqueous solution at the same temperature (Fig. 3.5). This differs from previous results with *Rps. viridis* reaction centers where the rate was found to decrease when glycerol was added.[23]

Choice of k_0 and k_1 The free energy, enthalpy and entropy change going from $P^+Q_A^-$ to P^+H^- can be obtained using equation 3.2, given the $P^+Q_A^-$ charge recombination rate through the direct electron tunneling route, k_0, and the charge recombination rate from P^+H^-, k_1. The direct electron tunneling rate from Q_A^- to P^+, k_0, is only weakly temperature dependent.[34,41] So for each Q_A, the low temperature value (~35 K) was used for k_0 at all temperatures. This rate was either measured here or taken from earlier studies.[41] For most of the Q_A's used here, the charge recombination rate is over 100 s^{-1} in the ambient temperature range. This is much larger than k_0, which is less than 30 s^{-1} so the fitting process is not sensitive to errors in k_0. However, for 1-Cl-AQ and 2-Cl-AQ, whose charge recombination rates (~20 s^{-1}) are of the same magnitude as k_0 (~10 s^{-1}), the fitting is sensitive to the choice of k_0. For these relatively high potential Q_A's, increasing k_0 by 1 s^{-1} increases the $T\Delta S^0$ estimate by 50 meV. Given k_0, the temperature dependence of the measured charge recombination rate can be fit using equation 3.2. The slope of the resultant line gives the standard enthalpy change between $P^+Q_A^-$ and P^+H^- (Fig. 3.4).

The charge recombination rate was measured down to 275 K with all 9 Q_A's. In this temperature range there is a clear, simple linear dependence between the rate and 1/T. Measurements of the rate were continued to 40 K for reaction centers with 3 of the Q_A's. Above ~210 K, the charge recombination rate

decreases with the temperature as predicted by equation 3.2 (Fig. 3.5) with essentially the same slope as found in the aqueous sample at room temperature. The entropy change is quite small in this temperature region. However, below ~210 K, the rate decreases much more slowly as the temperature decreases. The temperature dependence between 80 and 210 K suggests the reaction has a much smaller enthalpy (Fig. 3.6). For these two Q_A's the ΔH^0 is close to 300 meV above 200 K and only 30 meV below the transition temperature (Table 3.3). Below 210 K the kinetics do deviate more from a simple exponential decay. However, a double exponential function still fits the data well. The slow and fast phases have a similar temperature dependence and therefore have similar enthalpies (data not shown).

The kinetics for reaction centers with 2,3-dM-AQ was also measured in 33% glycerol buffer (Fig. 3.6b). As the temperature is lowered from room temperature the reaction rate and the enthalpy are independent of the solvent. However, the temperature of transition to a smaller enthalpy reaction occurs about 15 K higher in the low glycerol sample. Thus, this transition seems to relate to some property of the solvent. Below the transition temperature the temperature dependence of the rate is the same in both low and high glycerol solvent. Thus, the reaction enthalpy is unaffected by this change in solvent. However, the reaction ΔG^0 is dependent on the glycerol concentration as seen by the faster back reaction rate with lesser glycerol concentration. The solvent thus appears to change the reaction ΔS^0.

To determine the reaction free energy and entropy from the observed $P^+Q_A^-$ decay kinetics, the charge recombination rate of P^+H^-, k_1, is needed. This

decay rate has been previously established to be $5\sim8\times10^7$ s^{-1}.[37,40] For the calculation reported here, k_1 is taken to be 7.7×10^7 s^{-1}. Different values have been used when the triplet decay pathway was taken into consideration.[23,42] But as will be discussed later, the triplet pathway seems to be separate from the charge recombination pathway found in these reaction centers. k_1 has a weak temperature dependence.[37,40] The rate increases approximately 20% from 5 to 45°C, causing a -30 meV correction of the enthalpy measured in this temperature range for all the quinones. This correction is smaller (~ -10 meV) for the enthalpy measurements over the larger temperature range. The reported enthalpy was corrected for the temperature dependence of k_1.

The entropy, enthalpy and free energy. The free energy, enthalpy and entropy changes for reaction centers with 2-Me-AQ as Q_A are listed in Table 3.1. These values compare measurements in the ambient temperature range (278-318 K) and in 67% glycerol between 220 to 300 K. Remarkably the results show that the reaction entropy and enthalpy is temperature independent down to 220 K. The enthalpy change is the dominating term being close to the reaction free energy and so the entropy change is small. Thus the free energy is nearly temperature independent. The ΔG^0 value obtained for the single exponential fit is 265 meV (298 K). This is in good agreement with previous measurement of 270 meV.[12,18] The free energy difference between the fast and slow phase is about 30 meV (298 K), which reflects the approximately 3 fold difference in the two rate constants.

The parameters from the single exponential fit above the transition temperatures for reaction centers with nine different Q_A's are listed in Table 3.2.

The measured entropy and enthalpy change vs. the free energy change are plotted in Figure 3.7. The enthalpy change is slightly larger than the free energy change, and the difference becomes smaller when the ΔG^0 decreases. On average, ΔH^0 is within 10% of ΔG^0. AQ has the largest absolute entropy change, $T\Delta S^0$ =100 meV, while in 1-Am-AQ the entropy change is the largest fraction of the reaction free energy change. The entropy change is never more than 25% of the reaction ΔG^0.

The reaction enthalpy, entropy and free energy were determined below 210 K using the same thermal back reaction model and the same k_1 value (Table 3.3). The enthalpy drops about 250 meV below the transition temperature, and the entropic contribution to the free energy increase by the same amount. Now the free energy change decreases with temperature.

One possible source of error in the derivation of the thermodynamic parameters is the use of a constant value for k_0, especially at temperatures below 210 K. Previous studies[34,41] show that k_0 increases by 50 –100% from 210 K to 90 K in wild type RCs and in mutants with different P/P^+ midpoint potentials, which is in the opposite direction of the rate change observed here. The use of a constant for k_0 will cause the enthalpy of the reaction to be underestimated, but it is not nearly enough to explain the difference in the enthalpy change above and below the transition temperature. If k_0 is assumed to double over this temperature range in RCs with substituted quinones , the correction on the enthalpy data derived is less than 3 meV, within the error of the measurement.

Discussion

The temperature dependence of the $P^+Q_A^-$ charge recombination kinetics was measured from 40-318 K for reaction centers with low potential quinones substituted in the Q_A site. With these Q_A's the reaction occurs via an pre-equilibrium with the P^+H^- state.[22] Thus, the reaction kinetics provide a simple measurement of the *in situ* thermodynamics for the electron transfer from Q_A^- to H. The use of these different Q_A's allows the reaction ΔG^0 to be varied over a range of ≈200 meV. In the native RCs with ubiquinone as Q_A, the contribution of the uphill pathway is negligible. Here charge recombination mainly proceeds through the direct tunneling from Q_A^- to P. This reaction is close to temperature independent, therefore it provides little information about reaction thermodynamics.[11,13] The temperature at which the thermal route freezes out and the direct tunneling rate becomes the dominant pathway decreases as the quinone midpoint potential is lowered.[24]

When the charge recombination reaction proceeds through the thermally activated route via the P^+H^- state, the ΔG^0 between the $P^+Q_A^-$ and P^+H^- states can be determined from the charge recombination rate at a given temperature, and the temperature dependence of the rate provides ΔH^0 and ΔS^0. Above about 210 K, the reaction enthalpy is found to be close to the free energy change (Fig. 3.7). This is consistent with previous measurement on a smaller number of samples using the same method.[28,41] The entropy change is small (<3.3 mev/K) and positive, indicating that the intermediate P^+H^- state is somewhat more

disordered than $P^+Q_A^-$. Between 80 K and 200 K, ΔH^0 is much smaller, ΔG^0 becomes more strongly temperature dependent and ΔS^0 becomes significant.

The method used here for estimation of thermodynamic parameters of the reaction centers relies on the validity of the model illustrated in Figure 3.1. A few possible complications exist:

The identity of the intermediate state. The variation of the charge recombination kinetics with the energy of the $P^+Q_A^-$ state strongly supports a mechanism where $P^+Q_A^-$ pre-equilibrates with a higher energy intermediate (Fig. 3.2). This intermediate is most likely P^+H^-.[2,18,23] Some controversy exists in the literature regarding the exact free energy of this state. Measurements on the nanosecond or faster time scales find values varying from 90 meV to 250 meV below P*.[43-47] Explanations for the variation include relaxation following the initial charge separation and a distribution of free energies for P^+H^-. Using 7.7×10^7 s^{-1} for k_1 and a ΔG^0 between P* and $P^+Q_A^-$ of 860 meV for the native reaction centers, the thermal intermediate is 340 meV below P*. This estimate uses measurements on the micro- to millisecond time scale. The lower energy suggests the thermal intermediate state observed in $P^+Q_A^-$ charge recombination utilizes a more relaxed form of P^+H^- as the high energy intermediate.

The free energy change from $P^+Q_A^-$ to P* has also been measured independently using the delayed fluorescence method.[18] If the free energy change of $P^+Q_A^-$ to P* is compared to the free energy change between $P^+Q_A^-$ and

P^+H^-, the difference is a constant for the different quinones as Q_A (Fig. 3.2). Thus, the free energy of the thermally accessible P^+H^- state is independent of the identity of the quinone in the Q_A binding site. So regardless of the exact nature of the thermal intermediate, this state can be used as a reference point for determining the relative $P^+Q_A^-$ energy under different conditions.

Triplet formation on the charge combination pathway. Triplet states will be formed in quinone substituted reaction centers if the quantum yield for formation of $P^+Q_A^-$ is lower than 1. Some formation of triplet state in reaction centers containing 2-Me-AQ and 2,3-dM-AQ at low temperature is consistent with previous quantum yield measurement.[41]

The triplet state might also be formed in charge recombination via P^+H^-. Equation 3.1, does not account for this additional route for $P^+Q_A^-$ charge recombination. However, at low temperature the triplet decay rate is seen to be distinct from the decay of the $P^+Q_A^-$ state, indicating that the triplet state is not in equilibrium with the P^+H^- state. It has been observed previously that no extra triplet was formed from the thermal back reaction through the P^+H^- state for 2,3-dM-AQ substituted reaction centers.[18] Therefore the triplet pathway seems to be separate from the thermal back reaction route through the P^+H^- state. The observed triplet most likely arises in RC where $P^+Q_A^-$ is never formed.

Comparison with previous results. The temperature dependence of ΔG^0, ΔH^0, $-T\Delta S^0$ for reaction centers with 2-Me- as Q_A is illustrated in Figure 3.8. At

temperatures above 210K $\Delta G^0 \approx \Delta H^0$ and ΔS^0 is small. At lower temperatures, $-\Delta G^0$ diminishes with temperature. The interpretation presented here is a first order approximation, which assumes ΔH^0 and ΔS^0 are constant above and below the transition temperature.

The entropy and enthalpy differences between P* and $P^+Q_A^-$ have been obtained in the room temperature region by measuring the temperature dependence of the delayed fluorescence via the P* state. For UQ_{10}, the entropy change is 110 meV while the free energy difference is –860 meV.[17] For AQ and 2,3,5-trimethyl-NQ, $T\Delta S^0$ was 10 meV and –20 meV relative to ΔG^0 of –700 meV and –770 meV.[18] Thus, the reaction entropy between $P^+Q_A^-$ and P* is small.

The thermodynamic parameters of the charge separation from P* to $P^+Q_A^-$ have also been measured by a photoacoustic method, which is a more direct calorimetric measure of the enthalpy change. The results from photoacoustic measurements vary. Early estimate showed relatively small values of ΔS^0 in agreement with the delayed fluorescence measurement.[19,20] However a recent study using improved methodology and sub-microsecond time resolution found a surprisingly large portion of the free energy change (~50% for UQ_{10}) to be entropic.[21] Possible causes of this discrepancy were discussed in detail in that paper. One important factor may be the different time scales of the measurements. It was proposed that more relaxation of $P^+Q_A^-$ occurs in the slower delayed fluorescence measurements (10 μS to 100 ms) than in the fast photoacoustic measurement (<100 ns). The thermodynamic parameters obtained

here by the thermal charge recombination measurements are in good agreement with those found by delayed fluorescence. These methods both monitor the system during the lifetime of $P^+Q_A^-$.

The observation of a large entropy change at temperatures lower than 210 K also suggests that $P^+Q_A^-$ is formed in a state which can be trapped before relaxation. The reaction ΔS^0, if extrapolated to room temperature, is 300 mev (298 K) for 2,3-dM-AQ, which is comparable with the value of 210 meV measured by the photoacoustic method at the same temperature. At low temperature, protein motions are slowed down, and the $P^+Q_A^-$ state formed by the flash may not be able to fully relax in the milliseconds before the charge recombination. A trapped state can result from energy barriers internal to the protein and as well as from high solvent viscosity.[33] The reaction entropy and enthalpy changes are therefore different from their values at room temperature. Thus, a large ΔS^0 may be found by the photoacoustic method because an early intermediate is assayed, while similar results are found below 210 K where an unrelaxed state is trapped.

Extrapolating the $-\Delta G^0$ for electron transfer with 2-Me-AQ to 0 K show that the ebergy gap between $P^+Q_A^-$ and P^+H^- is 220 meV smaller than at room temperature (Fig. 3.8). The temperature dependence of the $P^+Q_A^-$ state is likely to be greater than of the P^+H^- state, which lives less than a nanosecond and so has little time for relaxation at any temperature. Several other, less direct estimates of the temperature dependence of the $P^+Q_A^-$ energy level exist from estimates of the temperature dependence of the free energy gap between $P^+Q_A^-$ and the

ground state. The rate of $P^+Q_A^-$ charge recombination by direct tunneling from Q_A^- to P^+ was analyzed using a distributed conformation model.[14] Analyzing the change in rate with quantum mechanical electron transfer theory, the average free energy difference between $P^+Q_A^-$ and P appears to increase by about 130 meV from room temperature to 5 K. This is consistent with $P^+Q_A^-$ being trapped in a higher energy state at low temperatures.

A similar study determined the temperature dependence of electron tunneling from Q_A^- to P^+ in mutants with different P/P^+ midpoint potentials.[34] The relationship between the electron transfer rate and driving force was analyzed using Marcus theory. The maximum of the theoretical curve, i.e. the driving force ($-\Delta G^0$) at which the electron transfer is optimized, shifts by -280 meV from room temperature to 10 K. This shift could be explained by either a decrease of the reorganization energy (λ) or an increase in the driving force ($-\Delta G^0$). The contribution of each variable could not be separated in the analysis. However, the results reported here suggest that a significant portion of the shift is due to an increase in $-\Delta G^0$ as $P^+Q_A^-$ is trapped at a higher energy at low temperature.

Conclusions

The free energy, entropy and enthalpy changes between $P^+Q_A^-$ and P^+H^- were determined for 8 anthraquinones and 1 naphthoquinone as Q_A. The temperature dependence of the charge recombination kinetics was studied from 40-318 K. The entropy changes are found to be small from 210 K to room temperature. However, in the temperature region 80-210 K a significant entropy change is observed and the free energy is strongly temperature dependent. Thus, at lower temperatures $P^+Q_A^-$ appears to be trapped in a higher energy state. This is consistent with early studies that inferred changes in the energy of this state at low temperature without being able to measure the *in situ* ΔG^0 directly.

References

(1) Feher, G.; Allen, J. P.; Okamura, M. Y.; Rees, D. C. *Nature* **1989**, *339*, 111-116.

(2) Gunner, M. R. *Current Topics in Bioenergetics* **1991**, *16*, 319-367.

(3) Blankenship, R. E.; Madigan, M. T.; Bauer, C. E. *Anoxygenic Photosynthetic Bacteria*; Kluwer Academic Publishers:, 1995; Vol. 2.

(4) Marcus, R. A.; Sutin, N. *Biochim. Biophys. Acta* **1985**, *811*, 265-322.

(5) DeVault, D. *Q. Rev. Biophys.* **1980**, *13*, 387-564.

(6) Gopher, A.; Blatt, Y.; Schonfeld, M.; Okamura, M. Y.; Feher, G.; Montal, M. *Biophys. J.* **1985**, *48*, 311-320.

(7) Lin, X.; Murchison, H. A.; Nagarajan, V.; Parson, W. W.; Allen, J. P.; Williams, J. C. *Proc. Natl. Acad. Sci. USA* **1994**, *91*, 10265-10269.

(8) Woodbury, N. W.; Allen, J. P. The pathway,kinetics and thermodynamics of electron transfer in wild type and mutant raction centers of purple nonsulfur bacteria. In *Anoxygenic Photosynthetic Bacteria*; Blankenship, R. E., Madigan, M. T., Bauer, C. E., Eds.; Kluwer: Dordrecht, 1995.

(9) Li, J.; Takahashi, E.; Gunner, M. R. *Biochemistry* **2000**, *39*, 7445-7454.

(10) Kleinfeld, D.; Okamura, M. Y.; Feher, G. *Biochemistry* **1984**, *23*, 5780-5786.

(11) Gunner, M. R.; Robertson, D. E.; Dutton, P. L. *J. Phys. Chem.* **1986**, *90*, 3783-3795.

(12) Gunner, M. R.; Dutton, P. L. *J. Am. Chem. Soc.* **1989**, *111*, 3400-3412.

(13) Franzen, S.; Boxer, S. G. *J. Phys. Chem.* **1993**, *97*, 6304-6318.

(14) McMahon, B. H.; Muller, J. D.; Wraight, C. A.; Nienhaus, G. U. *Biophysical Journal* **1998**, *74*, 2567-2587.

(15) Chidsey, C. E. D.; Takiff, L.; Slodstein, R. A.; Boxer, S. G. *Proc. Natl. Acad. Sci. USA* **1985**, *82*, 6850-6854.

(16) Polenova, T.; Mc Dermott, A. E. *J. Phys. Chem. B.* **1999**, *103*, 535-548.

(17) Arata, H.; Parson, W. W. *Biochim. Biophys. Acta* **1981**, *638*, 201-209.

(18) Woodbury, N. W.; Parson, W. W.; Gunner, M. R.; Prince, R. C.; Dutton, P. L. *Biochim. Biophys. Acta.* **1986**, *851*, 6-22.

(19) Arata, H.; Parson, W. W. *Biochim. Biophys. Acta* **1981**, *636*, 70-81.

(20) Puchenkov, O. V.; Kopf, Z.; Malkin, S. *Biochim. Biophys. Acta* **1995**, *1231*, 197-212.

(21) Edens, G. J.; Gunner, M. R.; Xu, Q.; Mauzerall, D. *J. Am. Chem. Soc.* **2000**, *122*, 1479-1485.

(22) Gunner, M. R.; Tiede, D. M.; Prince, R. C.; Dutton, P. L. Quinones as prosthetic groups in membrane electron-transfer proteins I: Systematic replacement of the primary ubiquinone of photochemical reaction centers with other quinones. In *Function of Quinones in Energy Conserving Systems*; Trumpower, B. L., Ed.; Academic Press: New York, 1982; pp 265-269.

(23) Shopes, R. J.; Wraight, C. A. *Biochim. Biophys. Acta* **1987**, *893*, 409-425.

(24) Page, C. C.; Moser, C. C.; Chen, X.; Dutton, P. L. *Nature* **1999**, *402*, 47-52.

(25) Takahashi, E.; Wells, T. A.; Wraight, C. A. Enviornmental control of the redox protential of Q_A in *Rb. sphaeroides* reaction centers: Polar replacement of Ile^{M260} causes marked change in Q_A and Q_B function. In *Proceedings of the XIth*

International Photosynthesis Congress; Garab, G., Ed.; Kluwer: Dordrecht, 1998; Vol. II; pp 17-22.

(26) Warncke, K.; Dutton, P. L. *Biochemistry* **1993**, *32*, 4769-4779.

(27) Kleinfeld, D.; Okamura, M. Y.; Feher, G. *Biophys. J.* **1985**, *48*, 849-852.

(28) Sebban, P. *Biochim. Biophys. Acta* **1988**, *936*, 124-132.

(29) Kakitani, T.; Kanitani, H. *Biochim. Biophys. Acta* **1981**, *635*, 498-514.

(30) Sebban, P.; Wraight, C. A. *Biochimica et Biophysica Acta* **1989**, *974*, 54-65.

(31) Vitcup, D.; Ringe, D.; Petsko, G. A.; Karplus, M. *Nature structural biology* **2000**, *7*, 34-38.

(32) Daniel, R. M.; Smith, J. C.; Ferrand, M.; Héry, S.; Dunn, R.; Finney, J. L. *Biophys. J.* **1998**, *75*, 2504-2507.

(33) Hagen, S. J.; Hofrichter, J.; Eaton, W. A. *Science* **1995**, *269*, 959-962.

(34) Ortega, J. M.; Mathis, P.; Williams, J. C.; Allen, J. P. *Biochemistry* **1996**, *35*, 3354-3361.

(35) Clayton, R. K.; Wang, R. T. *Methods Enzymol* **1971**, *23*, 696-704.

(36) Okamura, M. Y.; Isaacson, R. A.; Feher, G. *Proc. Natl. Acad. Sci. USA* **1975**, *72*, 3492-3496.

(37) Chidsey, C. E. D.; Kirmaier, C.; Holten, D.; Boxer, S. G. *Biochim. Biophys. Acta* **1984**, *766*, 424-437.

(38) Franzen, S.; Goldstein, R. F.; Boxer, S. G. *J. Phys. Chem.* **1990**, *94*, 5135-5149.

(39) Lavalette, D.; Tetreau, C.; Brochon, J.; Livesey, A. *Eur. J. Biochem.* **1991**, *196*, 591-598.

(40) Schenck, C. C.; Blankenship, R. E.; Parson, W. W. *Biochim. Biophys. Acta* **1982**, *680*, 44-59.

(41) Gunner, M. R. The temperature and ΔG dependence of long range electron transfer in reaction center protein from *Rhodobacter sphaeroides*. Ph.D., University of Pennsylvania, 1988.

(42) Norris, J. R.; Bowman, M. K.; Budil, D. E.; Tang, J.; Wraight, C. A.; Closs, G. L. *Proc. Natl. Acad. Sci.* **1982**, *79*, 5532-5536.

(43) Holzwarth, A. R.; Muller, M. G. *Biochem.* **1996**, *35*, 11820-11831.

(44) Woodbury, N. W. T.; Parson, W. W. *Biochim. Biophys. Acta* **1984**, *767*, 345-361.

(45) Goldstein, R. A.; Takiff, L.; Boxer, S. G. *BBA 42789* **1988**, 1-11.

(46) Ogrodnik, A.; Volk, M.; Michel-Beyerle, M. E. *Biochim. Biophys. Acta* **1988**, *936*, 361-371.

(47) Ogronik, A.; Keupp, W.; Volk, M.; Aumeier, G.; Michele-Beyerle, M. E. *J. Phys. Cem.* **1994**, *98*, 3432-3439.

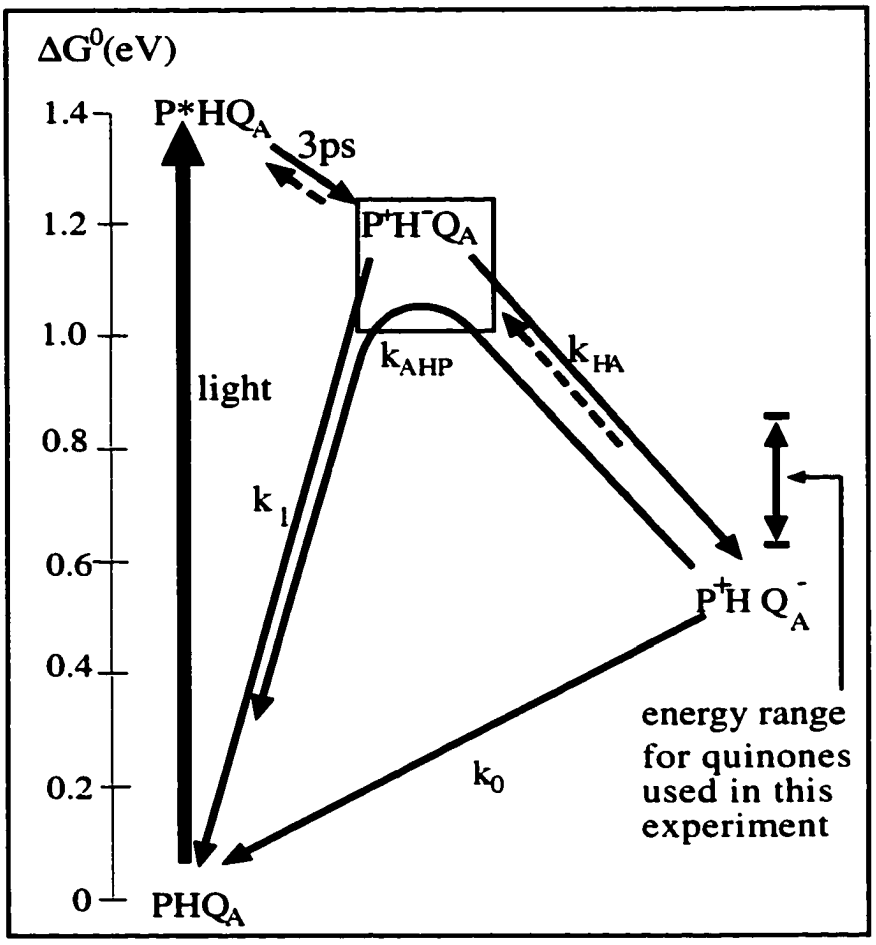

Figure 3.1. The electron transfer pathway and free energy level in *Rb. spharoides* RCs. The free energy level of the $P^+HQ_A^-$ state is shown for the native ubiquinone. The energy range for the substituted low potential quinones used as Q_A in the experiment is also shown. The uncertainty of the P^+H^- free energy level is indicated by the box (see discussion). With native RCs at room temperature, k_1 = 7.7×10^7 s^{-1} and is assumed to be independent of quinone at the Q_A site, k_{HA}= 5×10^9 s^{-1}, k_0 = 9.3 s^{-1}.

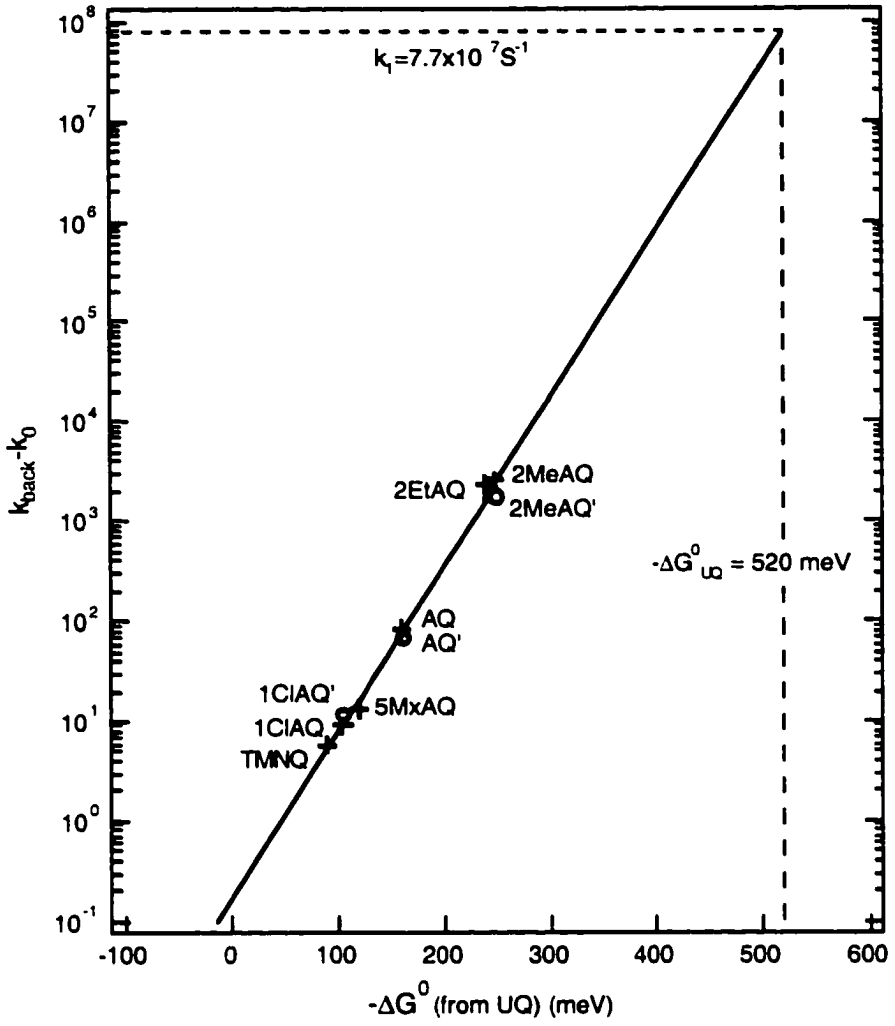

Figure 3.2. The relation between the $P^+Q_A^-$ charge recombination rate and the *in-situ* free energy measured by delayed fluorescence.[18] +, charge recombination rates taken from reference 41; o, values measured here. The line through the data was drawn so that the rate increases by a factor of 10 for each 60 meV increase in the energy of $P^+Q_A^-$ as predicted if the reaction mechanism involves equilibration of $P^+Q_A^-$ with a higher energy state. Assuming this state decays at 7.7×10^7 s^{-1}, as expected for P^+H^-, the intermediate is 520 meV above $P^+Q_A^-$ when Q_A is UQ.

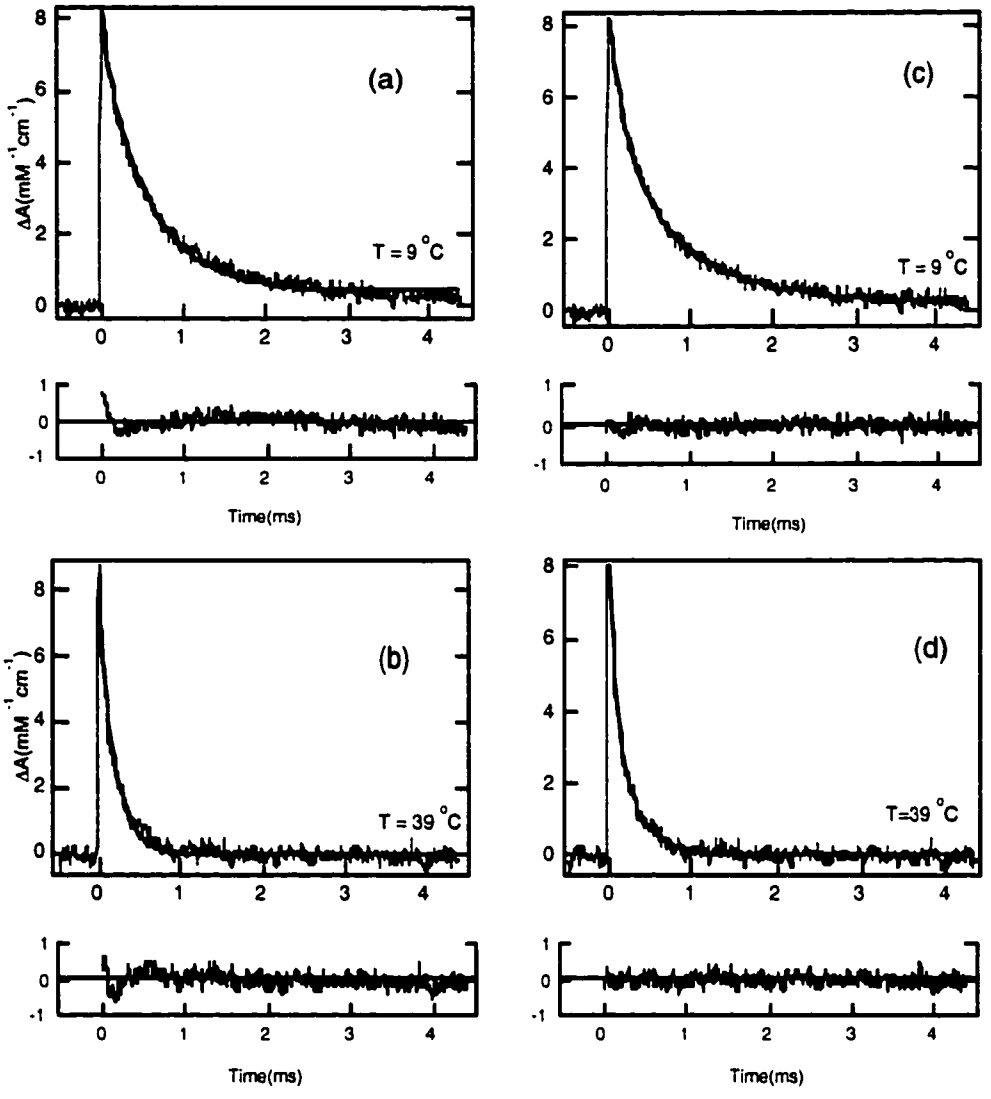

Figure 3.3. Flash induced absorption change for RCs with 2-Me-AQ as Q_A. The single (a and b) and double (c and d) exponential fit to the kinetics at two different temperature are shown. The residual error is also shown. pH =8.0, [RC]=400 nM, [2-Me-AQ]=4 μM. k_{single} is the rate obtained from the single exponential fit while k_f and k_s are the faster and slower components of the double exponential fit. The fit parameters are: at T =9°C, k_{single} =1.8x10^3 s^{-1}, k_f=1.2x10^3 s^{-1}(46% of total amplitude), k_s= 4.6x10^3 s^{-1}(54%), at T =39°C , k_{single} =5.4x10^3 s^{-1}, k_f=3.2x10^3 s^{-1}(55%), k_s=1.2x10^4 s^{-1}(45%). The constant in the single exponential fit is less than 5% of the total amplitude in both cases.

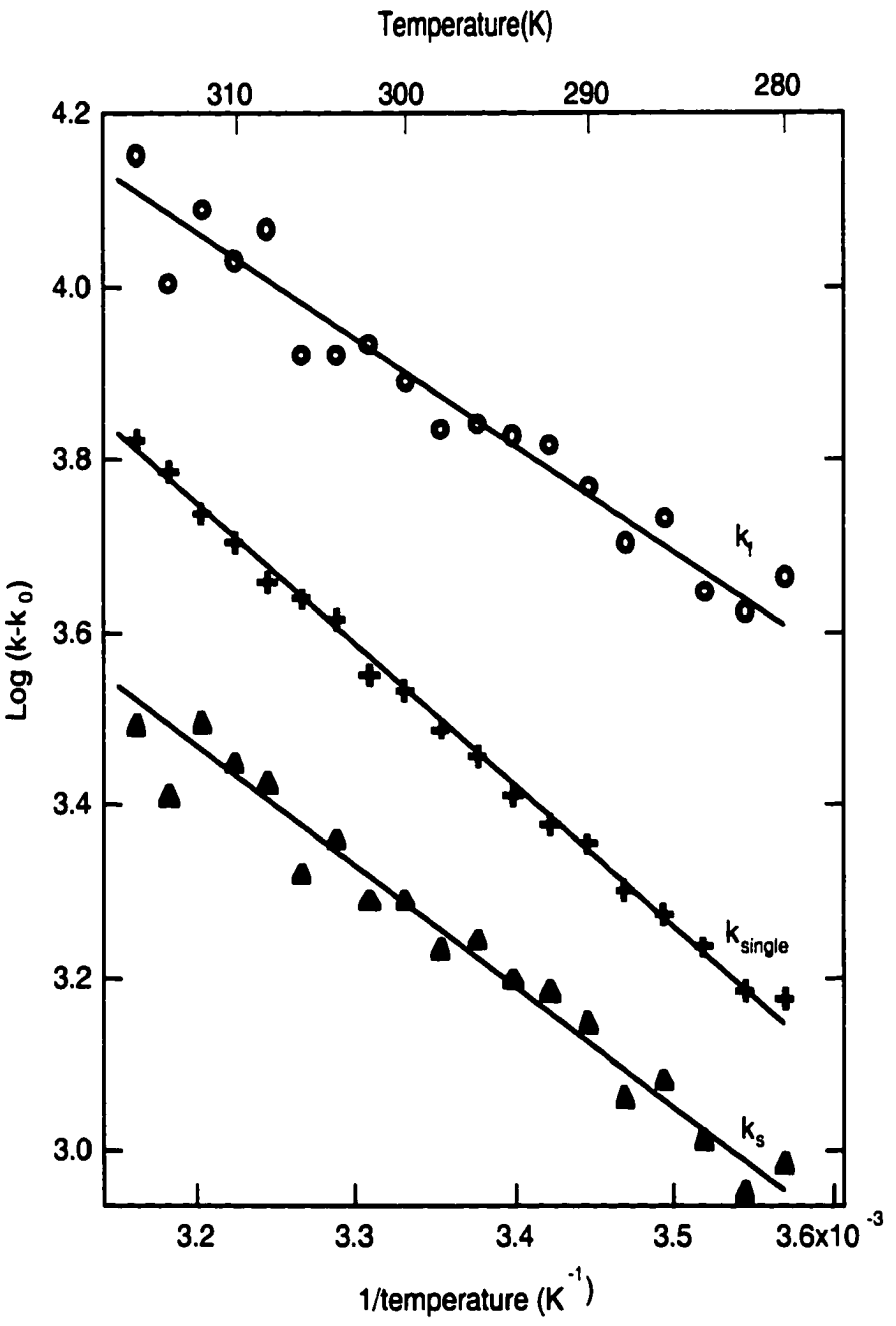

Figure 3.4. The Van't Hoff plot for the single exponential fit and for the 2 phases (k_f, k_s) of a double exponential fit of the charge recombination for 2-Me-AQ in the ambient temperature range. Fitting parameters are given in Table 3.1.

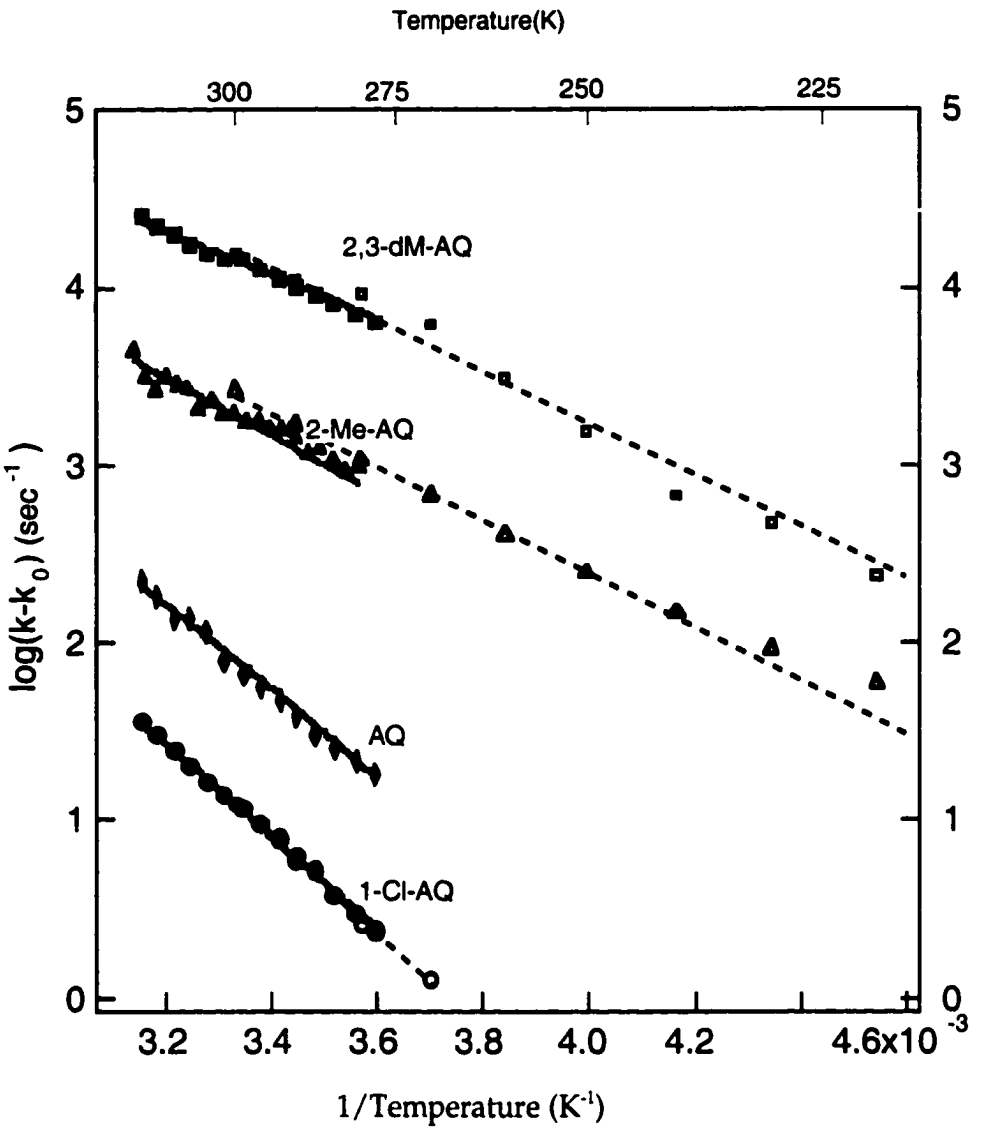

Figure 3.5. The temperature dependence of the $P^+Q_A^-$ charge recombination rates for reaction centers with four different Q_A's. The rates are obtained from single exponential fit to the kinetic data. Filled symbols represent values measured in the 210-300 K region (with 67% glycerol) and unfilled symbols represent values measured between 278 and 318 K. □,■ 2,3-dM-AQ, Δ, ▲ 2-Me-AQ, ♦, AQ, ○,●1-Cl-AQ. The lines shown are fit to equation 3.2. Fitting parameters are given in Table 3.2.

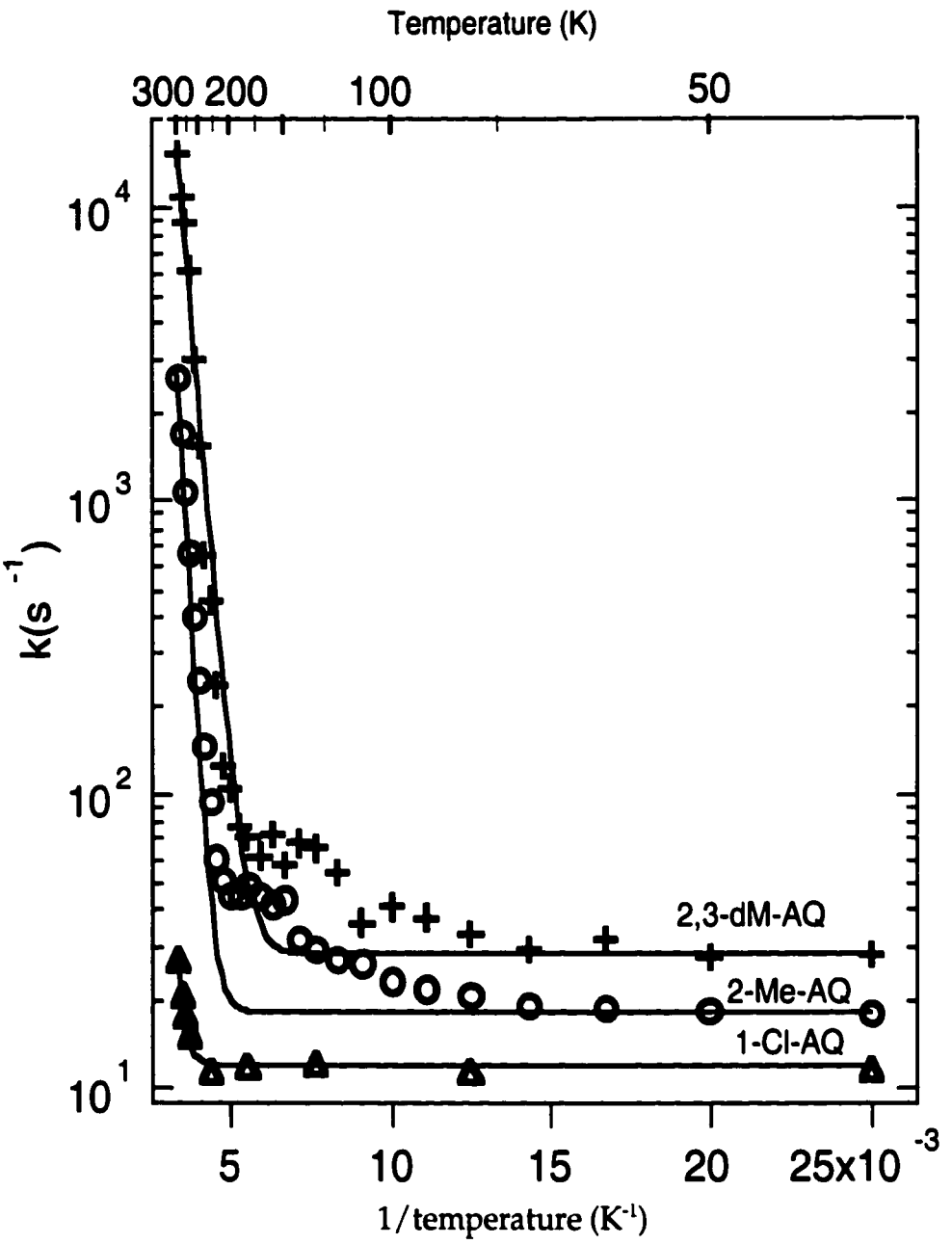

Figure 3.6. a

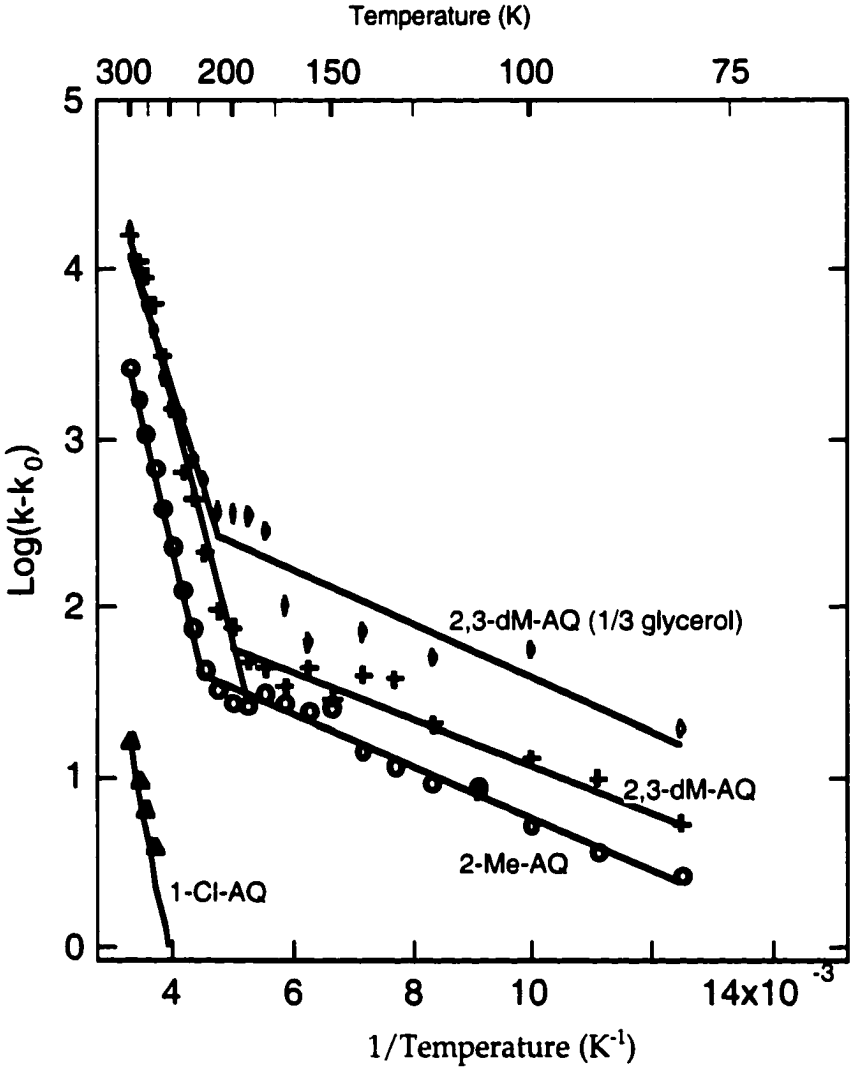

Figure 3.6. The temperature dependence of the $P^+Q_A^-$ charge recombination rate (single exponential fit) for three quinones as Q_A(40-300K). With 67% glycerol +, 2,3-dM-AQ, o,2-Me-AQ, ▲, 1-Cl-AQ; with 33% glycerol ◊, 2,3-dM-AQ (b only). Fitting parameter given in Table 3.3. (a) fit to equation 3.1. (b) Data fitted with contribution of direct tunneling pathway (k_0) subtracted and equation 3.2 fitted independently above and below transition temperature.

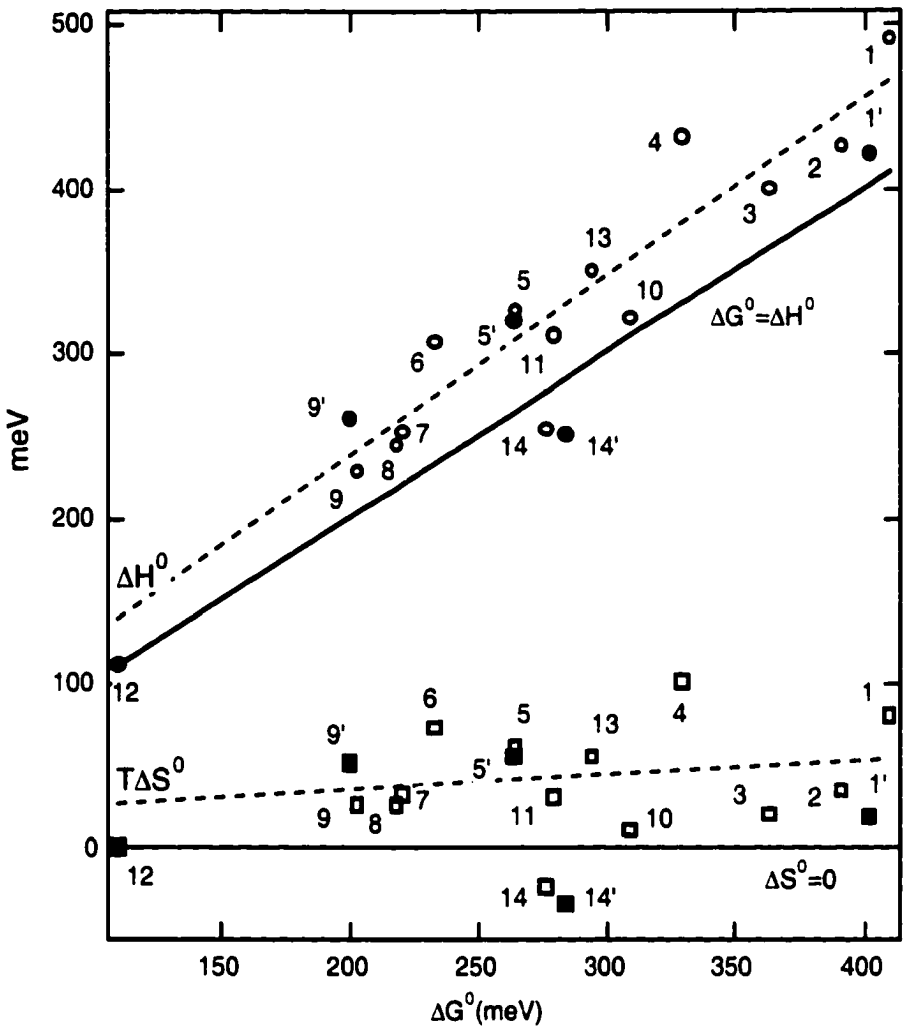

Figure 3.7. The enthalpy and entropy change vs free energy change for the reaction from $P^+Q_A^-$ to P^+H^- with eight anthraquinones and one naphthoquinone as Q_A. The lines through ΔH^0 and $T\Delta S^0$ have slopes of 1.1 and 0.1 respectively. A line where $\Delta G^0=\Delta H^0$ is also shown. Identity of each reaction center: (1-9): the data in table 3.2 measured between 278-318 K. The primed labels (1', 5', 9', and 14'): measured between 210 and 300K. (10-12): data with non-quinones substituted for Q_A from reference 26. 10: 1-nitroso-2-hydroxynaphthalene; 11: 2,4,7-trinitro-6-fluorenone; 12: 1,2,3,4-tetrafluoro-9-fluorenone. 10 and 11 are measured between 200 and 300 K; 12 is measured below 150K. 13: AQ as Q_A from reference 28. 14: *Rps. viridis* reaction centers with the native menaquinone as Q_A measured between 274 and 308 K.[23]

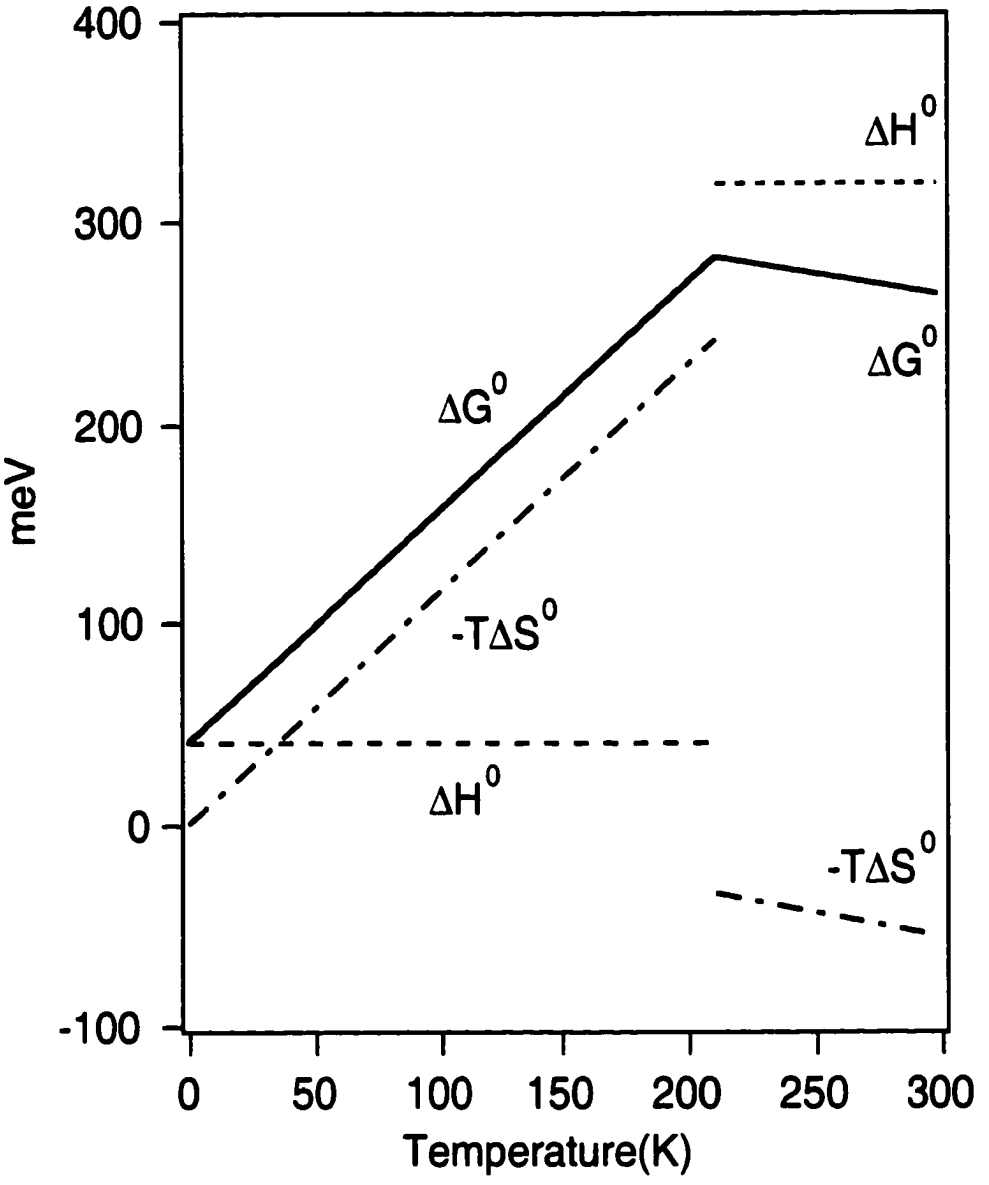

Figure 3.8. The temperature dependence of ΔG^0, ΔH^0 and $-T\Delta S^0$ from $P^+Q_A^-$ to P^+H^- in reaction centers with 2-Me-AQ as Q_A. The region below 80K is an extrapolation assuming constant values for ΔH^0 and ΔS^0.

Table 3.1. Free energy, enthalpy and entropy change from $P^+Q_A^-$ to P^+H^- in RCs with 2-Me-AQ as Q_A, using different fitting procedures.

	Rate		ΔG^0 (meV) (298K)	ΔH^0(meV)	$T\Delta S^0$(meV) (298K)
278-318 K	Single		265±7	326± 5	61± 5
	Double	Fast	240±23	240±16	0±16
		Slow	273±26	273±18	-3±19
210-300 K	Single		264±17	297±16	33±5
	Double	Fast	251±85	277±76	26±40
		Slow	280±53	305±45	25±28

Single: Charge recombination fitted with a single exponential.

Double: fast and slow phases of the two exponential analysis.

The error quoted here is the standard deviation of the fitting to the Van't Hoff plot (Temperature range 278-318 K) .

Table 3.2. Free energy, enthalpy and entropy change from $P^+Q_A^-$ to P^+H^- for RCs with nine different quinones as Q_A.

			278-318 K			210-300 K		
		k_0 (s^{-1})	ΔG^0(meV) (298 K)	ΔH^0 (meV)	$T\Delta S^0$(meV) (298 K)	ΔG^0(meV) (298 K)	ΔH^0 (meV)	$T\Delta S^0$(meV) (298 K)
1	2-Cl-AQ	12.2	410	460	50			
2	1-Cl-AQ	10.2	391	425	34	402	420	18
3	2-Am-NQ	10.0	364	400	20			
4	AQ	7.4	330	430	100			
5	2-Me-AQ	19.7	265	326	61	264	297	33
6	1-Am-AQ	6.8	234	306	72			
7	1,3-dM-AQ	20.0	221	252	31			
8	2,3-dM-AQ	27.7	219	244	25	200	282	82
9	2,7-dM-AQ	20.9	203	228	25			

The kinetics was fitted using a single exponential plus a constant. The uncertainty of the thermodynamic parameters is less than 25 meV. The values listed under 278-318 K were measured with samples in aqueous buffer (Tris pH=8) in this temperature range, while the values listed under 210-300 K were measured using 2 to 1 glycerol water mixture as the solvent.

Table 3.3. Comparison of free energy, enthalpy and entropy change from $P^+Q_A^-$ to P^+H^- above and below the transition temperature.

	ΔG^0(meV) (298 K)	ΔH^0(meV)	$T\Delta S^0$(meV) (298 K)
$P^+Q_A^- \rightarrow P^+H^-$			
2-Me-AQ[a]	264	297	33
2-Me-AQ[b]	350	30	-320
2,3-dM-AQ[a]	200	282	82
2,3-dM-AQ[b]	330	30	-300
$P^+Q_A^- \rightarrow P^*$			
2,3-dM-AQ[c]	570	360	-210

For comparison, all values are extrapolated to 298 K.

[a] Values measured in the temperature range 210-300 K

[b] Values measured in the temperature range 80-210 K, the ΔG values at 298 K are extrapolated from the measured values of ΔS and ΔH at low temperature. The operating ΔG at low temperature is much smaller (See figure 3.8).

[c] The difference between P^* and $P^+Q_A^-$ measured by photoacoustic method on the sub-microsecond time scale.[21]

Chapter 4

Trapping conformational intermediate states in the reaction center protein from photosynthetic bacteria

Abstract

In protein, conformational changes are often crucial for function but not easy to observe. Two functionally relevant conformational intermediate states of photosynthetic reaction center protein (RCs) are trapped and characterized at low temperature. RCs frozen in the dark do not allow electron transfer from the reduced primary quinone, Q_A^-, to the secondary quinone, Q_B. In contrast, RCs frozen under illumination in the product ($P^+Q_AQ_B^-$) state, with oxidized electron donor, P^+ and reduced Q_B^-, return to the ground state at cryogenic temperature in a conformation that allows a high yield of Q_B reduction. Thus, RCs frozen under illumination are found to be trapped above the ground state in a conformation that allows product formation. When the temperature is raised above 120 K, the protein relaxes to an inactive conformation which is different from the RCs frozen in the dark. The activation energy for this change is 87±8 meV, and the active and inactive states differ in energy by only 16±3 meV. Thus, there are several conformational substates along the reaction coordinate with different transition temperatures. The ground state spectrum of the RCs in active and inactive conformations report differences in the intra-protein electrostatic field demonstrating the dipole or charge distribution has changed. The electrochromic shift associated with the Q_A^- to Q_B electron transfer at low temperature was characterized. The electron transfer rate from Q_B^- to P^+ was

measured at cryogenic temperature and is similar to the rate at room temperature as expected for an exothermic, electron tunneling reaction in RCs.

Conformational flexibility is important for the function of proteins.[1,2] At room temperature, proteins fluctuate amongst many conformational states. At low temperature, protein will become trapped in harmonic motions near the conformation it was frozen into.[3-9] Intra-protein reactions are inhibited if this conformation can not access the transition state. When the temperature is raised, relaxation between conformational sub-states becomes possible. Elastic incoherent neutron scattering and x-ray crystallography measurements of bacteriorhodopsin[10] and myoglobin[4] show that different parts of the protein relax at different temperatures.[11]

Bacterial photosynthetic reaction center protein (RCs) has a number of physiological electron tunneling reactions that occur even at cryogenic temperatures. This system can therefore be used to characterize conformational sub-states of physiologically important reactions. Previous studies of RCs have characterized the protein at cryogenic temperatures. RCs can be trapped in a distribution of sub-states which exhibit a wider distribution of reaction rates.[12,13] Other studies have characterized unrelaxed product states.[14] In addition, reactions that normally do not occur at low temperatures have been observed when the protein is frozen into appropriate conformational states.[12]

The bacterial photosynthetic reaction center is the membrane protein that facilitates the conversion of light energy to chemical energy. Upon absorption of a photon, a separation of charge is achieved by a series of electron transfers between the cofactors bound to the protein. (For reviews, see Ref. 15-17) Charge separation starts with a very fast picosecond electron transfer from the primary electron donor

P, a dimer of bacteriochlorophyll, to the bacteriopheophytin in the L branch of the protein, BPh_L, followed by a slower reduction (~200 ps) of the primary quinone, Q_A. The electron is then transferred to the secondary quinone, Q_B. When no external electron donor is present, the electron returns to P^+ and the system is restored to the ground state (Fig. 4.1).

At cryogenic temperatures charge separation to form $P^+Q_A^-$ and charge recombination to regenerate the ground state occurs with rates and yields little different than found at room temperature. However, at low temperatures, the electron transfer from Q_A^- to Q_B stops, demonstrating that some activated step limits this electron transfer. Kleinfeld et al.[12] observed previously that RCs frozen under illumination in the $P^+Q_B^-$ state and then allowed to return to the ground state can support electron transfer from Q_A^- to Q_B. Thus, RCs can be trapped in an activated conformation. It is this observation that will be explored here.

The importance of conformational change in the Q_A^- to Q_B electron transfer has also been seen in kinetic studies at room temperature. Two kinetic phases can be found.[18,19] The slower ($\tau \approx 100\ \mu s$) is independent of the driving force, indicating that the electron transfer itself is not rate limiting and that the reaction is gated by some other process.[20] This is the predominate process in isolated, native RCs. The faster rate ($\tau < 10\mu s$), depends on the driving force as predicted by Marcus electron transfer theory,[21] indicating RCs can be prepared where the gate is open and the electron transfer itself determines the rate. Binding a Zn^{2+} or Cd^{2+} ion to a surface site on the RCs slows down the 100 μs phase of the Q_A^- to Q_B electron transfer. Thus ion binding impedes the rate limiting conformational change.[22,23]

High-resolution X-ray crystal structures can follow significant, heavy atom conformational changes along a reaction coordinate if an intermediate state can be trapped.[24-27] RC structures have been obtained at 2.2 and 2.6 Å resolution of the protein frozen in the dark in the ground state and under illumination in the $P^+Q_B^-$ state. Comparison reveals some structural differences even at this resolution, the most significant being that Q_B occupies a site 3.5 Å closer to Q_A in crystals frozen in the light rather than in the dark.[28] However, other processes may also contribute to the temperature dependence of Q_B reduction which could not be seen at the resolution of these structures. Experimental and computational studies suggest that proton transfer, changes in hydrogen bond patterns, and side chain reorientation need to occur for the electron transfer from Q_A^- to Q_B to be energetically favorable.[29-34]

In order to further characterize the conformational gating that controls electron transfer from Q_A^- to Q_B, RCs were trapped in an active state by freezing under illumination using methods developed by Kleinfeld et al.[12] The loss of activity in the dark adapted protein follows the temperature dependence of the rate of reduction of Q_B. The stability of the active conformation at different temperatures probes the shape of the energy landscape near the active conformation. Electrochromic shifts, that monitor changes in the electrostatic fields in the protein are compared in the ground states of light and dark adapted protein as well as in the $P^+Q_A^-$ and $P^+Q_B^-$ states at low temperature. In addition, the temperature dependence of the charge recombination reaction from $P^+Q_B^-$ to the ground state is characterized.

Materials and Methods

Engineered poly-histidine tagged, carotenoid containing, *Rb. sphaeroides* reaction centers were purified utilizing the high affinity interaction between the poly-Histidine tag and Ni-NTA (nitrilo-Tri-Acetic acid) resin.[35] Non-His-tagged carotenoid-less strain R-26 RCs was also used for comparison with previous measurements. No significant difference between the two strains was observed in the measurements reported here. The non-His-tagged protein was isolated following established procedures using lauryldimethylamine-N-oxide (LDAO) extraction and purified using ammonium sulfate and DEAE (diethylaminoethyl) chromatography.[36] The Q_B site is less than 5% occupied after either purification. Protein for Q_A reconstitution has the native ubiquinone-10, Q_A, extracted with 4% LDAO and 10 mM orthophenathroline using the method of Okamura [37] with minor modification.[38] After this treatment, the quinone content is: Q_B = 0% and $Q_A \leq 5\%$. The residual LDAO concentration from the RC stock solution is 0.025%.

Quinones added to the RCs, ubiquinone-10 (UQ10), ubiquinone-1 (UQ1) and manaquinone-4 (MQ4), were dissolved in 2% Triton X-100. The relatively insoluable UQ10 stock solution was heated for 5 seconds in a microwave oven before being added to the RCs. To reconstitute Q_A activity with MQ4, about 1.5 MQ4 per RC was added. Q_B was reconstituted with 15-20 UQ10 or UQ1 per RC.[39] RCs with MQ4 at Q_A and UQ10 at Q_B were prepared as described previously.[21]

Flash induced absorbance transients were measured with a flash spectrophotometer of local design. The sample was excited by a 2.2 joule, 10μs flash from a xenon flash lamp. A low pass filter with cutoff of 750nm (Oriel) filtered out

the shorter wavelengths. The transmitted light was detected by a Thorn EMI 9798QB photomultiplier. The electron transfer kinetics were monitored by following the difference in P and P^+ absorbance at 430nm.

Absorbance changes from 700nm to 950nm were measured with a liquid nitrogen cooled CCD detector (Princeton Instrument, LN/CCD-1024-EHRB/1). A weak, non-actinic xenon flash lamp (~0.4μS FWHM) (IBH Consultants, 5000XeF) provided the measuring light. The transmitted light was focused onto an optical fiber and into the spectrometer (Jobin-Yvon, HR460) with the CCD detector at the image plane. The absorbance was calculated by comparing the light transmitted through a buffer solution (I_0) and through the RCs after excitation I(t) at the same temperature. $A(t)=Log(I_0/I(t))$. The delay between the pump and probe flash was varied with a delay generator (Stanford Research DG535) to follow the time dependence of the reaction. As the absorbance changes are collected in the same spectral region as the exciting flash, a minimum delay of 20ms was needed to give the CCD time to remove the charges induced by the actinic flash.

The low temperature measurements were carried out in a closed cycle helium cryostat system (APD cryogenics, CSW202A) with a programmable temperature controller. The temperature resolution is 0.1K and controllability is ±0.4K.

For low temperature experiments, RCs in Tris buffer were mixed with two volumes of glycerol. The final RC concentration was 3-4 μM for single wavelength kinetics measurements and 30 μM for time resolved spectral measurements. The optical cell has a light path of 1 mm. The actinic and measuring light were perpendicular to each other with an incident angle of 45 degrees at the sample.

Two different methods were used to trap the protein in the light induced $P^+Q_B^-$ conformation. Following the method used by Kleinfeld et al.,[12] the sample was plunged into liquid nitrogen for about three seconds while under illumination, then transferred to the cryostat at 40 K. The sample was dark adapted for 30 minutes at 40 K to let the RCs reform the ground state, then brought to the measurement temperature. Helium gas was blown through the chamber when frozen samples were placed in the pre-cooled system. The cryostat temperature was found to increase by 40 K or less and then return to the set temperature in about three minutes. The protein was also trapped by cooling the sample slowly (at ≈5 K/minute) under a 75W continuous Xenon light or with actinic flashes repeated at 1HZ. A 675nm low pass filter (Corion) was used in either case.

When RCs are activated at any temperature with an actinic flash $P^+Q_A^-$ is formed. This can either yield $P^+Q_B^-$ by electron transfer from Q_A^- to Q_B (k_{AB}) or return to the ground state at k_{AP} (Fig. 4.1). The quantum efficiency of $P^+Q_B^-$ formation reflects the competition between these two steps. In dark adapted samples k_{AB} slows with temperature so that the rate can be estimated from the quantum efficiency, ϕ, of $P^+Q_B^-$ formed from $P^+Q_A^-$, where ϕ is:

$$\phi = \frac{k_{AB}}{k_{AB} + k_{AP}} = \frac{[P^+Q_B^-]_{t=0}}{[P^+Q_A^-]_{t=0} + [P^+Q_B^-]_{t=0}} \qquad (4.1)$$

Over the temperature range when k_{AB} and k_{AP} are comparable, ϕ differs from zero and 1.0, and Eqn. 4.1 can be used to derive k_{AB}. ϕ for $P^+Q_B^-$ formation is the fraction of excited RCs that form $P^+Q_B^-$. This can be readily determined from the kinetics of reduction of P^+ which occurs at very different rates from the $P^+Q_A^-$ and $P^+Q_B^-$ states. The rate k_{AP} has been well characterized, increasing from 9 s^{-1} to 37 s^{-1} as the

temperature is lowered from room temperature to 5 K.[12,13,40] In contrast, once formed $P^+Q_B^-$ returns to the ground state at rates between 1 and 0.02 s^{-1}.

The use of ϕ to determine k_{AB} can be tested by exciting a sample when most of the $P^+Q_A^-$ RCs have returned to the ground state, but the $P^+Q_B^-$ RCs have not. The second flash reforms $P^+Q_A^-$ of which a fraction ϕ should generate additional $P^+Q_B^-$. The yield of $P^+Q_B^-$ should be the same on each flash if the competition between k_{AB} and k_{AP} is the sole cause of the low $P^+Q_B^-$ yield. Here caution must be taken to correct for the incomplete saturation of the actinic light so that not all RCs form $P^+Q_A^-$ in a single flash and also for the portion of the RCs without bound Q_B.

When the temperature of light-adapted RCs is raised above 120 K, the trapped conformation which can form $P^+Q_B^-$ relaxes so that only the faster decaying $P^+Q_A^-$ RCs are seen after a flash. The relaxation rate was measured at different temperatures. Starting at 40K it takes ≈15 minutes to reach 200 K. The time at which the temperature reading reaches the set value is used as time zero. The position of the temperature and optical measurements are separated by about 0.5 cm.

For measurements at constant temperature, 5-10 flashes approximately 20 minutes apart were averaged. No averaging was carried out for the measurement of the relaxation processes in the 120-200 K temperature region.

The $P^+Q_B^-$ charge recombination kinetics were analyzed by two exponential decays plus a constant using a nonlinear least square fitting program of Levenberg-Marquardt algorithm (Igor Pro from WaveMetrics). The constant is 10% or less of the total amplitude. A more general distributed rate model can also be used to analyze this type of kinetics[41] where:

$$\Delta A(t) = \Delta A(0)\int_0^\infty D(k)e^{-kt}d\log k \qquad (4.2)$$

D(k) is the distribution of rates on the log(k) scale. This Laplace transformation can be inverted numerically using Tikhonov-Miller regularization method.[42]

Results

RCs trapped in the dark-adapted conformation. At low temperature, flash excitation yields $P^+Q_A^-$ in essentially 100% of the RCs.[43] $P^+Q_A^-$ returns to the ground state at ~9 s^{-1} (k_{AP}). When the electron is transferred to Q_B charge recombination slows to <1 s^{-1} at room temperature and becomes even slower at lower temperature (see below). Thus, it is possible to differentiate between RCs in $P^+Q_A^-$ and $P^+Q_B^-$ states by monitoring the rate at which the P^+ formed on a flash is rereduced to P at 430 or 890 nm. As the temperature is lowered, the slow component of charge recombination is lost (Fig. 4.2).[44] In native RCs at pH 8.0 (67% glycerol), the quantum yield of $P^+Q_B^-$ (ϕ) is 50% at ~225 K. At this temperature $k_{AB} = k_{AP} \approx 10\ s^{-1}$.

An estimate of the activation energy of 8±1 Kcal/mol for k_{AB} can be derived from the temperature dependence of quantum efficiency (Fig. 4.2). Equation 4.1 is used to estimate k_{AB} from ϕ for $P^+Q_B^-$ formation. Between 250K and 180 K electron transfer from Q_A^- to Q_B (k_{AB}) slows to where it can no longer compete with k_{AP} ($k_{AB} >> k_{AP}$ ($\phi \approx 1$) to $k_{AB} << k_{AP}$ ($\phi << 1$)) (Fig. 4.2).[12,45] Eqn. 4.1 makes the simplification that the electron transfer from Q_A^- to Q_B happens at a single exponential rate. Direct measurement indicates that the Q_A^- to Q_B kinetics become more inhomogeneous when temperature is lowered.[18] Therefore, the rate obtained from equation 4.1

represents a weighed average and the derived activation energy is a rough estimate of the true value. Given a single enthalpy barrier, the error will be small if the energy distribution of RCs is much smaller than the activation energy itself.

RCs trapped in light-adapted conformations. When RCs are frozen under illumination, 3 populations are seen after dark adaption. The near-IR spectrum shows a loss of the 890nm P absorbance indicating that some RCs are trapped in an inactive state where P^+ is remains oxidized (Fig. 4.3). At 110K, no change in this spectrum is observed in 24 hours. This inactive fraction has been seen previously [45] and may represent RCs frozen in a $P^+Q_AQ_B$ state where the quinone has been oxidized by adventitious mediators.[12] Generally, the stronger the illumination during freezing, the more RCs are trapped. The protein is not permanently damaged as it regains activity when thawed. This population will not be discussed further.

Under conditions used here more than 80% of the protein which is frozen in a charge separated state returns to the ground state after 30 minutes at low temperature. After an actinic flash two kinetic components are now seen for P^+ rereduction. Approximately, ten percent of the RCs lack Q_B. These form only the $P^+Q_A^-$ state, which decays back to the ground state at the characteristic 37 s^{-1} (40 K) after a flash. In a given sample, the fraction of RCs without Q_B at low temperature is unchanged, within 10% of that found at room temperature.

As has been seen previously,[12] RCs with bound Q_B frozen under illumination adopt a ground state conformation that supports electron transfer from Q_A^- to Q_B. In these RCs the P^+ formed by an actinic flash decays back to the ground state in tens of seconds (Fig. 4.4A). In contrast, the absorbance change decays to zero in less than a second in RCs frozen in the dark. (Fig. 4.4B) The quantum efficiency, ϕ, of the

electron transfer, determined with the multiple flash method, is greater than 98% in the light-adapted RCs at 40 K. Given the known k_{AP} value of about 10 s^{-1} in the light-adapted RCs at 40 K,[12] k_{AB} in the active conformation must be faster than ~$10^3 s^{-1}$ (Eqn. 4.1). The spectral changes associated with the slow phase are consistent with those expected for $P^+Q_B^-$ returning to the ground state.

The double difference spectrum ($\Delta\Delta A$) of the flash absorption change in RCs frozen under illumination (ΔA_L) and in the dark (ΔA_D) is $\Delta\Delta A=\Delta A_L-n\Delta A_D$ (Fig. 4.5). This difference between the [$P^+Q_B^-$ - ground state spectrum] (ΔA_L) and the [$P^+Q_A^-$ - ground state spectrum] (ΔA_D) provides the spectral difference between RCs with Q_B^- and Q_A^-. The normalization factor, n, matches the absorbance change in the 2 samples at 890nm. This corrects for the activity lost in the light adapted samples as well as for the decay of the P^+ signal during the 20ms between the actinic and measuring flashes. The latter is a small factor in the $P^+Q_B^-$ RCs, but more significant in the $P^+Q_A^-$ RCs.

The near-IR spectra of RCs is dominated by the absorbance bands of the bacteriochlorophyll dimer (P), monomers (B_L and B_M), and bacteriopheophytins (H_L and H_M) (see Fig. 4.3). The features of the double difference spectrum, where the changes at P are subtracted out, show band shifts which result from changes in the electric field at each chromophore. The spectrum qualitatively agrees with the Q_B^--Q_A^- spectrum at room temperature.[18] However, because the absorption bands are much narrower at 40 K, more features are seen. From previous assignments of the absorption peaks for each species,[46,47] the major features in the spectrum can be tentatively assigned (Fig. 4.3 and Fig. 4.5). The difference spectrum shows a ≈15 cm^{-1}

blue shift of $BChl_M$ and BPh_L, and a comparable red shift for $BChl_L$ and BPh_M. From the orientation of the four chromophores, this indicates an increase of the field intensity at $BChl_M$ and BPh_M, and decrease at $BChl_L$ and BPh_L. These shifts are consistent with the negative charge moving from Q_A to Q_B, reducing the distance to the M side cofactors and increasing it to the L side cofactors. The broad feature near 900 nm indicates some absorption change on the red side of P^+. This could represent either some relaxation process near P, or a difference between its long range electrostatic interaction with Q_A^- and Q_B^-.

Some changes must be trapped in the RCs frozen in the light to allow electron transfer from Q_A^- to Q_B. The difference between the ground state spectrum of RCs frozen in the light and the dark was measured to see if the electrostatic fields throughout the protein are different (Fig. 4.3). One complication here is that the population of RCs trapped in the inactive P^+ state also contributes to this difference spectrum. But as mentioned previously, the percentage of the RCs trapped in the inactive P^+ state can be varied by changing the illumination conditions. By comparing spectra with different percentage of the two species, the spectrum of the trapped RCs and the difference of the ground states for the light and dark adapted ground state spectra (Fig. 4.3) can be separated.

Although the signal to noise ratio is not ideal, there appears to be an electrochromic shift of the bacteriopheophytin (BPh) and monomer bacteriochlorophyll (BChl) bands when RCs are frozen in the light. The electrochromic shift of the bacteriopheophytin (BPh) and monomer bacteriochlorophyll (BChl) bands is caused by a change in the electrical field at the chromophores, i.e. a Stark shift. These shifts have been analyzed in detail for the

$P^+Q_A^-$ charge separation.[47] The shift caused by freezing RCs in the light is in the opposite direction from that induced by the $P^+Q_A^-$ or $P^+Q_B^-$ charge separation, indicating a difference in the electric field at the chromophores which is opposite to that induced by the $P^+Q_A^-$ or $P^+Q_B^-$ charge separation. The extra field's projection on the transition dipole of BPh or BChl can be estimated from the magnitude of the shift, which is proportional to the height of the difference signal when the shift is small comparing to the width of the peak. The change in the field projection is about 20% of that found for the $P^+Q_A^-$ or $P^+Q_B^-$ charge separated states.

$P^+Q_B^-$ charge recombination kinetics. In light-adapted RCs, the $P^+Q_B^-$ charge recombination kinetics can be examined in detail at low temperature for the first time. The rate of this reaction was measured at 430nm, monitoring the change of the P absorbance (Fig. 4.6). At 40 K the kinetics can be fit with two exponentials at 0.21 s^{-1} and 0.025 s^{-1} and a constant which is less than 10% of the total amplitude. Since the two rates differ by more than ten fold, they can be easily separated in the kinetic analysis (Fig. 4.6A).

The kinetics were also analyzed with a distributed rate model as Eqn. 4.2 (Fig. 4.6B). The distribution has rates centered around the same two values obtained in the 2 exponential fit. There may be a slightly broader distribution of the faster rate (data not shown). However, Fig. 4.6 shows that the residuals with the simpler, 2 exponential fit is comparable to that found with a distribution of exponential decays. Both charge recombination rates show little temperature dependence from 40 K to 110 K. (Fig. 4.7A). However, the fraction of the reaction at the faster rate decreases from 44% to 30% as the temperature is raised (Fig. 4.7B).

Since the light induced product state has a long lifetime, one practical concern is whether the weak measuring light will cause some RCs to be trapped in the product state, distorting the measured kinetics. To assess the contribution of the measuring light, its intensity was varied by 10 fold around the value normally used, from approximately 10^{11} to 10^{12} quanta/second. The charge recombination kinetics were independent of the measuring light intensity (data not shown) .

There are 2 pathways for charge recombination in $P^+Q_B^-$ RCs. One is by electron tunneling from Q_B^- to P^+. However, at room temperature, $P^+Q_B^-$ charge recombination proceeds predominantly via $P^+Q_A^-$ as an intermediate.[44,48] The rate is therefore dependent on a pre-equilibrium between the $P^+Q_A^-$ and $P^+Q_B^-$ so is sensitive to the energy level of Q_A^-.[21,49] The $P^+Q_B^-$ charge recombination rate was measured at 40 K in RCs with MQ4 rather than UQ10 as Q_A. Q_B is still UQ10. The free energy of the $P^+Q_A^-$ state with MQ4 is 30meV higher than with UQ10. If charge recombination depends on the thermal equilibration of the $P^+Q_A^-$ and $P^+Q_B^-$ as it does at room temperature, the rate would be expected to slow by more than 1000 fold at 40 K. However, the measured rate is independent of the energy of the $P^+Q_A^-$ state (Fig. 4.7). Thus, the contribution of this indirect route to the $P^+Q_B^-$ charge recombination is negligible and the reaction proceeds at a Q_A independent process via direct tunneling from Q_B^- to P^+.

Relaxation of the active, light-adapted conformation. Light-adapted RCs remain capable of forming $P^+Q_B^-$ on a flash for at least 24 hours at temperatures below 70K. However, when the temperature is then raised, the protein begins to relax to an

inactive conformation. There is no loss in the initial charge separation reaction since the amount of P^+ formed remains almost unchanged (Fig. 4.8). However, with time the amplitude of the slow, $P^+Q_B^-$, charge recombination decreases and that of the fast, $P^+Q_A^-$, component increases. The kinetics of $P^+Q_B^-$ charge recombination can be fitted with a two exponential decay with similar rates as at lower temperature. Fig. 4.8 shows that the percentage of the slower kinetic phase seems smaller than expected at early times. This might be caused by difference in the relaxation rate of the two substates of the active conformation. The relaxation rate becomes faster as the temperature is raised (Fig 4.9). The Van't Hoff plot of log(k) versus 1/temperature indicates the activation energy for inactivation is 87±8 meV. (Fig. 4.10)

As the RCs frozen in the light are allowed to come to equilibrium at temperatures between 120 and 200K, some $P^+Q_B^-$ activity remains even after 24 hours. Thus, at these temperatures an equilibrium is set up between an active and inactive conformations. As the temperature is raised the active fraction is larger. The multi-flash method shows the fractional activity does not represent a homogeneous population of RCs with a quantum yield less than 1, since a second actinic flash 1 s after the first yields no additional $P^+Q_B^-$. Rather, the system relaxes into a slowly equilibrating mixture of active and inactive ground state conformations.

The equilibrium constants derived from the ratio of the active and inactive conformations between 160 to 200 K yield a free energy difference of 16±3 meV. At 120 K and 140 K the free energy difference is smaller (4 meV and 8 meV) respectively. This may be caused by an overestimate of the active conformation

because the very slow reaction does not reach equilibrium at these temperatures. The RCs frozen in dark show no Q_B activity in this temperature range. Thus this relaxed conformation represents a previously unobserved intermediate state different from both the dark-adapted and active light-adapted conformations.

The most obvious conformational change between the RCs frozen in the dark and light in the crystallographic study is the position of the quinone.[28] Therefore the quinone movement is suggested to be the rate limiting conformational change. To check whether quinone movement is involved in the relaxation of the active conformation between 120-200 K, UQ1, which has a much shorter isoprene tail, was also used as Q_B. A much faster relaxation rate might be expected if rotation of the bulky tail limits the movement of the native quinone. Instead, similar relaxation rates were observed with UQ1 or UQ10 as Q_B.

Discussion

When reaction centers (RC) are frozen in dark, the yield of electron transfer from Q_A^- to Q_B diminishes with temperature so that almost no reaction is seen below 200 K. In contrast, in RCs frozen under illumination the reaction proceeds with high yield even at 50 K.[12] Thus, RCs frozen in the $P^+Q_B^-$ state must retain some conformational changes at low temperature so they return to the ground state in an altered conformation that now supports rereduction of Q_B. Below 70 K the dark and light adapted structures remain trapped for days. Between 120 and 200 K the active conformation relaxes into a nearby inactive state. There is an 87 meV activation energy for this relaxation. Active and inactive RCs remain in equilibrium

in this temperature range. In contrast, in protein frozen in the dark there is no activity at these temperatures. The relationship between the active and two inactive conformation are summarized in Fig. 4.11.

The charge recombination rate in the light conformation is consistent with direct electron transfer from Q_B^- to P^+.

The earliest observation that RCs could be frozen into an active conformation was made by Kleinfeld et al.[12] The general results reported here are in good agreement with that earlier study. The one significant difference in the observations is that $P^+Q_B^-$ returns to the ground state here much faster than previously reported, and at a rate that is temperature independent. The reason for the discrepancy is not clear, but the result presented here seems to be more consistent with that found for other electron tunneling processes in RCs at low temperature.

At room temperature, charge recombination in $P^+Q_B^-$ RCs proceeds at ~1 s^{-1} predominantly via the intermediate state of $P^+Q_A^-$. The direct electron transfer from Q_B^- to P^+ is much slower. The latter mechanism only becomes important when the free energy of either Q_A or Q_B is altered by quinone replacement[34,50,51] or by mutation[34,49,52] to make electron transfer via the indirect route slower than the direct route. The direct electron transfer from Q_B^- to P^+ occurs at 0.12-0.19 s^{-1} at room temperature.[34,50-52] Charge recombination in $P^+Q_B^-$ RCs in the light-adapted conformation at cryogenic temperature shows two phases at 0.2 s^{-1} and 0.02 s^{-1} with comparable amplitudes. The faster rate is similar to that seen at room temperature. At low temperature the conversion between the two states producing the two rates

is much slower than charge recombination. If the equilibration becomes faster at room temperature, the observed rate would be close to that of the faster component. Therefore the rate of electron tunneling from Q_B^- to P^+ appears to be essentially temperature independent.

This measurement of the direct tunneling along the M branch of the RCs from Q_B^- to P^+ at cryogenic temperature can be compared with the well characterized charge recombination along the L branch of the protein from Q_A^- to P^+. Both processes are somewhat biphasic, although the difference in rates is larger for the electron transfer from Q_B^- to P^+ than from Q_A^-.[14,53-55] In RCs frozen in the light in the absence of Q_B, Q_A^- to P^+ electron transfer is better analyzed by a distribution of exponentials than by one or two exponentials.[12,13] In contrast, in light-adapted RCs the Q_B^- to P^+ reaction remains well characterized by 2 exponentials (Fig. 4.6A).

The Q_B^- to P^+ reaction is independent of temperature below 110 K and the low temperature rate is comparable to that found at room temperature. This is again similar to that found with the Q_A^- to P^+ electron transfer. In RCs frozen under illumination, the $P^+Q_A^-$ charge recombination rate is almost the same at room and low temperature.[12,13] In RCs frozen in dark, the $P^+Q_A^-$ charge recombination rate is approximately 4 fold slower at room temperature than at low temperature, with much of the change occurring between 180 and 250 K.

The free energy dependence of the Q_A^- to P^+ electron transfer reaction has been shown to shift as the system is cooled from room temperature to cryogenic temperature.[56] Part of this comes from $P^+Q_A^-$ being trapped in a higher energy conformation at low temperature.[14] In addition, the reaction reorganization energy is diminished at low temperature because large protein changes become

inaccessible.[57] The reorganization energy of the Q_B^- to P^+ electron transfer is larger than found for Q_A^- to P^+ at room temperature.[51] The method described here should make it possible to monitor the free energy dependence of the electron transfer from Q_B^- at low temperature to more fully characterize this reaction. A smaller value for the reorganization energy would be expected in the light-adapted samples at low temperatures because smaller changes are needed in the light trapped conformation.

The temperature dependence of the electron transfer rate from Q_A^- to Q_B.

The electron transfer from Q_A^- to Q_B is measured to be 10^4 s^{-1} at room temperature in native RCs.[18,48,58-60] The driving force for this reaction can be modified by replacing the native ubiquinone Q_A with other low potential quinones. The rate is independent of driving force and so it appears to be limited by a conformational gating step rather than the electron transfer itself.[20,21] The rate of this conformational change decreases with temperature in dark adapted RCs, indicating that this is an activated process (Fig. 4.11). The loss of quantum yield shows the rate decrease to less than 1 s^{-1} below 200 K. In contrast, the estimated rate of Q_A^- to Q_B electron transfer is faster than 10^3 s^{-1} at 40 K in RCs frozen under illumination so the rate limiting conformational gate appears to be trapped in the open position in RCs frozen in the light.

In RCs with low potential Q_As, a faster phase (>10^5 s^{-1}) was observed for the Q_A^- to Q_B electron transfer. This rate is free energy dependent and so monitors the electron transfer itself not a conformational change.[19] Since the Q_A^- to Q_B electron transfer in RCs frozen in light is likely to be direct electron transfer, it's more appropriate to compare this rate with the fast phase observed at room temperature.

The rate has an activation energy of 3.8 Kcal/mol (2-25 °C).[18,19] If temperature is lowered further, this quantum tunneling rate would be predicted to become relatively temperature independent.[61,62] The lack of temperature dependence of the quantum yield in the light adapted RCs is consistent with a very small activation energy for the reaction.

The electrochromic shifts associated with the Q_A^- to Q_B electron transfer and with the trapped conformational changes.

The electrochromic Stark shifts in the cofactor absorbance bands are caused by changes in the electric field at the cofactor. For Q_A^- to Q_B electron transfer, this is caused by a change in the distance between the negative charge and the cofactors. Part of the shift may also come from the difference in the dielectric screening on the L and M sides of the protein.[47]

The electrochromic shifts associated with the Q_A^- to Q_B electron transfer at cryogenic temperature are qualitatively consistent with the kinetically measured difference spectrum at room temperature.[18] But because the absorption peaks are narrower at low temperature the resolution is significantly improved. In addition the spectrum measured at room temperature will contain contributions from the gating conformational changes and from relaxation after the electron transfer. In contrast, significant conformation changes will already be frozen into the ground state so will not be seen in the kinetic difference spectrum and much less relaxation would be expected at cryogenic temperature.

An electrochromic shift associated with the conformational change at low temperature can be observed in the spectrum of the ground state of the RCs frozen

in the light and in the dark (Fig. 4.3). The observed shift shows a change in the electric field at the chromophores opposite to the direction of the field produced by the negative charge in $P^+Q_A^-$ or $P^+Q_B^-$ in the active, trapped RC conformation. This more positive field could come from proton uptake, internal proton movement or other dielectric response of residues. These changes would help stabilize the Q_B^- state and make the electron transfer from Q_A^- to Q_B energetically more favorable. These changes are trapped in the light adapted RCs and should aid and may be required for the electron transfer from Q_A^- to Q_B.

Relaxation processes in frozen RCs.

The RCs trapped in the Q_B active conformation can relax slowly to an inactive conformation at temperatures above 120 K. The relaxation in the temperature region 120-200 K results in a slow equilibration between the active and a new inactive state. This relaxed, inactive state is distinct from the dark frozen state as the latter never accesses the active conformation. Thus, only part of the trapped conformational changes can be annealed out in this temperature region. The energy barrier and free energy difference between active and inactive states are quite small.Possible sources of relaxation to this inactive conformation include quinone movement, internal proton shift or more general dielectric response of residues nearby. The underlying conformational change makes the formation of $P^+Q_B^-$ energetically unfavorable or very slow.[29,33,34] The similar relaxation rates of RCs with UQ1 and UQ10 as Q_B suggest that quinone movement is unlikely to be the cause of this relaxation.

Quinone translocation between binding sites might be expected to have a higher activation energy and so would freeze out at higher temperature.

Other conformationally unrelaxed states have been previously characterized in RCs. When RCs are frozen under illumination in the absence of Q_B, the protein is also found to be trapped in a light adapted state, which is indicated by the slower and more distributed $P^+Q_A^-$ charge recombination rate.[12,13] As the RCs are warmed up slowly (> 10^3 s), an incomplete relaxation from the light adapted to the dark adapted conformation is observed in the 120-200 K temperature region.[12,13] This is the same temperature for relaxation to the partially inactive conformation found here. In addition, the RCs are found to be trapped in an unrelaxed conformation of the product state, $P^+Q_A^-$ below 200 K for the ms lifetime of this state.[14] The unrelaxed initial product state is at a energy level 200 meV higher (extrapolated to 0 K) than found for the room temperature relaxed state.

Implication for protein dynamics.

Motions in proteins are often critical for their biological function. The protein energy landscape can be described as a rugged hyperspace with many local minima corresponding to different conformational substates. At room temperature, proteins can fluctuate between substates. But at low temperature, the system is confined to harmonic oscillations near the conformation that it is frozen into.

Here RCs have been shown to be trapped into active or inactive conformational substates depending on the freezing procedure. The partial relaxation of the active conformation into a previously unobserved inactive

conformation shows substates with different enthalpy barriers near the active conformation. At 120-200 K, the protein is able to overcome only the lower tier of barriers in the light-adapted sample. This transition is to a state separated by only 16 meV from the active light-adapted protein. This would appear to represent a local change in the protein with its own transition temperature. From elastic incoherent neutron scattering and X-ray crystallography study of bacteriorhodopsin and myoglobin, the relation between the magnitude of fluctuation and temperature shows that different regions of the protein can have different glass transition temperature with tiers of barriers having different heights.[10,11] RCs now provide another example for this type of hierarchical organization of energy barriers.

Other conformational changes in RCs caused by freezing under illumination have been previously explored.[12,29,63-65] The original studies of the Q_A^- to Q_B electron transfer by Kleinfeld et al. suggested a key role for proton binding in the trapped active conformation.[12] Measurement of the pH buffering capacity of dark and light adapted RCs at room temperature shows four independent protonable groups may be involved, with their relative importance changing with pH.[64] Theoretical calculations suggest that proton transfer between 2 acidic residues in the Q_B pocket are required for electron transfer from Q_A^- to Q_B.[29] Recent theoretical calculations have highlighted the role of protein dynamics in promoting the electron transfer.[65] The measurements presented here show that even very small changes can transform RCs from active to inactive conformations, and factors in addition to quinone movement are important. Changes in RC spectra suggest active and inactive conformers differ in the intra-protein electrostatic potentials. Future studies, determining the temperature dependence of inactivation of both dark and light

adapted RCs as a function of pH and other parameters may provide a more detailed atomic picture of the energy surface between reactant and product for this reaction.

References:

(1) Frauenfelder, H.; Sligar, S. G.; Wolynes, P. G. *Science* **1991**, *254*, 1598-1603.

(2) Zaccai, G. *Science* **2000**, *288*, 1604-7.

(3) Parak, F.; Knapp, E. W.; Kucheida, D. *J Mol Biol* **1982**, *161*, 177-94.

(4) Doster, W.; Cusack, S.; Petry, W. *Nature* **1989**, *337*, 754-756.

(5) Loncharich, R. J.; Brooks, B. R. *J Mol Biol* **1990**, *215*, 439-55.

(6) Di Pace, A.; Cupane, A.; Leone, M.; Vitrano, E.; Cordone, L. *Biophys J.* **1992**, *63*, 475-484.

(7) Ferrand, M.; Dianoux, A. J.; Petry, W.; Zaccai, G. *Proc Natl Acad Sci U S A* **1993**, *90*, 9668-72.

(8) Andreani, C.; Filabozzi, A.; Menzinger, F.; Desideri, A.; Deriu, A.; Di Cola, D. *Biophys. J.* **1995**, *68*, 2519-2523.

(9) Vitcup, D.; Ringe, D.; Petsko, G. A.; Karplus, M. *Nature structural biology* **2000**, *7*, 34-38.

(10) Reat, V.; Patzelt, H.; Ferrand, M.; Pfister, C.; Oesterhelt, D.; Zaccai, G. *Proc Natl Acad Sci U S A* **1998**, *95*, 4970-5.

(11) Frauenfelder, H.; McMahon, B. *Proc Natl Acad Sci U S A* **1998**, *95*, 4795-7.

(12) Kleinfeld, D.; Okamura, M. Y.; Feher, G. *Biochemistry* **1984**, *23*, 5780-5786.

(13) McMahon, B. H.; Muller, J. D.; Wraight, C. A.; Nienhaus, G. U. *Biophysical Journal* **1998**, *74*, 2567-2587.

(14) Xu, Q.; Gunner, M. R. *J.Phys.Chem. B* **2000**, *104*, 8035-8043.

(15) Feher, G.; Allen, J. P.; Okamura, M. Y.; Rees, D. C. *Nature* **1989**, *339*, 111-116.

(16) Gunner, M. R. *Current Topics in Bioenergetics* **1991**, *16*, 319-367.

(17) Blankenship, R. E.; Madigan, M. T.; Bauer, C. E. *Anoxygenic Photosynthetic Bacteria*; Kluwer Academic Publishers:, 1995; Vol. 2.

(18) Tiede, D. M.; Vazquez, J.; Cordova, J.; Marone, A. P. *Biochemistry* **1996**, *35*, 10763-10775.

(19) Li, J.; Gilroy, D.; Tiede, D. M.; Gunner, M. R. *Biochemistry* **1998**, *37*, 2818-2829.

(20) Graige, M. S.; Feher, G.; Okamura, M. Y. *Proc. Natl. Acad. Sci. USA* **1998**, *95*, 11679-11684.

(21) Li, J.; Takahashi, E.; Gunner, M. R. *Biochemistry* **2000**, *39*, 7445-7454.

(22) Utschig, L. M.; Ohigashi, Y.; Thurnauer, M. C.; Tiede, D. M. *Biochemistry* **1998**, *37*, 8278-8281.

(23) Paddock, M. L.; Graige, M. S.; Feher, G.; Okamura, M. Y. *Proc. Natl. Acad. Sci. USA* **1999**, *96*, 6183-6188.

(24) Schlichting, I.; Berendzen, J.; Chu, K.; Stock, A. M.; Maves, S. A.; Benson, D. E.; Sweet, R. M.; Ringe, D.; Petsko, G. A.; Sligar, S. G. *Science* **2000**, *287*, 1615-22.

(25) Edman, K.; Nollert, P.; Royant, A.; Belrhali, H.; Pebay-Peyroula, E.; Hajdu, J.; Neutze, R.; Landau, E. M. *Nature* **1999**, *401*, 822-6.

(26) Luecke, H.; Schobert, B.; Richter, H. T.; Cartailler, J. P.; Lanyi, J. K. *Science* **1999**, *286*, 255-261.

(27) Genick, U. K.; Borgstahl, G. E. O.; Ng, K.; Ren, Z.; Pradervand, C.; Burke, P. M.; Srajer, V.; Teng, T.; Schildkamp, W.; McRee, D. E.; Moffat, K.; Getzoff, E. D. *Science* **1997**, *275*, 1471-1475.

(28) Stowell, M. H. B.; McPhillips, T. M.; Rees, D. C.; Soltis, S. M.; Abresch, E.; Feher, G. *Science* **1997**, *276*, 812-816.

(29) Alexov, E.; Gunner, M. *Biochemistry* **1999**, *38*, 8253-8270.

(30) Grafton, A. K.; Wheeler, R. A. *J. Phys. Chem* **1999**, *103*, 5380-5387.

(31) Alexov, E.; Miksovska, J.; Baciou, L.; Schifer, M.; Hanson, D.; Sebban, P.; Gunner, M. R. *Biochemistry* **2000**, *39*, 5940-5952.

(32) Beroza, P.; Fredkin, D. R.; Okamura, M. Y.; Feher, R. *Biophys. J.* **1995**, *68*, 2233-2250.

(33) Paddock, M. L.; Rongey, S. H.; Feher, G.; Okamura, M. Y. *Proc. Natl. Acad. Sci. USA* **1989**, *86*, 6602-6606.

(34) Takahashi, E.; Wraight, C. A. *Biochemistry* **1992**, *31*, 855-866.

(35) Goldsmith, J. O.; Boxer, S. G. *Biochim Biophys Acta* **1996**, *1276*, 171-175.

(36) Clayton, R. K.; Wang, R. T. *Methods Enzymol* **1971**, *23*, 696-704.

(37) Okamura, M. Y.; Isaacson, R. A.; Feher, G. *Proc. Natl. Acad. Sci. USA* **1975**, *72*, 3492-3496.

(38) Woodbury, N. W.; Parson, W. W.; Gunner, M. R.; Prince, R. C.; Dutton, P. L. *Biochim. Biophys. Acta.* **1986**, *851*, 6-22.

(39) McComb, J. C.; Stein, R. R.; Wraight, C. A. *Biochim. Biophys. Acta* **1990**, *1015*, 156-171.

(40) Gunner, M. R.; Robertson, D. E.; Dutton, P. L. *J. Phys. Chem.* **1986**, *90*, 3783-3795.

(41) Steinbach, P. J.; Chu, K.; Frauenfelder, H.; Johnson, J. B.; Lamb, D. C.; Nienhaus, G. U.; Sauke, T. B.; Young, R. D. *Biophysical society* **1992**, *61*, 235-245.

(42) Tikhonov, A. N.; Arsenin, V. Y. *Solution of ill-posed problems*; Wiley: New York, 1977.

(43) Gunner, M. R.; Dutton, P. L. *J. Am. Chem. Soc.* **1989**, *111*, 3400-3412.

(44) Mancino, L. J.; Dean, D. P.; Blankenship, R. E. *Biochim. Biophys. Acta* **1984**, *764*, 46-54.

(45) McElroy, J. D.; Mauzerall, D. C.; Feher, G. *Biochim. Biophys. Acta* **1974**, *333*, 261-277.

(46) Breton, J. Low temperature linear dichroism study of the orientation of the pigments in reduced and oxidized reaction centers of *Rps. viridis* and *Rb. sphaeroides*. In *The photosynthetic bacterial reaction center: structure and dynamics.*; Breton, J., Vermeglio, A., Eds.; Plenum: New York and London, 1988; pp 59-69.

(47) Steffen, M. A.; Lao, K.; Boxer, S. G. *Science* **1994**, *264*, 810-816.

(48) Kleinfeld, D.; Okamura, M. Y.; Feher, G. *Biochim. Biophys. Acta* **1984**, *766*, 126-140.

(49) Labahn, A.; Paddock, M. L.; McPherson, P. H.; Okamura, M. Y.; Feher, G. *J. Phys. Chem.* **1994**, *98*, 3417-3423.

(50) Labahn, A.; Bruce, J. M.; Okamura, M. Y.; Feher, G. *Chem. Phys.* **1995**, *97*, 355-366.

(51) Allen, J. P.; Williams, J. C.; Graige, M.; Paddock, M. L.; Labahn, A.; Feher, G.; Okamura, M. Y. *Photosynth. Res.* **1998**, *55*, 227-233.

(52) Paddock, M. L.; Rongey, S. H.; McPherson, P. H.; Juth, A.; Feher, G.; Okamura, M. Y. *Biochemistry* **1994**, *33*, 734-745.

(53) Shopes, R. J.; Wraight, C. A. *Biochim. Biophys. Acta* **1987**, *893*, 409-425.

(54) Franzen, S.; Boxer, S. G. *J. Phys. Chem.* **1993**, *97*, 6304-6318.

(55) Sebban, P. *Biochim. Biophys. Acta* **1988**, *936*, 124-132.

(56) Ortega, J. M.; Mathis, P.; Williams, J. C.; Allen, J. P. *Biochemistry* **1996**, *35*, 3354-3361.

(57) Dutton, P. L.; Moser, C. C. *Proc. Natl. Acad. Sci.* **1994**, *91*, 10247-10250.

(58) Vermeglio, A.; Clayton, R. K. *Biochim. Biophys. Acta* **1977**, *461*, 159-165.

(59) Wraight, C. A. *Biochim. Biophys. Acta* **1979**, *548*, 309-327.

(60) Takahashi, E.; Maroti, P.; Wraight, C. A. Coupled proton and electron transfer pathways in the acceptor quinone complex of reaction centers from *Rhodobacter sphaeroides*. In *Electron and Proton Transfer in Chemistry and Biology*; Muller, A., Ed.; Elsevier:, 1992; Vol. Vol. 78; pp pgs. 219-236.

(61) Marcus, R. A.; Sutin, N. *Biochim. Biophys. Acta* **1985**, *811*, 265-322.

(62) DeVault, D. *Q. Rev. Biophys.* **1980**, *13*, 387-564.

(63) Brzezinski, P.; Andreasson, L. E. *Biochemistry* **1995**, *34 no.22*, 7498-7506.

(64) Kalman, L.; Sebban, P.; Hanson, D. K.; Schiffer, M.; Maroti, P. *Biochim Biophys Acta* **1998**, *1365*, 513-521.

(65) Balabin, I. A.; Onuchic, J. N. *Science* **2000**, *290*, 114-7.

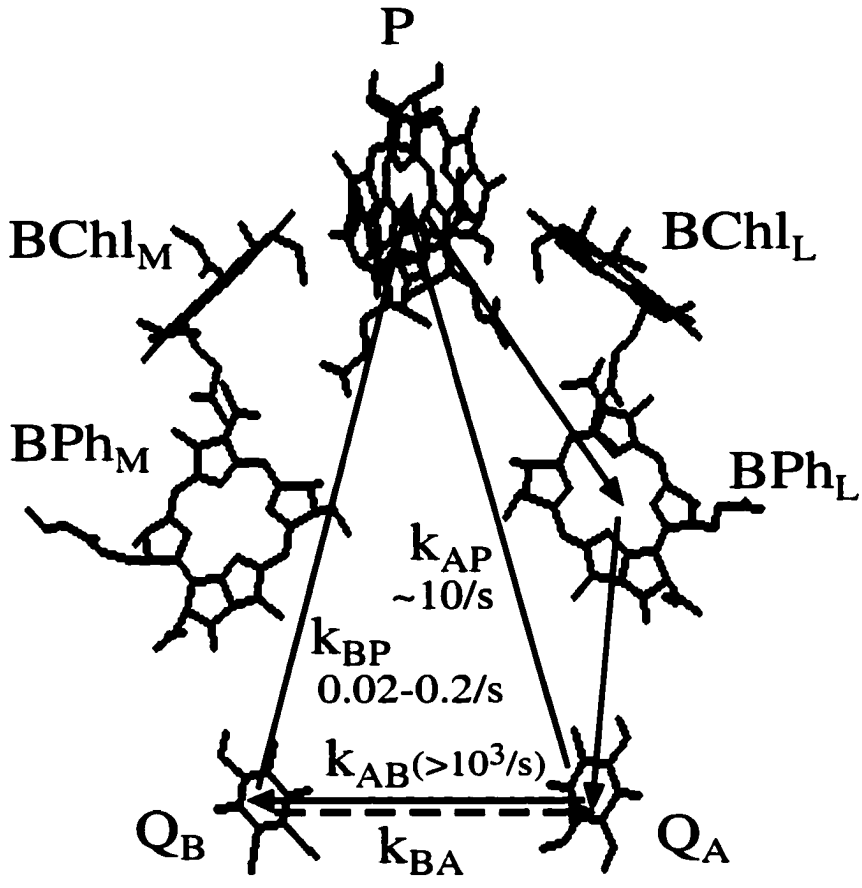

Figure 4.1. Cofactor arrangement and electron transfer pathway in *Rb. sphaeroides* RCs. At room temperature, the electron on Q_B^- returns to P^+ by thermal repopulation of the $P^+Q_A^-$ state. At cryogenic temperature, the direct tunneling at k_{BP} is seen. Approximate rate constants at cryogenic temperatures in the light-adapted protein are given. The values for k_{BP} and k_{AP}[12,13] were determined directly. The value for k_{AB} is estimated from the high quantum yield of $P^+Q_B^-$ formation.

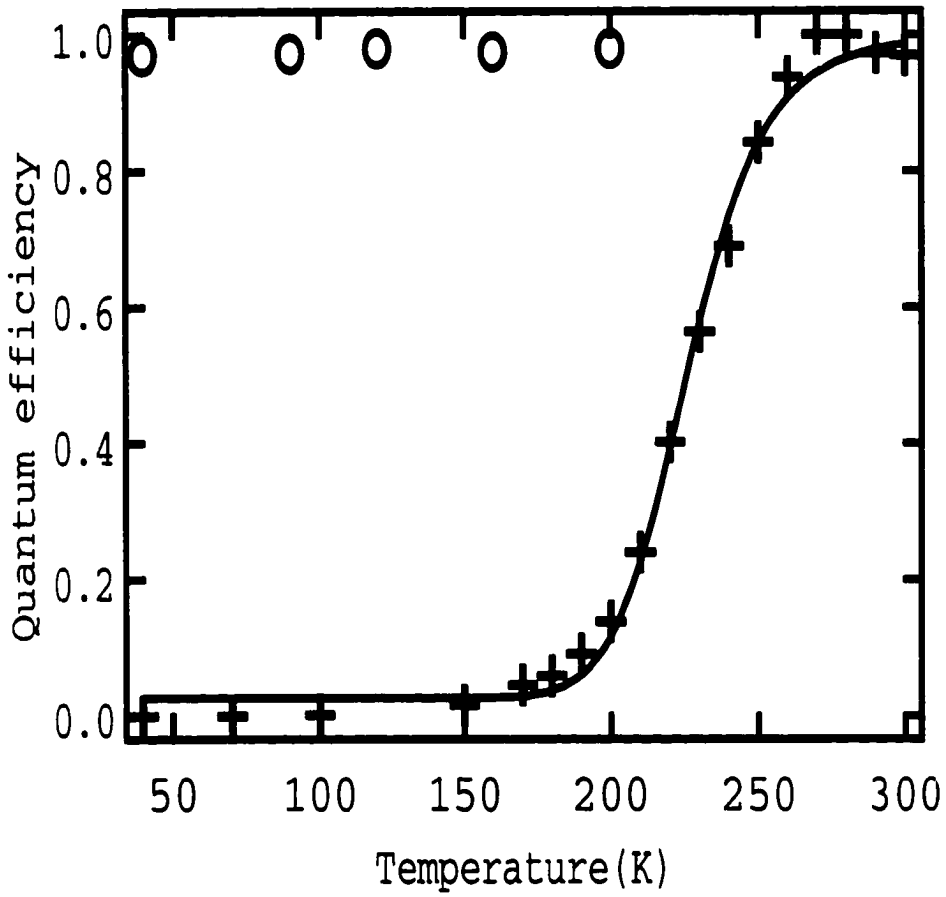

Figure 4.2. The fraction of RCs that show the slow, $P^+Q_B^-$ component of P^+ decay after an actinic flash. [RC]=4 μM, pH=8.0. For RCs frozen in dark, the amplitude was normalized against the value at 300 K. For RCs frozen under illumination, the maximum amplitude after 10 flashes (0.1 seconds interval) is taken as 1. Such normalization corrects for the portion of RCs without bound Q_B or RCs trapped in an inactive state. The fall-off in Q_B reduction in the dark-adapted RCs is fit using equation 4.1, assuming that k_{AP} is temperature independent and k_{AB} is an activated process, $k_{AB}= k_0 \text{ Exp}(-E_a / kT)+k_1$. k_{AP} is 9 s^{-1} and k_{AB} is 10^4 s^{-1} at 300K.[19] k_1 is a constant for the fitting. If the process has a single activation energy of 8 Kcal/mol (340 meV), k_{AP} will equal k_{AB} and the quantum efficiency will be 50% at ~225 K.

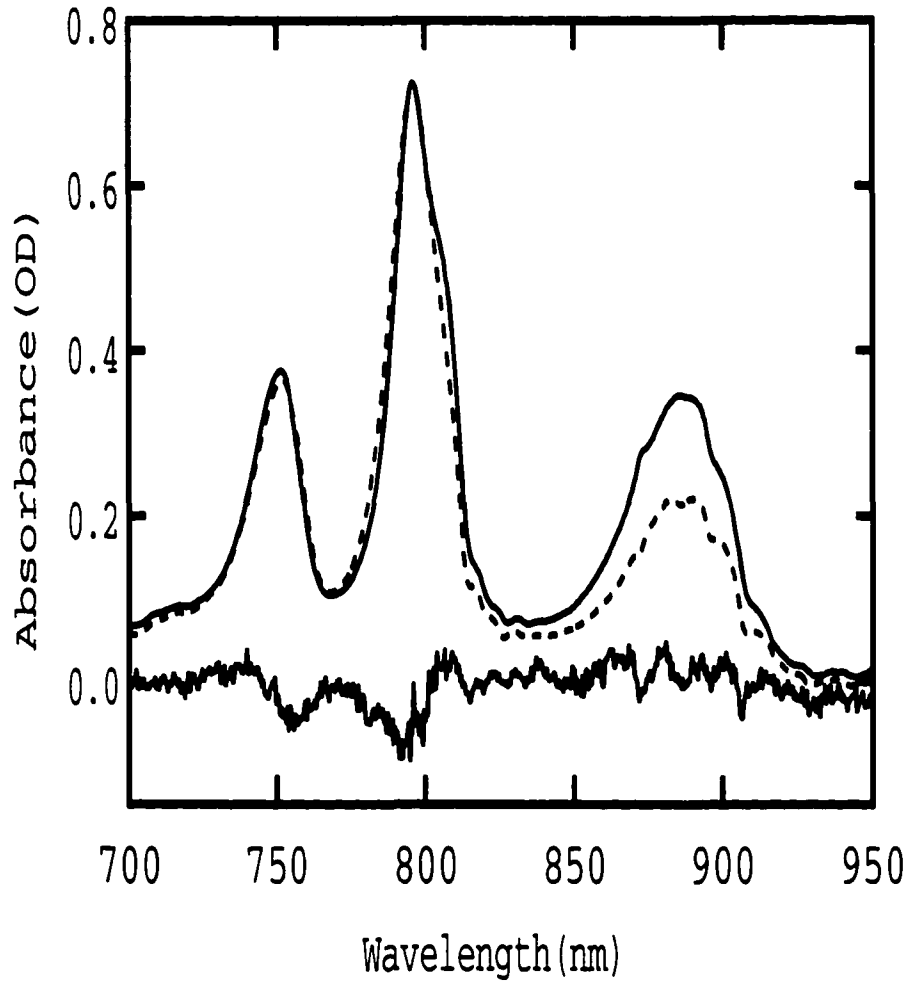

Figure 4.3. The spectrum of the RC ground state for protein frozen in the dark (solid line) and under illumination (dashed line). The peak assignments are from Ref. 46. The difference between the two spectrum is also shown. The difference spectrum is corrected for a trapped population of P^+ as described in the text. [RC] = 31μM, T = 40 K.

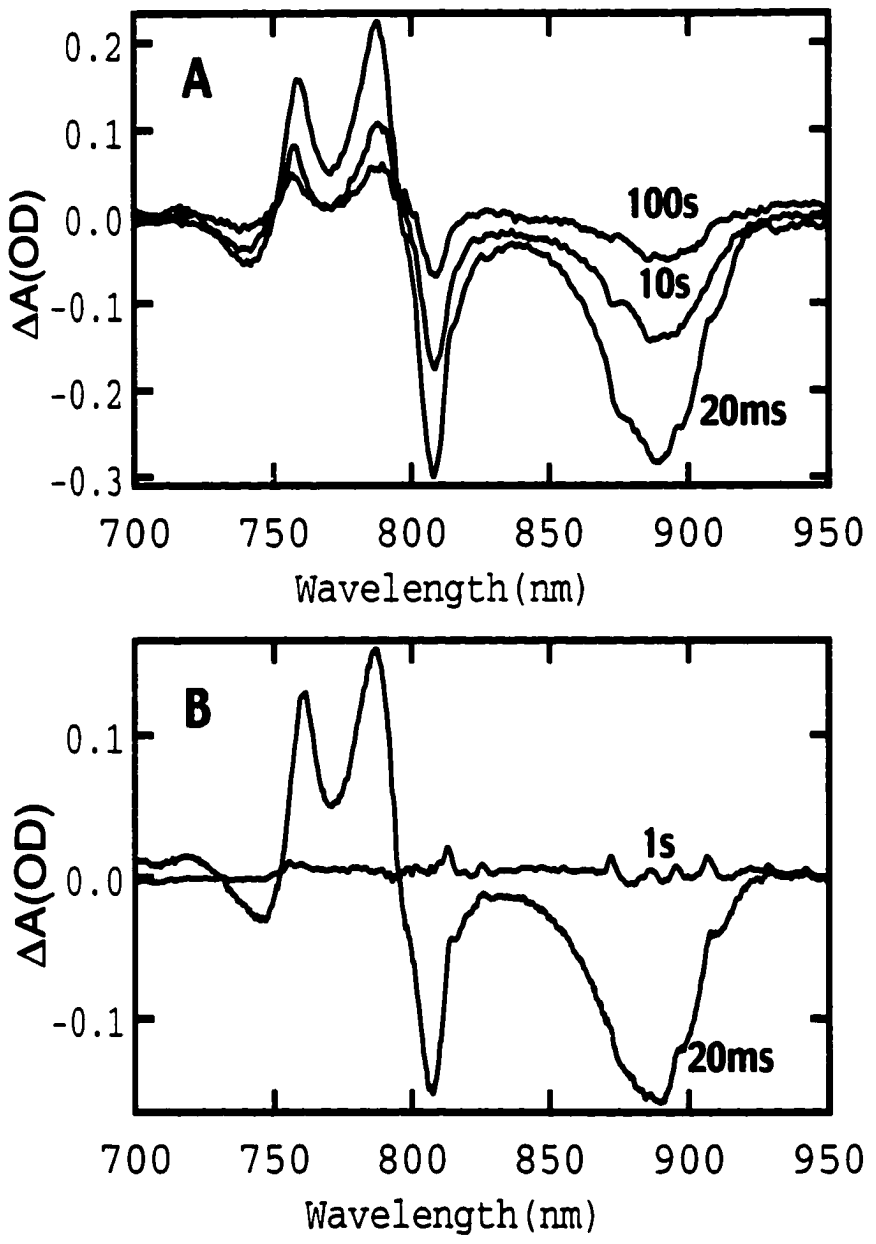

Figure 4.4. The time dependence of the absorption change at 40 K after an actinic flash in RCs frozen under illumination (A) and in the dark (B) at 40 K. The narrow peaks, most prominent in the 1s trace (4B) are lines in the weak Xenon measuring flash. Five transients were averaged at each time.

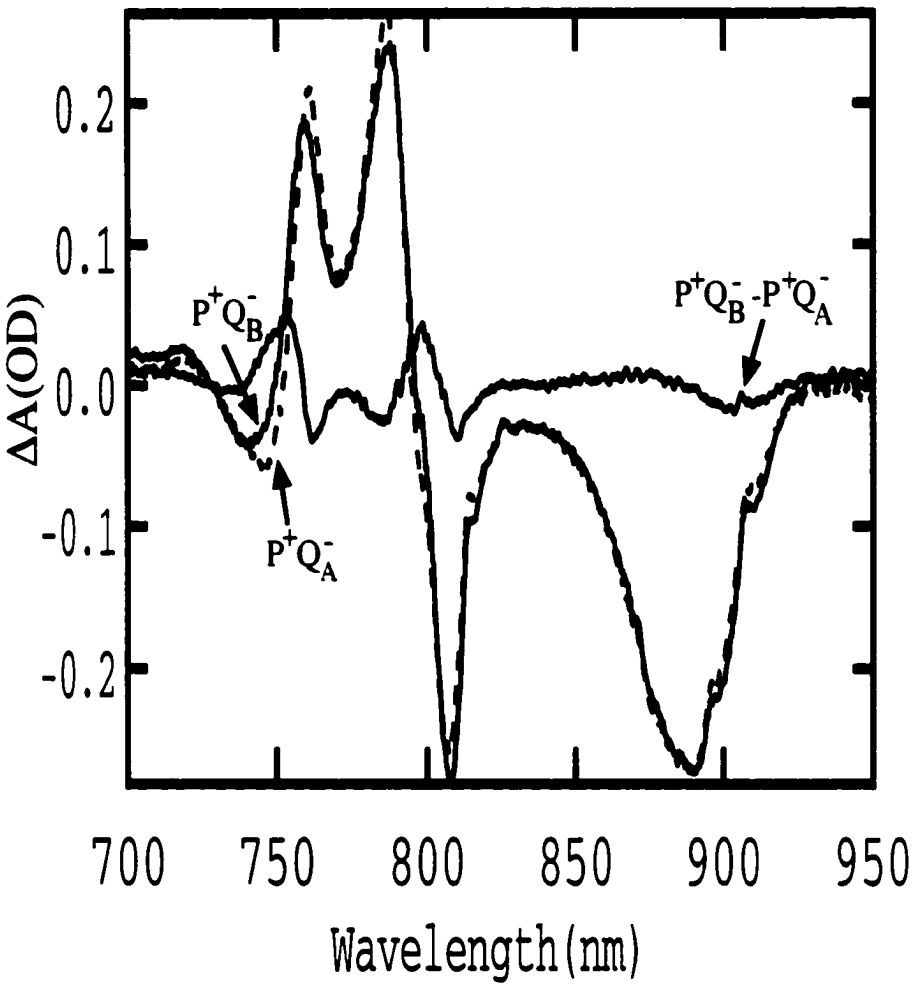

Figure 4.5. Comparison between the light induced absorption change in RCs frozen under illumination ($P^+Q_B^-$) and in the dark ($P^+Q_A^-$) at 40 K. The spectra are normalized to match the P^+ signal at 890 nm. The difference shows the shifts in the cofactor spectra in the presence of Q_B^- instead of Q_A^-.

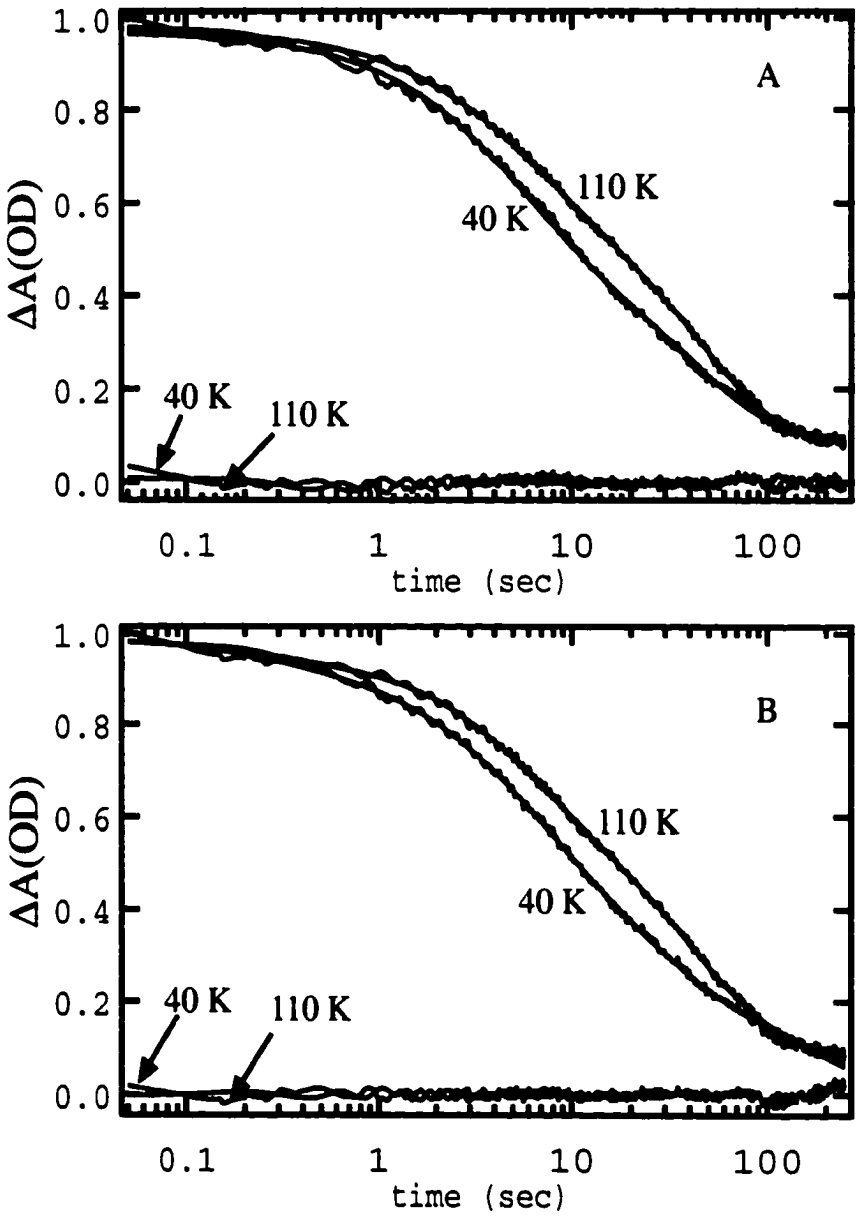

Figure 4.6. The kinetics of the $P^+Q_B^-$ charge recombination fitted by (A) double exponential fit and by (B) distributed rate model (Eqn. 4.2). The lines at the bottom are the residuals from each fit. The fitting parameters for (A) are given in Fig. 4.7.

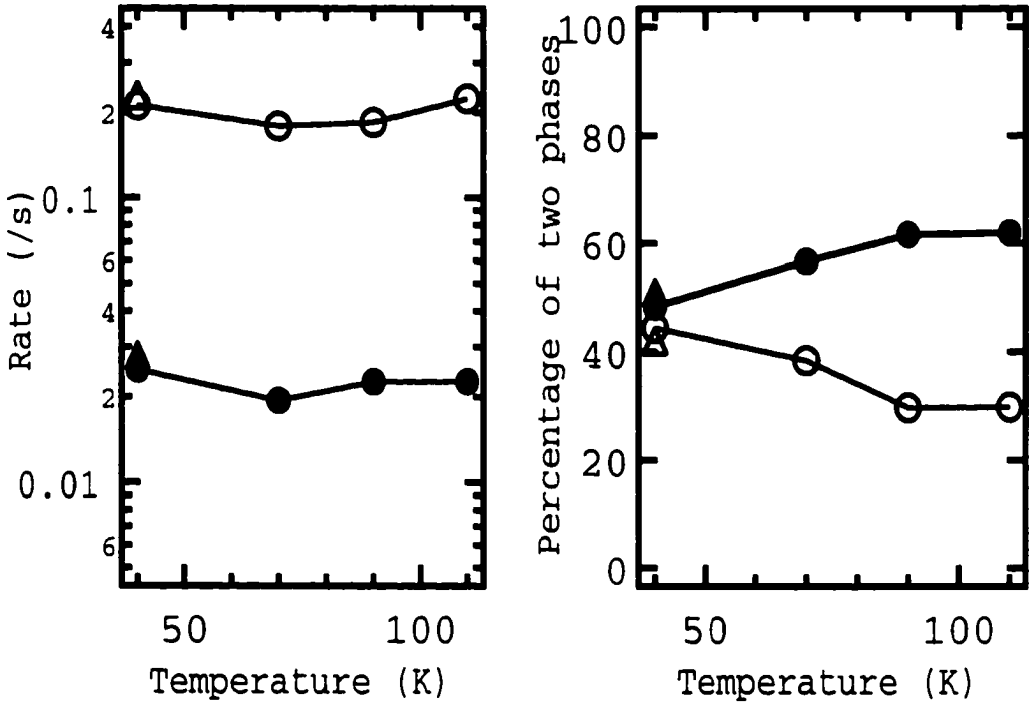

Figure 4.7. The temperature dependence of the two components for the $P^+Q_B^-$ charge recombination from the double exponential fit. (A) The rates. (B) The amplitude. Filled symbols the slower component, open the faster rate. Circle, UQ_AUQ_B; triangle, MQ_AUQ_B (40 K only).

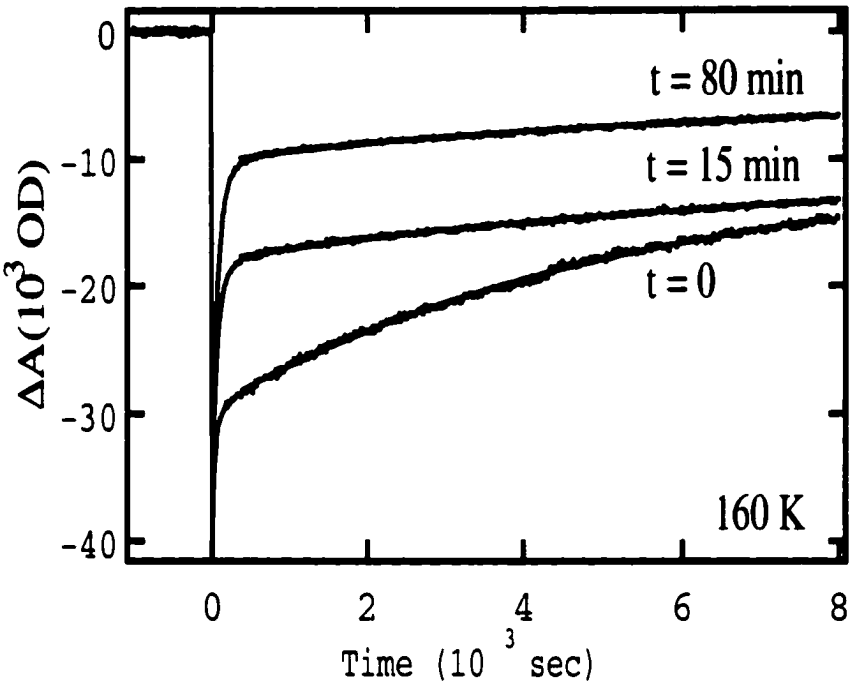

Figure 4.8. The charge recombination kinetics after the RCs trapped in the active state are warmed up to 160 K from 40 K. t=0 is the time when the thermometer reading reaches 160 K. The RCs return quickly to the ground state from $P^+Q_A^-$, while those that form $P^+Q_B^-$ show much slower charge recombination. The difference in the $P^+Q_B^-$ charge recombination kinetics at early time might be due to a difference in the relaxation rates of the two substates of the active conformation. The traces were fitted with two exponentials plus a constant fixed at 10% of the total amplitude. The fractional constant is estimated from measurements on a longer time scale. The fitting parameters are: t=0, k_1=0.20 s^{-1} (55%), k_2=0.02 s^{-1} (35%); t=15 min, , k_1=0.27 s^{-1} (22%), k_2=0.02 s^{-1} (68%); k_1=0.28 s^{-1} (28%), k_2=0.02 s^{-1} (62%).

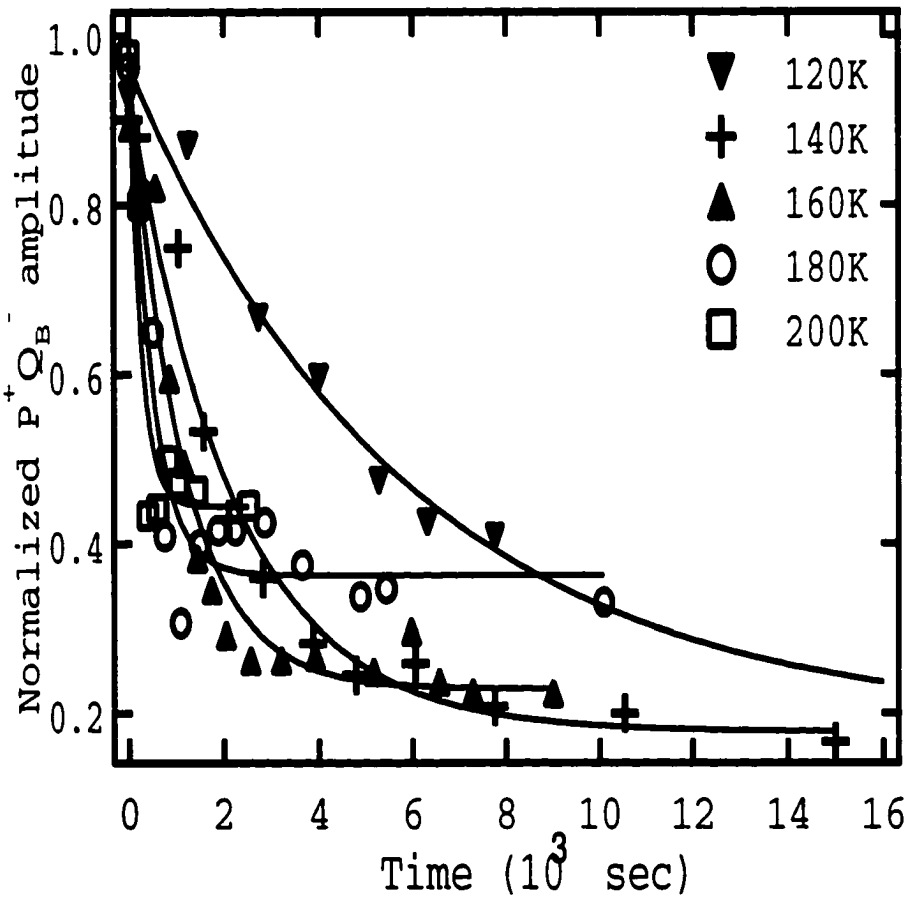

Figure 4.9. The percentage of the $P^+Q_B^-$ component in the charge recombination kinetics as a function of time. The RCs were frozen under illumination to 40 K, equilibrated for 30 min. and brought up to the measuring temperature in 10-15 min. The relaxation of the active, light-adapted RCs into a conformation where $P^+Q_B^-$ is not formed is fitted to an exponential decay at each temperature.

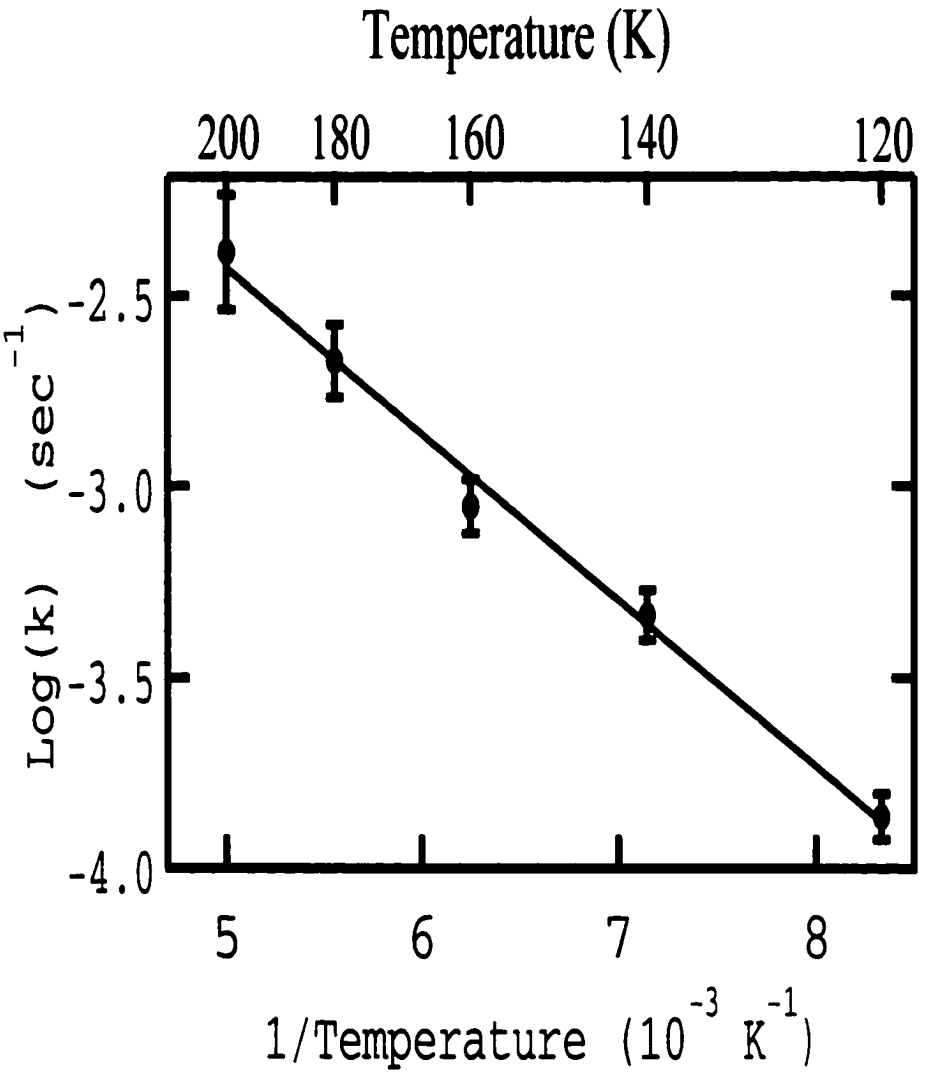

Figure 4.10. The temperature dependence of the relaxation of light-adapted RCs into an inactive conformation (Fig. 4.9). The activation energy is 87±8 meV and the rate at infinite temperature is 2 s^{-1}.

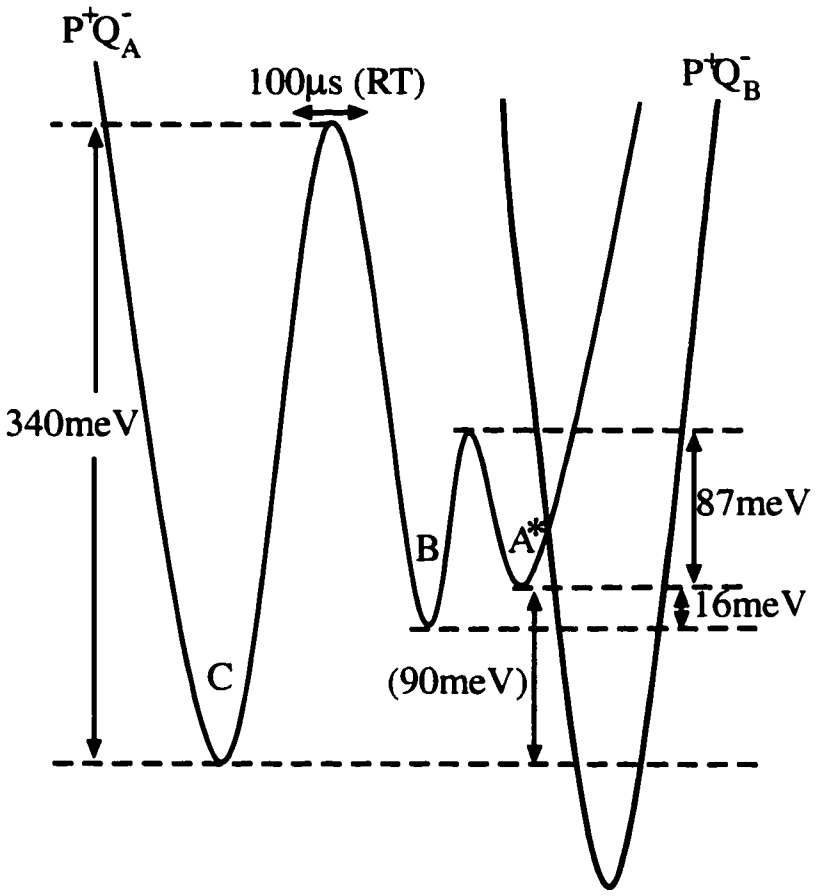

Figure 4.11. A model of the three conformational states characterized here. In dark adapted RCs, the protein is trapped in the inactive C conformation. In light adapted RCs, protein is trapped in the active A* conformation. When RCs trapped in the active conformation are warmed above 120 K, the protein relaxes into another inactive state B, which remains in equilibrium with A*. The free energy difference between A* and C is derived from the model of Li et al.[21] The activation energy between C and A* is estimated from the data in Figure 4.2.

Chapter 5

Exploring the energy profile for the Q_A^- to Q_B electron transfer along the reaction coordinate

I. pH dependence of the conformational gating step

Abstract

The ability to transform from one conformation to another at the appropriate rate is often crucial for the function of a protein. In isolated photosynthetic reaction centers (RCs), the electron transfer from the reduced primary quinone, Q_A^-, to the secondary quinone, Q_B is rate limited by a conformational change. The dependence of this conformational gating step on the protonation state of the protein was investigated by measuring and analyzing the temperature dependence of the kinetics at different pH. The energy barrier which is the rate limiting step is proposed to depend on the equilibrium between the protonated and unprotonated population. The apparent pK is 9.7. The energy barrier to the protonation step limits the electron transfer rate at high pH. This study demonstrates that the correct protonation state must be reached before the electron transfer could take place and the method has the potential for further elucidate the nature of the conformational gating step.

Reaction rates in proteins are often determined by the time scale at which the reactant can undergo conformational changes.[1,2] The energy barriers associated with required transformations cause reactions to slow and then stop at low temperature.[3-6] Large scale conformational changes have been seen in time resolved studies[7,8] or by trapping the intermediate states of the reaction process.[9,10] Evidence for substrate motion has been found by trapping photosynthetic reaction centers (RCs) in different redox states.[11] But often only small-scale motions such as changes in protonation states or hydrogen bonding pattern are required. These cannot be observed in any but the very highest resolution protein structures.

Structural studies may show what changes between reactant and product, they cannot provide the energetics of reaction barriers. Rather kinetic analysis of the temperature dependence of rates and free energy are required. Detailed kinetic measurements as a function of a variety of conditions such as pH, substrate, and mutation can provide clues as to what aspects of the protein structure contribute to the barriers to reaction. The well characterized photosynthetic bacterial reaction centers (RCs) is an excellent model system for such study. In this system it is possible to initiate the reaction with a pulse of light allowing single turn-over measurements at any time-scale. Reactions are reversible, allowing signal averaging. In addition, a remarkable scope for temperature dependence measurements is provided by the functionality of the protein even at cryogenic temperatures. Lastly, it is possible to determine

reaction free energies and associated thermodynamic parameters below 200 K for several intra-protein reactions, including the one considered here.

In the bacterial photosynthetic reaction centers from *Rb. sphaeroides*, the electron transfer from the reduced primary quinone, Q_A^- to the secondary quinone, Q_B is rate limited by a conformational change in isolated RCs with native ubiquinone as Q_A and Q_B.[12] When RCs are frozen in the product $P^+Q_B^-$ state they can return to the ground state even at 40K. When prepared in this manner the required conformational changes are trapped and electron transfer from Q_A^- to Q_B will occur with high yield.[13]

X-ray crystallography[11,14] and other experimental[15-18] and theoretical[19-24] methods have been used in the attempt to characterize the conformational change needed for the electron transfer from Q_A^- to Q_B. In the crystal structure of the reaction centers frozen under illumination (in the $P^+Q_B^-$ state), the Q_B quinone occupies a site which is about 2.7 Å closer to Q_A than is found in protein frozen in the dark. This shift of the quinone position has been proposed to be the conformational gating step.[11,14] Other studies suggest that proton shift or proton uptake, hydrogen bonding pattern change might also be involved.[20,22]

The dependence of the conformational gating step on the protonation state of the residues nearby Q_B was investigated through the analysis of the temperature dependence of the kinetics as a function of pH. A model is proposed where the protein must cross over additional barriers at high pH when active residues are deprotonated in the reactant state. The activation energy, enthalpy, and entropy of this barrier is characterized. In addition, the free

energy of the electron transfer from Q_A^- to Q_B is determined from room temperature to 260 K from pH 6 to 10.5.

Materials and Methods

Engineered poly-histidine tagged strain of *Rb. sphaeroides* reaction centers[25] were used. The isolation of the reaction centers has been described in the Chapter 2, as well as the protocol for the quinone reconstitution.

pH buffers Mes,[pH5.5-6.5], Hepes, [pH 6.9-8.0], Tris,[pH 7.5-8.5], Ches[pH 8.6-10.0] and Caps[pH 9.7-11.1] were used for different pH range. The pH values were given at 25°C. They were also measured at 5°C. The value at 5°C is 0.5-0.6 pH units higher than at 25°C except for Mes and Hepes which increases by about 0.2-0.3 from 25 to 5°C. The magnitude of the temperature dependence is consistent with previous reports.[26-29] The effect of the temperature dependence of pH on the experimental result will be explored later in the discussion.

The low temperature optical setup has been described in chapter 4. The charge recombination kinetics is measured by monitoring the decay of the P^+ signal at 430 nm with a photomultiplier(Thron EMI 9798QB). A 10 μs Xenon flash lamp with a long pass filter (750nm) provides the actinic light. The concentration of the RCs is 3-4 μM for the experiment. The measurement starts 15 minute after the set temperature is reached to allow for thermal equilibrium. The signal is average 10 times at 2 minute interval.. The sample was cooled in an APD closed-cycle Helium cryostat.

The kinetics of the return of the P^+ to the ground state was fitted to a two exponential function using the nonlinear least square fitting algorithm in the program IGOR Pro (WaveMetrics). The slower component ($<1s^{-1}$) is the charge recombination from RCs with Q_B^- while the faster component ($\sim 10\ s^{-1}$) is the charge recombination from Q_A^-. The kinetics is modeled using the program Mathematica 3.0 (Wolfram Research).

The quantum yield of the Q_A^- to Q_B reaction can be experimentally decided from the percentage of the slow phase. One complication to this approach is the small percentage of RCs (5-20%) without Q_B quinone due to the incomplete reconstitution. They must be subtracted from the fast phase before the calculation of the quantum efficiency. The contribution of the RCs without Q_B to the fast phase can be decided at room temperature, where the quantum efficiency is close to 1 for RCs with reconstituted Q_B. Correction at all temperatures is made assuming the Q_B site occupancy is temperature independent.

Results and Analysis

When the $P^+Q_A^-$ state is formed, the electron on Q_A^- can go either forward to reduce Q_B (at k_{AB}) or back to P^+ (at k_{AP}) reforming the ground state (Fig 4.1). The quantum yield (Φ) for Q_B^- formation is determined given the amplitude of the slow (A_S) and fast (A_F) components of the P^+ charge recombination. The slower component ($<1s^{-1}$) follows charge recombination

from Q_B^- while the faster component (~10 s^{-1}) is the charge recombination from Q_A^-. Thus:

$$\Phi = \frac{A_S}{A_S + A_F} = \frac{k_{AB}}{k_{AB} + k_{AP}} \tag{5.1}$$

k_{AP} can be independently measured in RCs with no Q_B and has been found to be essentially temperature [30,31] and pH [32] independent. Given k_{AP}, k_{AB} can be determined from a measurement of Φ. This analysis assumes that k_{AP} and k_{AB} can be well modeled with discrete rate constants at all temperatures. The consequences of this assumption will be discussed below.

The temperature dependence of Q_B^- formation was measured from pH 6 to 10.5 in the temperature range 150-300 K (Figure 5.1). The quantum yield decreases as the temperature is lowered until no Q_B^- is formed. At high pH the reaction freezes out at warmer temperature than at neutral pH. At pH near 9.5, the temperature dependence of Φ has s a more stretched, bimodal shape. The temperature dependent decrease in Φ monitors the slowing of the Q_A^- to Q_B electron transfer rate k_{AB}. The pH dependence of Φ indicates that the reaction is dependent on proton binding.

The model of the reaction. To fit the temperature and pH dependence of Φ (Fig. 5.1), a minimal model with 3 states is used (Fig 5.2). The reactant $P^+Q_A^-$ state can be protonated (A) or unprotonated (A'). The 2 populations are in equilibrium with an apparent pK of 9.7 (at room temperature). The product state (B) is assumed to be always protonated. At pH below 8 there is less than 0.3 protons

bound from solution on electron transfer from Q_A^- to Q_B.[33,34] Thus, protonated reactant and product states have essentially the same number of protons bound so as the pH changes, the energy of A and B change by the same amount keeping ΔG_1 constant. A and B may shift relative to the ground state, but this will not influence the reactions considered here. However, the A and B states shift relative to A'. Thus, ΔG_1 will be assumed to be pH independent, while the free energy of the reaction from the unprotonated reactant (ΔG_2) is pH dependent with $\Delta G_2=\Delta G_1-2.3\ k_bT(pH-pK_2)$. k_b is the Boltzman constant and T is the temperature.

The rate determining step for electron transfer depends on the pH. At low pH the reactant is in the A state and the barrier is $\Delta G_1^{\ddagger}$. At higher pH most RCs are in the unprotonated (A') reactant state. Now the taller, pH dependent barrier representing proton uptake must be crossed. In the model $\Delta G_2^{\ddagger}$ is the barrier to the pH independent transformation from A to A'. The forward direction activation energy for proton binding is $\Delta G_2^{\ddagger}+2.3k_bT(pH-pK_2)$. When the pH is near pK_2 there is a mixed population of protonated and unprotonated reactant. Both populations are seen in the stretched temperature dependence of Φ because the transformation from A' to A is slower than from A to B. If ΔG_1 and ΔG_2 are known then the dependence of Φ on temperature will provide $\Delta G_1^{\ddagger}$ and $\Delta G_2^{\ddagger}$ and the associated activation entropies and enthalpies for the reaction.

Determination of the free energy, enthalpy and entropy change between the three states. In RCs the equilibrium constant between $P^+Q_A^-$ and $P^+Q_B^-$ can be determined in situ from the rate at which $P^+Q_B^-$ returns to the ground state (PQ_AQ_B) (k_{BP}^{obs}).[32,35,36] There are 2 basic pathways. (Fig. 4.1) One is direct electron transfer from Q_B^- to P^+ (at k_{BP}). The second is an uphill pathway reforming $P^+Q_A^-$ which then returns to the ground state. At room temperature, the indirect pathway dominates, while as the temperature falls this slows so now the direct route is used. The rate of the indirect process is dependent on the fraction of RCs in the $P^+Q_A^-$ (A or A') rather than $P^+Q_B^-$ state and so monitors the equilibrium constant between these states. At physiological pH, charge recombination goes from the protonated product (B) through the protonated reactant (A) back to the ground state (Fig5.2). The pH independent free energy difference is ΔG_1. At high pH the protonated product equilibrates with the unprotonated reactant (A') with the free energy difference of $\Delta G_2+2.3k_bT(pH-pK_2)$. At room temperature, $\Delta G_{BA}=\Delta G_{BA'}$ at pH 9.7, identifying this as the $pK_{AA'}$ for proton uptake. Assuming equilibrium between A, A' and B, the charge recombination rate is determined by:

$$k_{BP}^{obs} = k_{BP} + k_{AP}[A] + k_{A'P}[A'] = k_{BP} + \frac{k_{AP}e^{-\Delta G_{BA}/k_bT} + k_{A'P}e^{-\Delta G_{BA'}/k_bT}}{1 + e^{-\Delta G_{BA}/k_bT} + e^{-\Delta G_{BA'}/k_bT}} \qquad (5.2a)$$

The $P^+Q_A^-$ charge recombination rate (k_{AP}) is relatively pH independent so $k_{A'P}$ is assumed to equal k_{AP}. Equation 5.2a can be transformed to recover the more familiar formula.[32,35,36]

$$k_{BP}^{obs} = k_{BP} + \frac{k_{AP}}{1 + \Big/\left(e^{-\Delta G_{BA}/k_bT} + e^{-\Delta G_{BA'}/k_bT}\right)} = k_{BP} + \frac{k_{AP}}{1 + K_{AB}} \qquad (5.2b)$$

where K_{AB} is the measured equilibrium constant between $P^+Q_B^-$ (B) and the $P^+Q_A^-$ state (A or/and A') found at a given pH and temperature. Both k_{AP} [30,31] and k_{BP} is only slightly temperature dependent. (Fig. 4.7) k_{AP} is assigned to be 10 and k_{BP} 0.1 s^{-1}.[37-39] The temperature dependence of ΔG_1 is determined at pH 8.0 where the $P^+Q_A^-$ state is fully protonated, while the temperature dependence of ΔG_2 is determined at pH 10.5 where the unprotonated A' state predominates (Table 5.1).

At an arbitrary pH, ΔG_2 is assumed to be ΔG_2(at pH 10.5)–2.3 k_bT(pH-10.5). The room temperature pH is used here. The solution pH is quite temperature dependent, however the buffers used (Tris, Ches and Caps) have very similar temperature dependence.[26-29] The estimate of ΔG_2 thus assumes that the pH differs from the buffer at pH 10.5 (298 K) by the same amount at all temperatures. The lines for K_{AB} at intermediate pH's in figure 5.3 are thus not the best fit to k_{BP}^{obs} but derived from ΔG_1 determined at the lowest pH, ΔG_2 obtained at the highest pH, and the assumption that the difference in pH of different samples is the same at each temperature.

The equilibrium constant K_{AB} was determined down to 240 K at pH 8.0 while at pH 10.5 where ΔG_{AB} is more negative, the indirect route which provides K_{AB} becomes slower than k_{BP} by 260 K (figure 5.3). The back reaction rate, even at room temperature and low pH is two fold slower in 60% glycerol than in aqueous solution. Thus, ΔG_1 is 20 meV more favorable. This change has been

ascribed to dehydration of the protein due to the osmotic stress at the glycerol concentration used for the cryosolvent.[40]

The reaction entropy and enthalpy is derived from the temperature dependence of the equilibrium constant (Table 5.1). Again the temperature dependence at pH 8.0 is used to determine the thermodynamic parameters for the electron transfer between protonated reactant and product, while that at pH 10.5 provides the entropy and enthalpy for the reaction from state A' to B. The correction for the temperature dependence of the pH will be discussed later.

	A' -> B (pH 10.5)		A-> B		RC proton uptake (pH10.5) (if pH T independent)		Caps Buffer at pH 10.5 (Temp correction pH)
meV at 298[a]	$\Delta G_{\alpha B}$	=	ΔG°_{AB}	+	$2.3\ k_BT(pH_{25^{\circ}C} - pK_{\alpha})$	+	$2.3\ k_BT(pH_T - pH_{25^{\circ}C})$
ΔG	−45 ± 5	=	−90 ± 10	+	45 ± 11	+	0
ΔH	−330 ± 10	=	−230 ± 20	+	-603 ± 22	+	503 ± 1
$-T\Delta S$	-(-285 ± 10)	=	-(-140 ± 20)	+	−(-648 ± 22)	+	−(503 ± 1)

Table 5.1. The equilibrium free energy, enthalpy and entropy change between the A, A' and B substates derived from Figure 5.3. The buffer proton dissociation enthalpy of Caps is obtained from Fukada et al.[29] The thermodynamic parameters for the proton uptake of the protein is calculated as explained in discussion.

Determination of the energy barriers. The reaction rate can be obtained assuming that state A can go on to A' (at $k_{AA'}$) to B (at k_{AB}) and to the ground state (at k_{AP}) and is formed from A' (at $k_{A'A}$) or B (k_{BA}). State A' can go to A, B, or the ground state and is reformed from A. State B can go to A or the ground state and be formed from A. State B and A' do not inter-convert directly but must pass through A. Formation of the ground state is irreversible. All reactions which do not involve A' are unimolecular. Thus, they are dependent

on the reactant concentration and a unimolecular rate constant. For example, for the electron transfer between A and B:

$$k_{AB} = \frac{k_b T}{h}\exp[\frac{\Delta S_1^{\ddagger}}{k_b}]\exp[-\frac{\Delta H_1^{\ddagger}}{k_b T}]$$
$$k_{BA} = k_{AB}\exp[\frac{\Delta S_1}{k_b}]\exp[-\frac{\Delta H_1}{k_b T}] \qquad (5.3)$$

$\hbar$ is the Planck constant. Similar relationships are assumed for all other unimolecular rates.

The electron transfer from A' to A is bimolecular as it depends on proton binding. Thus, the psudo-first order rate $k_{A'A}$ is proportional to proton concentration,

$$k_{A'A} = k_0[H^+] \qquad (5.4)$$

The constant k_0 is second order rate constant. $k_{A'A}$ can also be calculated from the equilibrium between the A and A′ state. At pH 10.5,

$$k_{A'A}(pH = 10.5) = k_{AA'}\exp[\frac{\Delta S_2 - \Delta S_1}{k_b}]\exp[-\frac{\Delta H_2 - \Delta H_1}{k_b T}] \qquad (5.5)$$

ΔS_1, ΔH_1 are entropy and enthalpy change from B to A state, ΔS_2 and ΔH_2 are the entropy and enthalpy change going from B to A′ state.(Table 5.1) From equ. 5.4, $k_{A'A}$ is proportional to the proton concentration, therefore at arbitrary pH,

$$k_{A'A} = k_{AA'} \bullet 10^{pH-10.5} \bullet \exp[\frac{\Delta S_2 - \Delta S_1}{k_b}]\exp[-\frac{\Delta H_2 - \Delta H_1}{k_b T}] \qquad (5.6)$$

The initial condition are assumed to represent equilibrium between A and A' given the pH and $pK_{A'}$. There is no B.

$$A[t=0]=\frac{1}{1+10^{pH-pK}}$$
$$A'[t=0]=\frac{10^{pH-pK}}{1+10^{pH-pK}} \qquad (5.7)$$
$$B[t=0]=0$$

The quantum efficiency (Φ) is calculated given the kinetic model (Fig. 5.2) assuming k_{AB} can be derived from Φ using eqn. 5.1. As before, k_{AP} is assigned to be 10/s and k_{BP} 0.1/s. The thermodynamic values for the reactions are derived from the rate of reformation of the ground state (Table 5.1). The data in Fig 5.1 is used to obtain the activation energies, enthapies, and entropies given in table 5.2. As before for the reaction connecting A' and A, the activation parameters are given relative to the protonated (A) $P^+Q_A^-$ state (Fig 5.2). The simulation using the 3 states model is generally consistent with the experimental data. Although accurate assessment of the error for these parameters is difficult to obtain, The range of the parameters that can fit the data can be estimated from visual inspection of the simulation result. The second order rate constant for proton uptake k_0 can be calculated combing equ. 5.4 and 5.6. The obtained k_0 at room temperature is ~10^{12} M^{-1} S^{-1}..

	$\Delta G^{\ddagger}$(meV) 298 K	$\Delta H^{\ddagger}$(meV)	$-T\Delta S^{\ddagger}$(meV), 298K
Barrier I	500±100	420±80	80±60
Barrier II	620± 60	830±50	-210±40

Table 5.2. The activation energy, enthalpy and entropy obtained from the simulation. Barrier I refers to the barrier between A and B , barrier II is the barrier between A′ and A.

Model II. The simulation predicts that the quantum yield at lower pHs will decay faster at low temperature than is found (Fig. 5.1). This suggests the presence of a protonated reactant state with a smaller barrier to reaction, A*. A state of this kind has been characterized previously. RCs can be trapped in a conformation that is active at low temperature by freezing the protein under illumination.[13] RCs in this light adapted state has the proper conformation for the Q_A^- to Q_B electron transfer to occur. In addition, faster, driving force dependent electron transfer reaction, with a smaller barrier to electron transfer has been observed when the ubiquinone Q_A is replaced by other quinones with lower *in situ* midpoint potentials.[41]

Model I was modified to included an adapted state (A*) in equilibrium with the other two $P^+Q_A^-$ states (A and A').(Figure 5.4) The barrier to the Q_A^- to Q_B electron transfer in this conformation is assumed to be so low that the electron transfer from A* doesn't slow down significantly in the temperature range of the measurement therefore all the RCs in this substate will proceed to the $P^+Q_B^-$ state rapidly after the actinic flash. The free energy level of this state is

assumed to be 40meV above the protonated $P^+Q_A^-$ state, and for simplicity ΔS is assumed to be zero. The equations for Model I remains the same and only the initial condition is changed to

$$A[t=0] = \frac{1}{1+10^{pH-pK}+e^{-\Delta G_0/k_bT}}$$
$$A'[t=0] = \frac{10^{pH-pK}}{1+10^{pH-pK}+e^{-\Delta G_0/k_bT}} \qquad (5.8)$$
$$B[t=0] = A^*[t=0] = \frac{e^{-\Delta G_0/k_bT}}{1+10^{pH-pK}+e^{-\Delta G_0/k_bT}}$$

The result of the simulation is also shown in Figure 5.1.(Dashed line) The low temperature tail from the freeze out curve at low pH is well fitted using this model but the quantum efficiency becomes a bit overestimated in the pH region near the pK. If the energy barrier from A to A' is raised, the freeze out curve at a pH close to pK can be fitted better, but the low temperature part of the low pH freeze curve is underestimated again. This problem may show a breakdown of the assumption that only the level of A' state shifts relative to other states when the pH is changed.

Discussion

The temperature dependence of the quantum yield of the Q_A^- to Q_B electron transfer is measured at the pH range of 6 to 10.5. At all pH values, the quantum yield diminishes as temperature is lowered. But the detail of the freeze out is pH dependent with an apparent pK of 9.7. At higher pH, the freeze out happens at higher temperature. At pH~pK, two populations are observed. It appears that a proton uptake step is necessary for the Q_A^- to Q_B electron transfer in the unprotonated population and this is rate determining at low temperature.

Simulation based on such models fit the experimental data nicely. The thermodynamic parameters of the different substates and the barriers are obtained.

Validity of the models. A model with two different energy barriers is the simplest model necessary to explain the experimental data. A single barrier that changes with pH can't explain the stretched, bimodal behavior of the freeze out curve at pH~pK. The model assumes a sequential mechanism where unprotonated A' state must bind a proton to form A before B can be formed. A' does not go to B, a path that would require formation of an unprotonated $P^+Q_B^-$ state (β) as an intermediate. The proton binding groups are predominately near the Q_B site. Thus, the energy difference between A and A' is modest as the electron on Q_A is interacting with ionized, acidic residues in the Q_B site.[42] In contrast, a β state would require Q_B^- to be formed quite close to a cluster of unprotonated acidic residues.[20] Thus, β would be expected to be at much higher energy than B and so is ignored.

The addition of the A* state to model I is necessary to explain the low temperature residual activity on the low pH freeze out curve. It is assumed that the electron transfer from A* to Q_B happens more quickly and is less temperature dependent than from A. This assumption is based on the study described in Chapter 4. The A* state is likely to be the light adapted state.

Limitation of the models. The proposed model here treats each state as a homogeneous population with the overall kinetics a sum of two or three exponential functions with discrete rate connecting the substates. This is a simplification as in the real protein every state is likely to consist of an

inhomogeneous population which will results in kinetics with distributed rates.[43,44] The conversion among the substates is usually fast enough at room temperature for the reaction to appear homogeneous. But the distribution of the rates becomes more apparent when temperature is lowered as the interconversion slows down. Indeed when the Q_A^- to Q_B electron transfer is measured directed, this effect is observed.[40] So the energy barrier obtained from the model should be regarded as an average value with possibly some error caused by this effect. This complication should cause the enthalpy barrier to be overestimated and entropy barrier underestimated, because the substates with faster rates will contribute more to the kinetics at higher temperature. The exact magnitude of the error depends on the exact distribution of the rates. This is difficult to measure because the absorption change used to follow electron transfer also contain contribution from the charge compensating effects which happens after the electron transfer.[41] These become especially hard to distinguish when they occur in overlapping time scale as is found at low temperature.[45] Thus the easier method of estimating the rates from the quantum yield is used here. If the rate distribution is reasonably limited, for example, within 2 orders of magnitude at 200 K, then the activation enthalpy is likely to be overestimated by no more than 30%, but that the activation entropy can be underestimated by as much as 120 meV. Therefore while the model gives us reasonably good estimate of the activation enthalpy, the activation entropy might be not so accurate.

Temperature dependence of the buffer pH. One complication in the experiment is the temperature dependence of the buffer pH. In the experiment, the pH is given at 25°C. The temperature dependence of various buffers have been measured previously in aqueous solution from 0 to 50 °C[26,29] or in cryosolvent

from -50 to 20 °C.[27,28] The temperature factor for the buffers used in the experiment, except Mes and Hepes, was reported to be about -0.03/°C. Mes and Hepes have smaller temperature factor at -0.01/°C. The pH value measured in this experiment at 5°C in the glycerol/buffer mixture is similar to previous reports. In the model used here,

$$\Delta G_{A'A} = \Delta G_1 - \Delta G_2 = -2.3k_BT(pH - pK) = -2.3k_BT(pH - pH_{25°C}) + 2.3k_BT(pH_{25°C} - pK) \quad (5.8)$$

The first term is the contribution from the temperature dependence of the buffer, the second term is the corrected enthalpy for proton uptake by the protein at pH value measured at 25°C. The temperature dependence of the buffer pH comes from the enthalpy (ΔHi) and heat capacity change of the deprotonation for the buffer. The heat capacity change is usually small, and pH at arbitrary temperature is

$$pH = pH_{T_0} + \frac{\Delta H_i}{2.3k_B}\left(\frac{1}{T} - \frac{1}{T_0}\right) \quad (5.9)$$

ΔHi is measured to be about 500 meV for CAPS. The enthalpy for the Tris and CHES is not reported. But from the temperature factor that has been reported for these two buffers, their enthalpy should be similar to CAPS. Using this value, the corrected enthalpy for proton uptake by RCs can be calculated (Table 5.1).

One concern here is whether the stretched bimodal shape at pH~pK is an artifact caused by the pH shift. This is unlikely as this would require the pH to shift in the opposite direction abruptly in a small temperature range around 250 K. And even such a shift is true, such a pH shift will cause the rate to increase with decreasing temperature in this region and this is not observed. Therefore again, the two barriers model is necessary for the explanation of the observation reported here.

The free energy, entropy, enthalpy change along the reaction pathway. The equilibrium parameters in table 5.1 and the activation parameters in table 5.2 gives a profile of the free energy, entropy and enthalpy along the reaction coordinate for the Q_A^- to Q_B electron transfer. For the electron transfer from the protonated state, the system needs to cross a barrier which is 80% enthalpic at room temperature. The electron transfer from A to B has favorable enthalpy change and unfavorable entropy change. For the proton uptake step, a energy barrier which is about twice as high needs to be crossed. Again this barrier is mostly enthalpic. The proton uptake step has favorable enthalpy change and unfavorable entropy change. Depending on the pH, the entropy change($-T\Delta S$) can be larger or smaller than the enthalpy change, thus making the proton uptake unfavorable or favorable.

Comparison with previous results. The pH dependence of the Q_A^- to Q_B electron transfer have been previously measured at room temperature from the electrochromic shift of the bacteriopheophytin.[46] The rate is constant below pH 9 and it decrease above pH 9 with an apparent pK of 9.5. The model proposed here is obviously consistent with this observation. The Q_B quinone is not directly protonated in the semiquinone state, so the observed pK comes from amino acid groups close to the Q_B site change protonation. Several mutants have been found to have different pH dependence than the wild type. For example, in the Glu L212-> Gln mutant the pH dependence is eliminated[47] while in Asp L213-> Asn, the pK is shifted to below 7[37]. The Glu L212 is suggested to be the protonation

site associated with the pK value of 9.5 and Asp L213 interacts strongly with Glu L212.[37,47-49] The temperature dependence of the kinetics in these two mutant RCs is currently being investigated.

The temperature dependence of the Q_A^- to Q_B electron transfer rate at neutral pH has been previously measured over smaller temperature range.[35,40,41] A much higher activation enthalpy of 14.3 kcal/mol was reported with the kinetics being fitted by one exponential phase.[35] In more recent results, the kinetics was resolved to two exponential phases, and the activation enthalpy for them are 2.7-4.5 kcal/mol for the faster phase and 9.5-11.5 kcal/mol for the slower phase.[40,41] The result here is more in line with these results.

The protonation kinetics. The apparent bimolecular rate constant of 10^{12} $M^{-1}s^{-1}$ at room temperature is larger than expected for a simple diffusion limited reaction, but it is actually consistent with previously reported value. For the $P^+Q_A^-$ state, a bimolecular rate of 2×10^{13} $M^{-1}s^{-1}$ at pH10 was reported by Maroti and Wraight.[50] These authors argued that proton transfer reactions in solution are not generally limited by the diffusion of H^+ or OH^-. The large activation enthalpy observed here also indicate that this protonation step is not diffusion limited, since diffusion limited reaction usually have activation enthalpy in the range of 0.08-0.15 eV. Again the observation of a high enthalpy barrier is similar to that have been reported for $P^+Q_A^-$ state,[50] although the activation enthalpy here is much larger. The energy barrier, as suggested for the $P^+Q_A^-$ state, may come from the conformational change between the proton accessible and inaccessible state.

Further work. The study presented here provides the energy profile along the reaction coordinate of the Q_A^- to Q_B reaction. Although the parameters obtained, especially preexponential factors or activation entropy should be regarded as rough estimates, this provide a useful model for further study of the conformational gating process. Factors such as mutation or quinone replacement may change the energy barrier of a particular step thus help assessing the contribution of those factors to the gating step. For example, the study presented here argues that the proper protonation state is a prerequisite for this electron transfer step.

References:

(1) Frauenfelder, H.; Sligar, S. G.; Wolynes, P. G. *Science* **1991**, *254*, 1598-1603.

(2) Zaccai, G. *Science* **2000**, *288*, 1604-7.

(3) Parak, F.; Knapp, E. W.; Kucheida, D. *J Mol Biol* **1982**, *161*, 177-94.

(4) Doster, W.; Cusack, S.; Petry, W. *Nature* **1989**, *337*, 754-756.

(5) Loncharich, R. J.; Brooks, B. R. *J Mol Biol* **1990**, *215*, 439-55.

(6) Vitcup, D.; Ringe, D.; Petsko, G. A.; Karplus, M. *Nature structural biology* **2000**, *7*, 34-38.

(7) Genick, U. K.; Borgstahl, G. E. O.; Ng, K.; Ren, Z.; Pradervand, C.; Burke, P. M.; Srajer, V.; Teng, T.; Schildkamp, W.; McRee, D. E.; Moffat, K.; Getzoff, E. D. *Science* **1997**, *275*, 1471-1475.

(8) Srajer, V.; Teng, T.; Ursby, T.; Pradervand, C.; Ren, Z.; Adachi, S.; Schildkamp, W.; Bourgeois, D.; Wulff, M.; Moffat, K. *Science* **1996**, *274*, 1726-9.

(9) Petsko, G. A.; Ringe, D. *Curr Opin Chem Biol* **2000**, *4*, 89-94.

(10) Schlichting, I.; Chu, K. *Curr Opin Struct Biol* **2000**, *10*, 744-52.

(11) Stowell, M. H. B.; McPhillips, T. M.; Rees, D. C.; Soltis, S. M.; Abresch, E.; Feher, G. *Science* **1997**, *276*, 812-816.

(12) Graige, M. S.; Feher, G.; Okamura, M. Y. *Proc. Natl. Acad. Sci. USA* **1998**, *95*, 11679-11684.

(13) Kleinfeld, D.; Okamura, M. Y.; Feher, G. *Biochemistry* **1984**, *23*, 5780-5786.

(14) Lancaster, R.; Michel, H. *Structure* **1997**, *5*, 1339-1359.

(15) Nabedryk, E.; Bagley, K. A.; Thibodeau, D. L. *FEBS Letter* **1990**, *266*, 59-62.

(16) Brzezinski, P.; Andreasson, L. E. *Biochemistry* **1995**, *34 no.22*, 7498-7506.

(17) Cherepanov, D. A.; Bibikov, S. I.; Bibikova, M. V.; Bloch, D. A.; Drachev, L. A.; Gopta, O. A.; Osterhelt, D.; Semenov, A. Y.; Mulkidjanian, A. Y. *Biochim. Biophys. Acta.* **2000**, *1459*, 10-34.

(18) van Mourik, F.; Reus, M.; Holzwarth, A. R. *Biochim Biophys Acta* **2001**, *1504*, 311-8.

(19) Lancaster, C. R. D.; Michel, H.; Honig, B.; Gunner, M. R. *Biophys. J.* **1996**, *70*, 2469-2492.

(20) Alexov, E.; Gunner, M. *Biochemistry* **1999**, *38*, 8253-8270.

(21) Sham, Y. Y.; Muegge, I.; Warshel, A. *Proteins: Structure, Function, and Genetics* **1999**, *36*, 484-500.

(22) Grafton, A. K.; Wheeler, R. A. *J. Phys. Chem* **1999**, *103*, 5380-5387.

(23) Rabenstein, B.; Ullmann, G. M.; Knapp, E. W. *Biochemistry* **2000**, *39*, 10487-96.

(24) Zachariae, U.; Lancaster, C. R. *Biochim Biophys Acta* **2001**, *1505*, 280-90.

(25) Goldsmith, J. O.; Boxer, S. G. *Biochim Biophys Acta* **1996**, *1276*, 171-175.

(26) Good, N. E.; Winget, G. D.; Winter, W.; Connolly, T. N.; Izawa, S.; Singh, R. M. *Biochemistry* **1966**, *5*, 467-77.

(27) Maurel, P.; Hoa, G. H.; Douzou, P. *J Biol Chem* **1975**, *250*, 1376-82.

(28) Taylor, M. J.; Pignat, Y. *Cryobiology* **1982**, *19*, 99-109.

(29) Fukada, H.; Takahashi, K. *Proteins* **1998**, *33*, 159-66.

(30) McElroy, J. D.; Mauzerall, D. C.; Feher, G. *Biochim. Biophys. Acta* **1974**, *333*, 261-277.

(31) Gunner, M. R.; Robertson, D. E.; Dutton, P. L. *J. Phys. Chem.* **1986**, *90*, 3783-3795.

(32) Kleinfeld, D.; Okamura, M. Y.; Feher, G. *Biochim. Biophys. Acta* **1984**, *766*, 126-140.

(33) Maroti, P.; Wraight, C. A. *Biochim. Biophys. Acta* **1988**, *934*, 329-347.

(34) McPherson, P. H.; Okamura, M. Y.; Feher, G. *Biochim. Biophys. Acta* **1988**, *934*, 348-368.

(35) Mancino, L. J.; Dean, D. P.; Blankenship, R. E. *Biochim. Biophys. Acta* **1984**, *764*, 46-54.

(36) Wraight, C. A.; Stein, R. R. *FEBS Letts.* **1980**, *113*, 73-77.

(37) Takahashi, E.; Wraight, C. A. *Biochemistry* **1992**, *31*, 855-866.

(38) Labahn, A.; Paddock, M. L.; McPherson, P. H.; Okamura, M. Y.; Feher, G. *J. Phys. Chem.* **1994**, *98*, 3417-3423.

(39) Labahn, A.; Bruce, J. M.; Okamura, M. Y.; Feher, G. *Chem. Phys.* **1995**, *97*, 355-366.

(40) Tiede, D. M.; Vazquez, J.; Cordova, J.; Marone, A. P. *Biochemistry* **1996**, *35*, 10763-10775.

(41) Li, J.; Gilroy, D.; Tiede, D. M.; Gunner, M. R. *Biochemistry* **1998**, *37*, 2818-2829.

(42) Alexov, E.; Miksovska, J.; Baciou, L.; Schifer, M.; Hanson, D.; Sebban, P.; Gunner, M. R. *Biochemistry* **2000**, *39*, 5940-5952.

(43) Austin, R. H.; Beeson, K. W.; Eisenstein, D. L.; Frauenfelder, E. H.; Gunsalus, I. C. *Biochem.* **1975**, *24*, 5355-5373.

(44) McMahon, B. H.; Muller, J. D.; Wraight, C. A.; Nienhaus, G. U. *Biophysical Journal* **1998**, *74*, 2567-2587.

(45) Tiede, D. M.; Utschig, L.; Hanson, D. K.; Gallo, D. M. *Photosynth. Res* **1998**, *55*, 267-273.

(46) Kleinfeld, D.; Okamura, M. Y.; Feher, G. *Biochim. Biophys. Acta* **1985**, *809*, 291-310.

(47) Paddock, M. L.; Rongey, S. H.; Feher, G.; Okamura, M. Y. *Proc. Natl. Acad. Sci. USA* **1989**, *86*, 6602-6606.

(48) Hienerwadel, R.; Grzybek, S.; Fogel, C.; Kreutz, W.; Okamura, M. Y.; Paddock, M. L.; Breton, J. *Biochemistry* **1995**, 34, 2832-2843.

(49) Breton, J.; Nabedryk, E. *Photosynthesis Research* **1998**, 55, 301-307.

(50) Maroti, P.; Wraight, C. A. *Biophys. J.* **1997**, 73, 367-381.

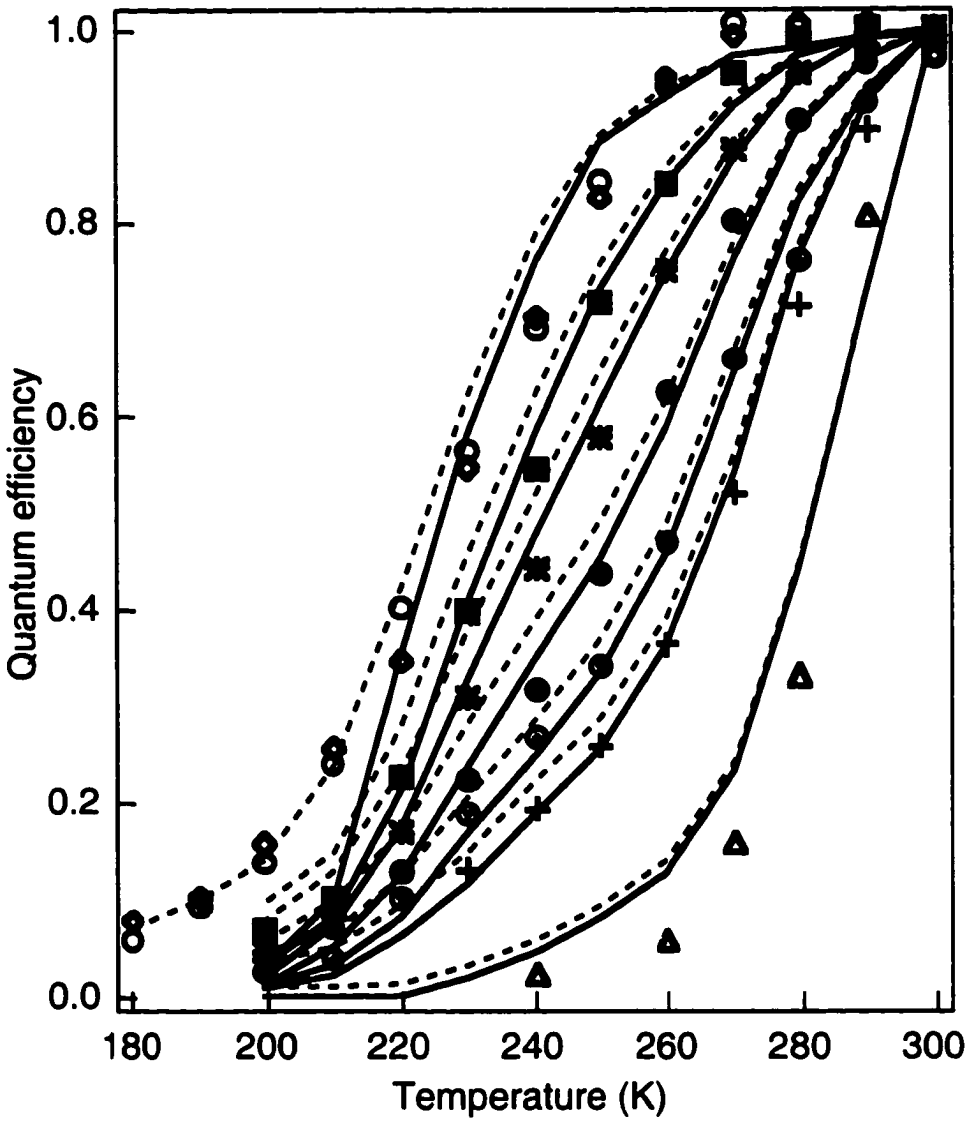

Figure 5.1. The temperature dependence of the quantum efficiency for the Q_A^- to Q_B electron transfer. The different symbols represent different pH value of the sample. At room temperature: ◊, pH 6.0; o, pH 8.0; ⊠, pH 9.3; *, pH 9.6; ●, pH 9.8; ⊕, pH 10.0; +, pH 10.2; Δ, pH 10.5. The solid line is the result of the simulation using Model I (Figure 5.2) and the dashed line with Model II. (Figure 5.4) The pH value is allowed to shift slightly (no more than 0.1 pH unit) from the measured value to get better fit.

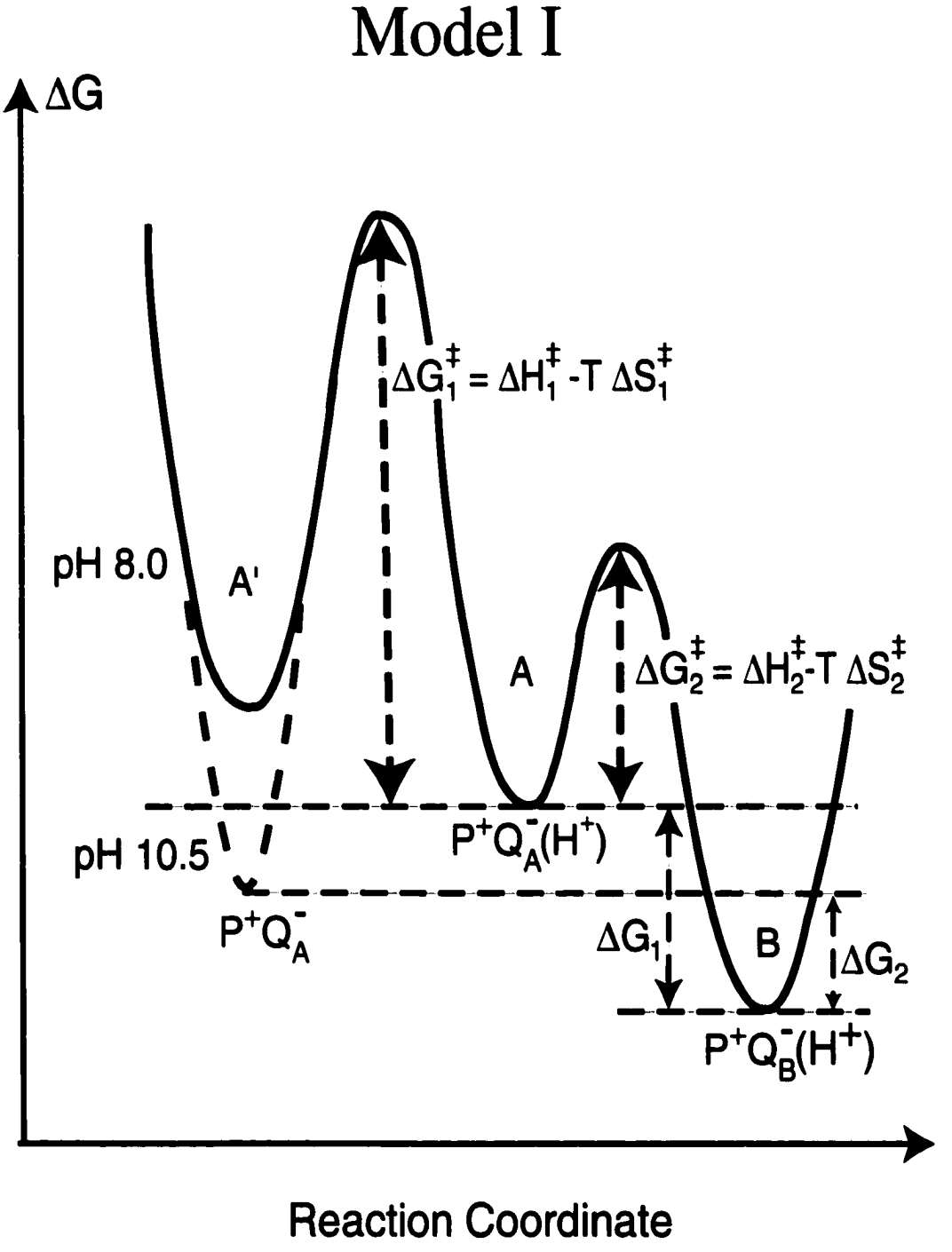

Figure 5.2. The free energy change along the reaction coordinate in Model I. A' state, which is the unprotonated $P^+Q_A^-$ state, shifts in energy with pH relative to the A and B state.

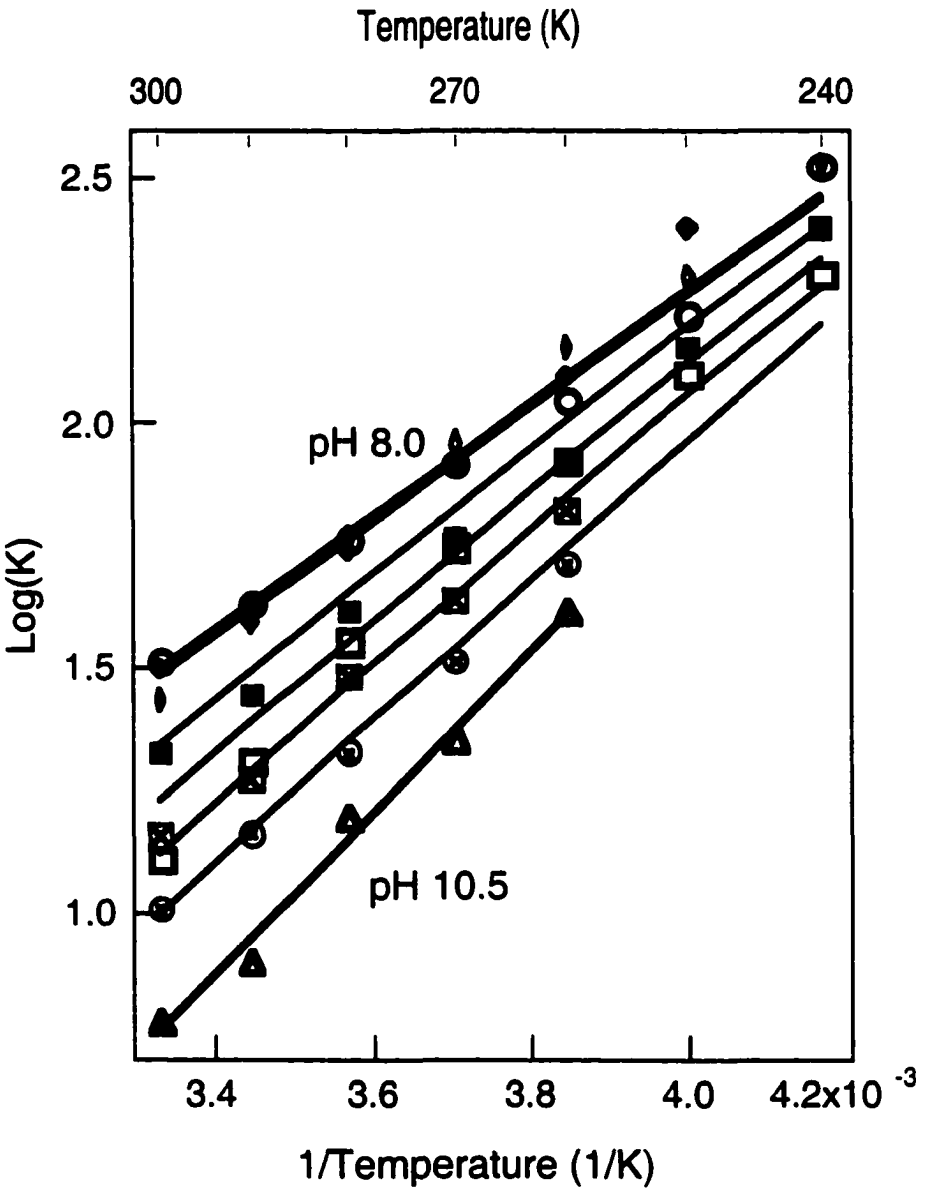

Figure 5.3. Temperature dependence of the equilibrium constant between the $P^+Q_A^-$(combining A and A′ substates) and $P^+Q_B^-$ state. The lines are from calculation from Equ. 5.2 using parameters decided from the highest and lowest pH line. Symbols: ♦, pH 7.0, ■, 8.7, □, 9.0. The other symbols are same as in Figure 5.1.

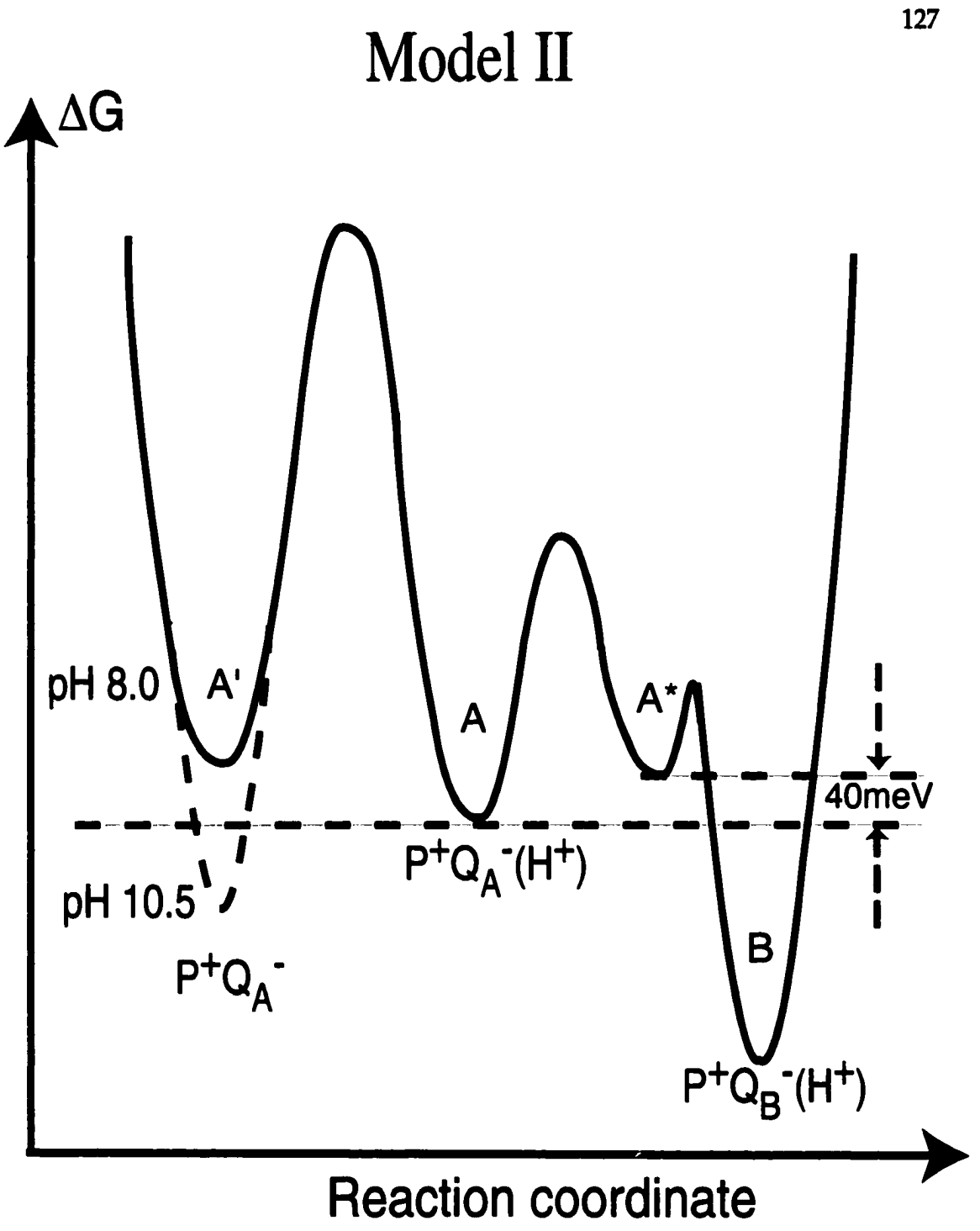

Figure 5.4 The free energy change along the reation coordinate in Model II. The only difference from Model I is the addition of the A* state, which is an activated $P^+Q_A^-$ state. The energy barrier between A* and B is assumed to be very low.

Chapter 6

Exploring the energy profile for Q_A^- to Q_B electron transfer along the reaction coordinate

II. Substrate and L209 Proline mutational effects on the conformational gating step

Abstract

The electron transfer step Q_A^- to Q_B in photosynthetic reaction center (RCs) is rate limited by a conformational change. It has been suggested that the movement of the Q_B quinone from a distal binding site to a proximal site is this conformational change. This hypothesis is tested using three L209 Proline mutants and also using ubiquinones with different hydrocarbon tail length. One of the L209 mutant, L209PY, has been shown to have Q_B quinone trapped in the proximal site even in the dark state by X-ray crystallography. The temperature dependence of the quantum efficiency for the Q_A^- to Q_B electron transfer for L209 mutants is found to differ from the wild type RCs. Entropy-enthalpy compensation is found to be responsible for the similar kinetics at room temperature. But the electron transfer reaction still stops at low temperature for all three mutants. No dependence on the quinone tail length is observed for the electron transfer. These observations suggest that a simple shift of the Q_B quinone is unlikely to be the only conformational gating step. Other processes such as the flip of the quinone ring or protonation of the residues near the quinone also play a role.

The bacterial photosynthetic reaction center is the membrane protein where the light reaction of the bacterial photosynthesis takes place. The absorption of a photon by the electron donor, which is a pair of bacteriochrolophyll, can trigger a series of electron transfers between cofactors bound to the protein and create a separation of charge.(For reviews, see Ref. 1-3) RCs prove to be a useful model system for studying factors that control the electron and proton transfer process in protein. The electron transfer from the reduced primary quinone, Q_A^- to the secondary quinone, Q_B is rate limited by a conformational change process in isolated RCs from *Rhodobacter sphaeroides* with native ubiquinone as Q_A and Q_B.[4]

The conformational change step needed for the electron transfer from Q_A^- to Q_B has a significant activation enthalpy thus the reaction freezes out at low temperature. It was observed that if the reaction center is frozen under illumination, it can be trapped in a different conformation that now allows the efficient electron transfer from Q_A^- to Q_B.[5,6] Temperature dependence of the kinetics has been measured to investigate the energy profile of this conformational gating step in the Chapter 5. The pH dependence of the freeze out curve reveals that an extra protonation step is required for the electron transfer above an apparent pK of 9.7.

Several possible protonation uptake pathways have been proposed given results of the structural,[7] mutational[8,9] and metal ion binding[10,11] experiments. One of those proposed proton pathways involves a water chain close to the L209 Proline residue.[12] A series of mutations is made at this site to test the importance of this water chain.[13] The crystal structure for three of these mutants is now

available.[14] One unexpected observation is that the mutation of L209 Pro to Tyr causes the Q_B quinone to shift to a new position. Two sites have been observed previously in the crystallography studies of RCs. When RCs from *Rb. sphaeroide* are frozen in the dark, the quinone mainly occupies the distal site, while in RCs frozen under illumination, the quinone occupies the proximal site which is about 2.7 Å closer to Q_A. In the L209 Pro to Tyr mutant structure, the Q_B quinone is in the proximal site even in the dark state. This provides an opportunity to assess the contribution of the quinone movement to the electron transfer.

Another way to check the contribution of the quinone motion is to measure the effect of replacing the native UQ-10 with shorter tail ubiquinones, which will be expected to be more mobile. Kinetics measured at room temperature show no significant dependence on the quinone tail length.[15,16] It was suggested that the rate limiting step in the quinone shift might be protein breathing motion or quinone breaking away from the distal site instead of the pure diffusion.[4] Lowering the temperature of the measurement might reveal more difference between the kinetics as the viscosity of the solution increases, the diffusion step could become rate limiting.

In this report, the mutation effects of the residue L209 Proline is investigated and the effect of shortening the Q_B quinone isoprenoid tail is also studied.

Materials and Methods

The reaction centers from the three L209 mutants were prepared as described in Ref. 13. The optical measurement and the data analysis has been

described in detail in Chapter 4. For quinone isoprenoid tail dependence measurement, the his-tagged *Rhodobacter Sphaeroides* strain was used. The ubiquinones used are UQ-1(from Sigma), UQ-4(Fluka) and UQ-10(Sigma). The mutant RCs can be trapped in the light adapted state as described in Chapter 4. All the measurements are done in Tris buffer, pH 8.0.

Results.

The L209 Pro mutants. The loss in quantum yield for the Q_A^- to Q_B electron transfer was measured in RCs when Pro L209 was mutated to Tyr, Glu and Thr. As in the reaction centers from the wild type bacteria, the quantum efficiency of the Q_A^- to Q_B electron transfer decreases with temperature in all three mutants.(Figure 6.1) But the temperature at which this electron transfer step freezes out differs significantly with the different mutants. In both the L209 PT and L209 PE, the quantum efficiency decreased to 50% at ~260K, much higher than in the wild type. The falloff in L209PE seems to be more abrupt than in the L209PT mutant. In contrast, the freeze out happens at lower temperatures in the L209 PE mutant than the wild type protein. The shift is significant. Although the shift on the temperature axis is only ~15K, the quantum efficiency in the L209PY mutant is much higher below 240K than in the wild type at the same temperature.

The loss of the quantum efficiency is due to the slow down of the Q_A^- to Q_B electron transfer rate. As the forward electron transfer rate decreases, more RCs in the $P^+Q_A^-$ state will proceed through the back reaction from P^+ to Q_A^- to the ground state at k_{AP}, which is almost temperature independent. When the

forward and backward electron transfer rate are equal to each other, the quantum efficiency drops to 50%. In the wild type RCs, the temperature dependence can fitted with a single energy barrier at pH 8. The fitting results for the mutants are shown with the parameters in Table 6.1 (Figure 6.1). As in the wild type RCs, this simple fit underestimate the quantum efficiency at low temperature in the Tyr mutant, which is not completely frozen out above 100 K. As in the analysis for the wild type, this can be compensated by adding the "light adapted substate" which corresponds to the conformation the RCs can be trapped into when they are frozen under illumination (see Fig. 5.4). As in the wild type RCs, the light adapted substate is about 40meV higher in energy than the dark adapted substate. But in contrast to the wild type RCs, the free energy difference has to be mostly entropic in order to fit the temperature dependence of the quantum efficiency (Table 6.1). One underlying assumption in the model, as discussed in Chapter 5, is that the states are assumed to be in equilibrium before the reaction starts. This is probably true above 200 K, but is questionable below the glass transition. It has been observed in RCs and other systems that the conformational relaxation kinetics became non-exponential below 200 K and that the higher tiers of the energy barriers for relaxation are only crossed very slowly. Therefore an alternative explanation for the low temperature "tail" of the L209 Tyr mutant is that a small population is trapped in the light state during the cooling.

	$\Delta G^{\ddagger}$(meV) 298 K	$\Delta H^{\ddagger}$(meV)	$-T\Delta S^{\ddagger}$(meV), 298K
Wild type	500±100	420±80	80±60
L209PY	540± 60	260±40	280±40
L209PE	520± 70	530±60	-10± 40
L209PT	550± 70	500±60	50±40

Table 6.1. The activation energy, entropy and enthalpy for the wild type RCs and L209 mutants at pH 8.0. The parameters is obtained from simulation using Model II (Figure 5.4) discussed in the last chapter.

No such low temperature tail is observed for the other two mutants, suggesting that the activated or light state is probably at higher energy in these mutants. The enthalpy barrier is considerably higher than in the wild type RCs for both mutants. However it is not as high as the enthalpy barrier for proton uptake in the wild type RCs at high pH (Fig. 5.2). For each mutant, the free energy barrier for the electron transfer is similar at room temperature to the wild type.

The effect of the isoprenoid tail on the kinetics. The temperature dependence of the Q_A^- to Q_B quantum efficiency is almost identical for RCs with UQ1, UQ4 and native UQ10 as Q_B (Figure 6.2). The independence of the kinetics on the isoprenoid tail length has been observed previously at room temperature.[15,16] When the RCs trapped in the light adapted active conformation are warmed up to the 120-200 K, the RCs relax to an inactive conformation (Fig. 4.8). This

relaxation kinetics is also found to be independent of the isoprenoid tail length (Chapter 4).

Discussion.

The temperature dependence of the Q_A^- to Q_B electron transfer reaction were measured for three L209 Proline mutants and compared with the wild type. Although the kinetic rate at room temperature is similar for the mutants and wild type RCs,[13] differences were observed when the temperature is lowered. Of particular interest is the freeze out behavior for the L209 PY mutant, the crystal structure of which shows that the Q_B quinone occupies the proximal position even in the dark.[14]

The role of the quinone movement. The freeze out curve for the L209 mutant and wild type RCs with the shorter tail quinones were measured to test the role of the quinone movement in the Q_A^- to Q_B electron transfer process. Two binding sites for the Q_B quinone were previously observed in crystallography studies of both *Rhodobacter sphaeroides*[17,18] and *Rhodopseudomonas viridis* RCs.[7] The two sites are displaced by about 4 Å along the path of the isoprenoid tail. In addition, the quinone ring planes differ by a 180° rotation around the isoprenoid tail. The quinone movement from the distal site to the proximal site, which is closer to the non-heme iron, has been suggested to be the rate limiting conformational change in the Q_A^- to Q_B electron transfer.[7,17] The evidence supporting this suggestion comes from the comparison between the crystal structure of the RCs frozen in the dark and frozen under illumination.[17] It was known previously that the Q_A^- to Q_B electron transfer can proceed in RCs frozen under illumination but it stops in

RCs frozen in the dark.[5,6] The Q_B quinone is found to occupy predominately the distal site in the dark structure but proximal site in the light structure. Molecular dynamics simulation indicates that the proximal site is the preferred site after the reduction of Q_A to semiquinone and the proton uptake in response to the Q_A reduction.[19] While the shift of the quinone from the distal to the proximal site can happen spontaneously, the flip of the ring plane can't be seen on the time scale of the simulation and a high energy barrier is expected for such a flip even at the most favorable binding position.[20]

One interesting feature in the crystal structure for the L209 PY mutant is that Q_B occupies the proximal position even in the dark structure although the orientation of the quinone ring is undetermined with respect to the 180° rotation. This change in the favored position indicates a change in the relative free energy of the two binding sites. The replacement of the proline L209 with tyrosine also causes the displacement of several residues close to the Q_B binding site including Asp L213, Glu H173, Thr L226 and Phe L216. The measured Q_A^- to Q_B electron transfer rate is similar to the wild type at room temperature and this electron transfer still freeze out at low temperature.

The similarity of the wild type and the L209PY mutant kinetics at low temperature could have several explanations. One possibility is that the quinone ring might be in the wrong orientation in the L209 PY mutant and the flip of the quinone ring is still the rate limiting step. The two orientations of the ring have different hydrogen bonding patterns. Although the distance between Q_A^- and Q_B is similar in the two ring orientations, the free energy difference and/or reorganization energy might be quite different so that the electron transfer can't

proceed when the ring is in the wrong orientation. The flip of the quinone ring inside the protein is expected to be difficult. Molecular dynamics simulation shows that even at the most optimized position, the activation barrier could still be larger than 20 kcal/mol.[20] Thus the quinone may need to dissociate from the protein in order for the quinone to flip around.

The second possibility is that some process other than the quinone shift is the rate limiting step although the quinone movement happens before or after the electron transfer. The rate limiting step could include protonation of key residues such as Glu L212, Asp L213, hydrogen bonding pattern change through the water channels near the Q_B site. Such processes will stabilize the Q_B^- state thus make the electron transfer favorable.

It seems unlikely that the displacement of the residues near Q_B caused the failure at low temperature since the rates at room temperature are so close to that found in wild type RCs.[13] If the rate limiting step in the L209 PY mutant is different from wild type, a change in the room temperature kinetics is expected.

The observation of the identical temperature dependence for RCs with UQ-1, UQ-4 and UQ-10 as Q_B also demonstrates that a simple shift of the quinone without flipping the ring is unlikely to be the rate limiting step. The electron transfer rate measured at room temperature was also found to be independent of the quinone tail length.[15,16] Since the barrier to a flip could come mainly from the head group, which is same for all the quinones used, these measurements don't disprove that the flip of the ring might be rate limiting.

The shift of the freeze out curves in the mutants. Although the room temperature kinetics for the Q_A^- to Q_B electron transfer is almost same for all

three mutants,[13] the freeze out behavior is quite different. The L209 PY mutant freezes out at lower temperature than the wild type, while the other two mutants freeze out at higher temperature. The freeze out is due to the activation energy barrier of the rate limiting process. The analysis of the energy barrier indicates the activation enthalpy and entropy change significantly from the wild type RCs, but the effect of these two contribution are opposite to each other and at room temperature they largely cancel out. This explains why the rate is similar at room temperature. The enthalpy-entropy compensation effect is common in biological processes, including protein folding and macromolecule interaction.[21] Therefore, the specific favorable or unfavorable interaction between the protein and quinone or semiquinone caused by the mutation here is large compensated by the entropy change to give the Q_A^- to Q_B reaction the proper driving force. As temperature is lowered, the entropy contribution decreases and the different changes becomes evident.

References :

(1) Feher, G.; Allen, J. P.; Okamura, M. Y.; Rees, D. C. *Nature* **1989**, *339*, 111-116.

(2) Gunner, M. R. *Current Topics in Bioenergetics* **1991**, *16*, 319-367.

(3) Blankenship, R. E.; Madigan, M. T.; Bauer, C. E. *Anoxygenic Photosynthetic Bacteria*; Kluwer Academic Publishers:, 1995; Vol. 2.

(4) Graige, M. S.; Feher, G.; Okamura, M. Y. *Proc. Natl. Acad. Sci. USA* **1998**, *95*, 11679-11684.

(5) Kleinfeld, D.; Okamura, M. Y.; Feher, G. *Biochemistry* **1984**, *23*, 5780-5786.

(6) Xu, Q.; Gunner, M. R. *Biochemistry* **2001**, *40*, 3232-3241.

(7) Lancaster, R.; Michel, H. *Structure* **1997**, *5*, 1339-1359.

(8) Paddock, M. L.; Feher, G.; Okamura, M. Y. *Biochemistry* **1995**, *34*, 15742-15750.

(9) Paddock, M. L.; Feher, G.; Okamura, M. Y. *Proc. Natl. Acad. Sci.* **2000**, *97*, 1548-1553.

(10) Utschig, L. M.; Ohigashi, Y.; Thurnauer, M. C.; Tiede, D. M. *Biochemistry* **1998**, *37*, 8278-8281.

(11) Paddock, M. L.; Graige, M. S.; Feher, G.; Okamura, M. Y. *Proc. Natl. Acad. Sci. USA* **1999**, *96*, 6183-6188.

(12) Baciou, L.; Michel, H. *Biochemistry* **1995**, *34*, 7967-7972.

(13) Tandori, J.; Sebban, P.; Michel, H.; Baciou, L. *Biochemistry* **1999**, *38*, 13179-13187.

(14) Kuglstatter, A.; Miksovska, J.; Sebban, P.; Fritzsch, G. *FEBS Letts.* **2000**, *472*, 114-6.

(15) McComb, J. C.; Stein, R. R.; Wraight, C. A. *Biochim. Biophys. Acta* **1990**, *1015*, 156-171.

(16) Li, J.; Takahashi, E.; Gunner, M. R. *Biochemistry* **2000**, *39*, 7445-7454.

(17) Stowell, M. H. B.; McPhillips, T. M.; Rees, D. C.; Soltis, S. M.; Abresch, E.; Feher, G. *Science* **1997**, *276*, 812-816.

(18) Ermler, U.; Fritzsch, G.; Buchanan, S. K.; Michel, H. *Structure* **1994**, *2*, 925-936.

(19) Grafton, A. K.; Wheeler, R. A. *J. Phys. Chem* **1999**, *103*, 5380-5387.

(20) Zachariae, U.; Lancaster, C. R. *Biochim Biophys Acta* **2001**, *1505*, 280-90.

(21) Dunitz, J. D. *Chem Biol* **1995**, *2*, 709-12.

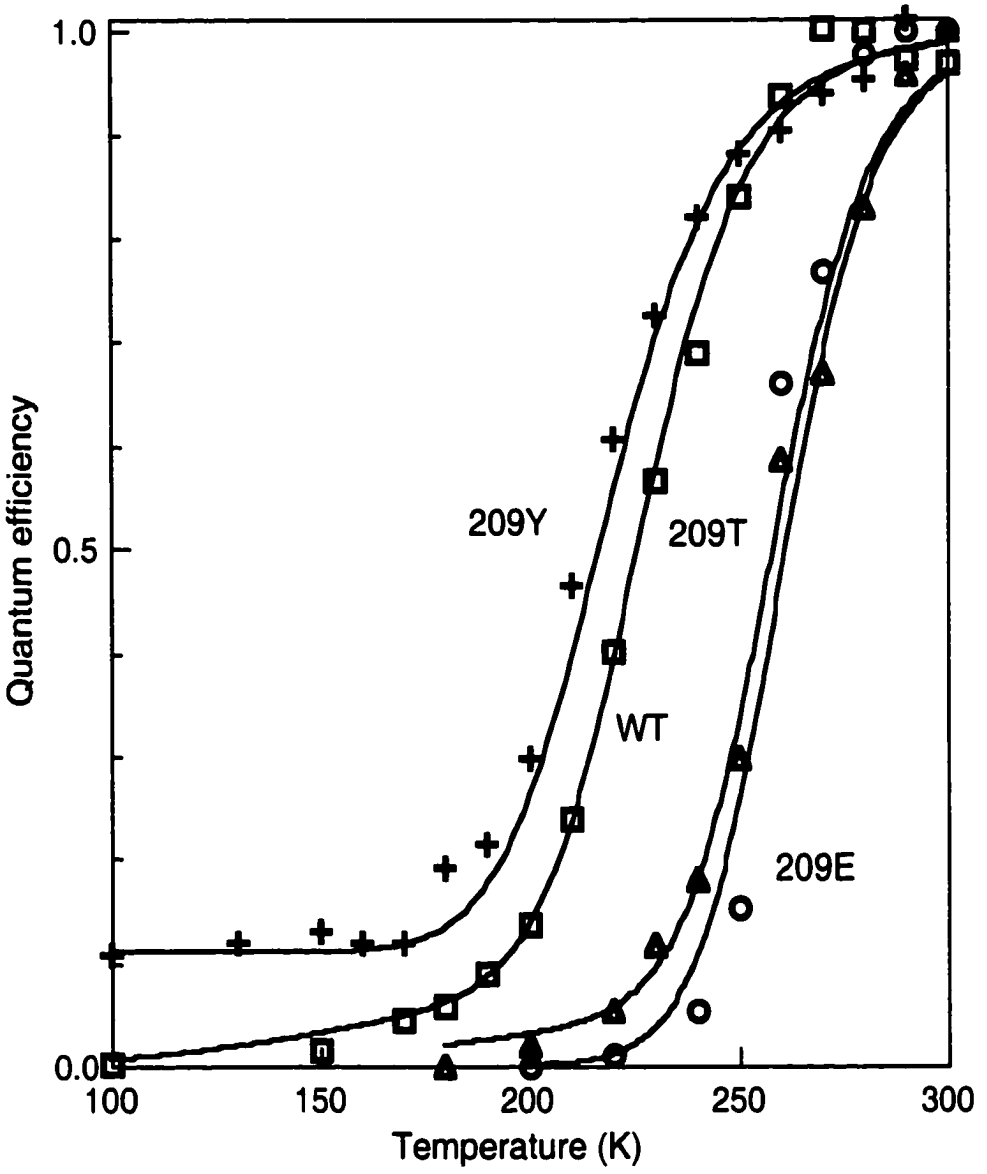

Figure 6.1. The temperature dependence of the quantum efficiency for the wild type RCs and for the three L209 mutants. The solid line is the result of the fitting using Model II in Chapter 5. (Figure 5.1 and 5.4)

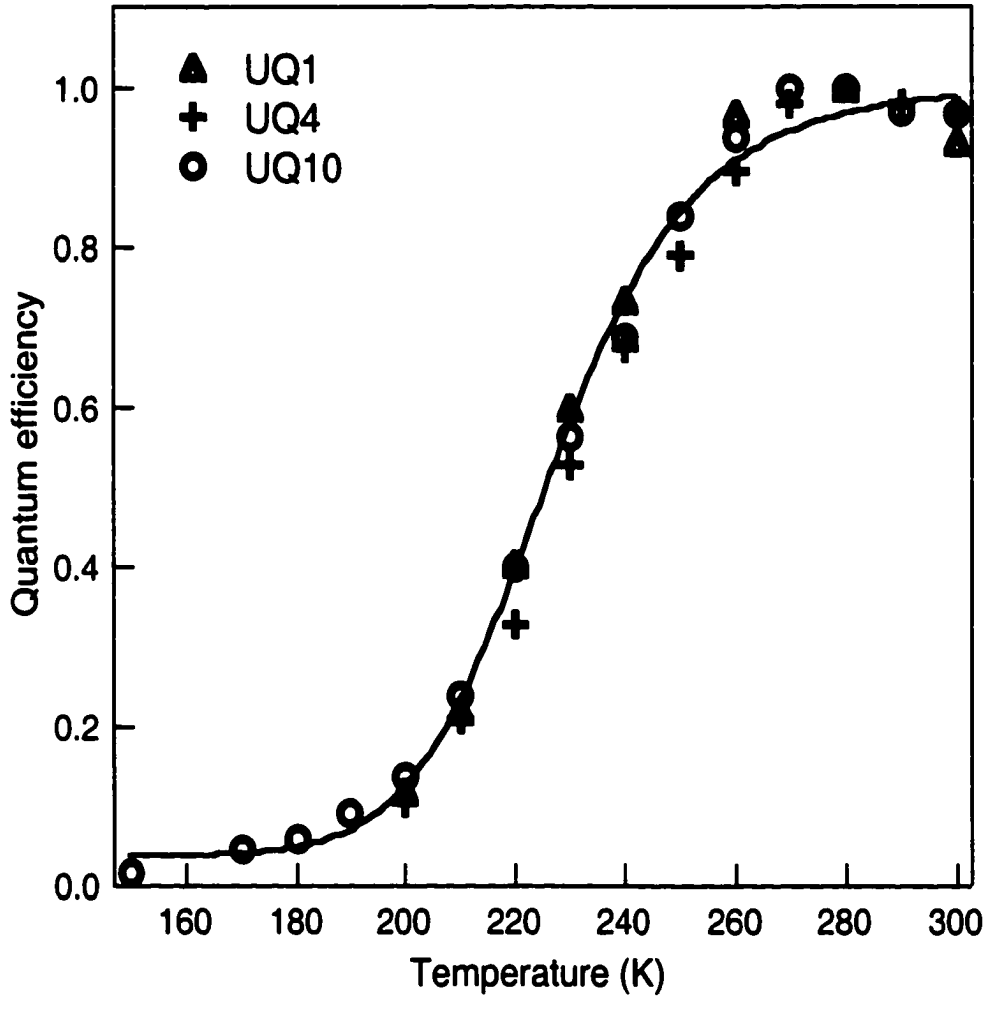

Figure 6.2. The temperature dependence of the Q_A^- to Q_B electron transfer step for wild type RCs with ubiquinone with different hydrocarbon tail.

Conclusions

Using the reaction center protein from photosynthetic bacteria as a model system, we investigated the role of conformational change in two electron transfer reactions. By extending the temperature range from room temperature to 40 K, a series of conformational substates has been trapped and characterized. For the $P^+Q_A^-$ charge separation, conformational change is found to help stabilize the product state through an enthalpy driven relaxation. For the Q_A^- to Q_B electron transfer, a profile of the energy landscape along the reaction pathway is becoming established by the characterization of a series of conformational substates. Factors such as pH, side chain mutation and substrate itself that perturb the energetics along the reaction pathway were investigated to provide clues for the identity of the rate limiting conformational change. The right protonation state of residue near the Q_B site is found to be a prerequisite for the Q_A^- to Q_B electron transfer. The method established here has potential for the further elucidation of reaction mechanism for electron transfer process in reaction centers.

References

Chapter 1.

(1) Gunner, M. R. The temperature and ΔG dependence of long range electron transfer in reaction center protein from *Rhodobacter sphaeroides*. Ph.D., University of Pennsylvania, 1988.

(2) Friesner, R., A.; Won, Y. *Biochim. Biophys. Acta* **1989**, *977*, 99-122.

(3) Moser, C. C.; Keske, J. M.; Warncke, K.; Farid, R.; Dutton, P. L. *Nature* **1992**, *355*, 796-802.

(4) Gray, H. B.; Winkler, J. R. *Annu Rev Biochem* **1996**, *65*, 537-561.

(5) Page, C. C.; Moser, C. C.; Chen, X.; Dutton, P. L. *Nature* **1999**, *402*, 47-52.

(6) Maroti, P.; Hanson, D. K.; Baciou, L.; Marianne, S.; Sebban, P. *Proc. Natl. Acad. Sci.* **1994**, *91*, 5617-5621.

(7) Okamura, M. Y.; Feher, G. Proton-coupled electron transfer reactions of Q_B in reaction centers from photosynthetic bacteria. In *Anoxygenic Photosynthetic Bacteria*; Blankenship, R., Madigan, M., Bauer, C., Eds.; Kluwer Academic Publishers: Dordrecht, 1995; Vol. 2; pp 577-593.

(8) Tiede, D. M.; Utschig, L.; Hanson, D. K.; Gallo, D. M. *Photosynth. Res* **1998**, *55*, 267-273.

(9) Alexov, E.; Gunner, M. *Biochemistry* **1999**, *38*, 8253-8270.

(10) Kleinfeld, D.; Okamura, M. Y.; Feher, G. *Biochemistry* **1984**, *23*, 5780-5786.

(11) McMahon, B. H.; Muller, J. D.; Wraight, C. A.; Nienhaus, G. U. *Biophysical Journal* **1998**, *74*, 2567-2587.

(12) Goushcha, A. O.; Kapoustina, M. T.; Kharkyanen, V. N.; Holzwarth, A. R. *J.Phys.Chem.B* **1997**, *101*, 7612-7619.

(13) Clayton, R. K.; Wang, R. T. *Methods Enzymol* **1971**, *23*, 696-704.

(14) Deisenhofer, J.; Michel, H. *The EMBO Journal* **1989**, *8*, 2149-2170.

(15) Allen, J. P.; Feher, G.; Yeates, T. O.; Komiya, H.; Rees, D. C. *Proc. Natl. Acad. Sci. USA* **1987**, *84*, 5730-5734.

(16) Allen, J. P.; Feher, G.; Yeates, T. O.; Komiya, H.; Rees, D. C. *Proc. Natl. Acad. Sci. USA* **1987**, *84*, 6162-6166.

(17) Chang, C.-H.; El-Kabbani, O.; Tiede, D.; Norris, J.; Schiffer, M. *Biochemistry* **1991**, *30*, 5352-5360.

(18) Stowell, M. H. B.; McPhillips, T. M.; Rees, D. C.; Soltis, S. M.; Abresch, E.; Feher, G. *Science* **1997**, *276*, 812-816.

(19) Feher, G.; Allen, J. P.; Okamura, M. Y.; Rees, D. C. *Nature* **1989**, *339*, 111-116.

(20) Gunner, M. R. *Current Topics in Bioenergetics* **1991**, *16*, 319-367.

(21) Blankenship, R. E.; Madigan, M. T.; Bauer, C. E. *Anoxygenic Photosynthetic Bacteria*; Kluwer Academic Publishers:, 1995; Vol. 2.

(22) Paddock, M. L.; Rongey, S. H.; Feher, G.; Okamura, M. Y. *Proc. Natl. Acad. Sci. USA* **1989**, *86*, 6602-6606.

(23) Takahashi, E.; Wraight, C. A. *Biochemistry* **1992**, *31*, 855-866.

(24) Lin, X.; Murchison, H. A.; Nagarajan, V.; Parson, W. W.; Allen, J. P.; Williams, J. C. *Proc. Natl. Acad. Sci. USA* **1994**, *91*, 10265-10269.

(25) Alexov, E.; Miksovska, J.; Baciou, L.; Schifer, M.; Hanson, D.; Sebban, P.; Gunner, M. R. *Biochemistry* **2000**, *39*, 5940-5952.

(26) McAuley-Hecht, K. E.; Fyfe, P. K.; Ridge, J. P.; Prince, S. M.; Hunter, C. N.; Issac, N. W.; Cogdell, R. J.; Jones, M. R. *Biochemistry* **1998**, *37*, 4740-4750.

(27) Okamura, M. Y.; Isaacson, R. A.; Feher, G. *Proc. Natl. Acad. Sci. USA* **1975**, *72*, 3492-3496.

(28) Gunner, M. R.; Tiede, D. M.; Prince, R. C.; Dutton, P. L. Quinones as prosthetic groups in membrane electron-transfer proteins I: Systematic replacement of the primary ubiquinone of photochemical reaction centers with other quinones. In *Function of Quinones in Energy Conserving Systems*; Trumpower, B. L., Ed.; Academic Press: New York, 1982; pp 265-269.

(29) Woodbury, N. W.; Parson, W. W.; Gunner, M. R.; Prince, R. C.; Dutton, P. L. *Biochim. Biophys. Acta.* **1986**, *851*, 6-22.

(30) Graige, M. S.; Feher, G.; Okamura, M. Y. *Proc. Natl. Acad. Sci. USA* **1998**, *95*, 11679-11684.

(31) Li, J.; Takahashi, E.; Gunner, M. R. *Biochemistry* **2000**, *39*, 7445-7454.

(32) Gunner, M. R.; Robertson, D. E.; Dutton, P. L. *J. Phys. Chem.* **1986**, *90*, 3783-3795.

(33) Gunner, M. R.; Dutton, P. L. *J. Am. Chem. Soc.* **1989**, *111*, 3400-3412.

(34) Deisenhofer, J.; Epp, O.; Miki, K.; Huber, R.; Michel, H. *J. Mol. Biol.* **1984**, *385*, 385.

(35) Deisenhofer, J.; Epp, O.; Miki, R.; Michel, H. *Nature* **1985**, *318*, 618-624.

(36) Chang, C. H.; Tiede, D.; Tang, J.; Smith, U.; Norris, J.; Schiffer, M. *FEBS Lett.* **1986**, *205*, 82-86.

(37) Allen, J. P.; Feher, G.; Yeates, T. O.; Komiya, H.; Rees, D. C. *Proc. Natl. Acad. Sci. USA* **1988**, *85*, 8487-8491.

(38) Allen, J. P.; Feher, G.; Yeates, T. O.; Komiya, H.; Rees, D. C. **1988**, 5-11.

(39) Austin, R. H.; Beeson, K. W.; Eisenstein, D. L.; Frauenfelder, E. H.; Gunsalus, I. C. *Biochem.* **1975**, *24*, 5355-5373.

(40) Frauenfelder, H.; Sligar, S. G.; Wolynes, P. G. *Science* **1991**, *254*, 1598-1603.

(41) Zaccai, G. *Science* **2000**, *288*, 1604-7.

(42) Doster, W.; Cusack, S.; Petry, W. *Nature* **1989**, *337*, 754-756.

(43) Reat, V.; Patzelt, H.; Ferrand, M.; Pfister, C.; Oesterhelt, D.; Zaccai, G. *Proc Natl Acad Sci U S A* **1998**, *95*, 4970-5.

(44) Daniel, R. M.; Smith, J. C.; Ferrand, M.; Héry, S.; Dunn, R.; Finney, J. L. *Biophys. J.* **1998**, *75*, 2504-2507.

(45) Parak, F. *Methods Enzymol* **1986**, *127*, 196-206.

(46) Garbers, A.; Reifarth, F.; Kurreck, J.; Renger, G.; Parak, F. *Biochemistry* **1998**, *37*, 11399-11404.

(47) Vitcup, D.; Ringe, D.; Petsko, G. A.; Karplus, M. *Nature structural biology* **2000**, *7*, 34-38.

(48) Genick, U. K.; Borgstahl, G. E. O.; Ng, K.; Ren, Z.; Pradervand, C.; Burke, P. M.; Srajer, V.; Teng, T.; Schildkamp, W.; McRee, D. E.; Moffat, K.; Getzoff, E. D. *Science* **1997**, *275*, 1471-1475.

(49) Schlichting, I.; Berendzen, J.; Chu, K.; Stock, A. M.; Maves, S. A.; Benson, D. E.; Sweet, R. M.; Ringe, D.; Petsko, G. A.; Sligar, S. G. *Science* **2000**, *287*, 1615-22.

(50) Luecke, H.; Schobert, B.; Richter, H. T.; Cartailler, J. P.; Lanyi, J. K. *Science* **1999**, *286*, 255-261.

(51) Schlichting, I.; Chu, K. *Curr Opin Struct Biol* **2000**, *10*, 744-52.

(52) Petsko, G. A.; Ringe, D. *Curr Opin Chem Biol* **2000**, *4*, 89-94.

(53) Arata, H.; Parson, W. W. *Biochim. Biophys. Acta* **1981**, *638*, 201-209.

(54) Edens, G. J.; Gunner, M. R.; Xu, Q.; Mauzerall, D. *J. Am. Chem. Soc.* **2000**, *122*, 1479-1485.

(55) DeVault, D.; Chance, B. *Biophys. J.* **1966**, *6*, 825-847.

(56) McElroy, J. D.; Mauzerall, D. C.; Feher, G. *Biochim. Biophys. Acta* **1974**, *333*, 261-277.

(57) Vermeglio, A.; Clayton, R. K. *Biochim. Biophys. Acta* **1977**, *461*, 159-165.

(58) Wraight, C. A. *Biochim. Biophys. Acta* **1979**, *548*, 309-327.

(59) Kleinfeld, D.; Okamura, M. Y.; Feher, G. *Biochim. Biophys. Acta* **1985**, *809*, 291-310.

(60) Li, J.; Gilroy, D.; Tiede, D. M.; Gunner, M. R. *Biochemistry* **1998**, *37*, 2818-2829.

(61) Wraight, C. A. *Biochim. Biophys. Acta* **1977**, *459*, 525-531.

(62) Maroti, P.; Wraight, C. A. *Biochim. Biophys. Acta* **1988**, *934*, 329-347.

(63) McPherson, P. H.; Okamura, M. Y.; Feher, G. *Biochim. Biophys. Acta* **1988**, *934*, 348-368.

(64) Kleinfeld, D.; Okamura, M. Y.; Feher, G. *Biochim. Biophys. Acta* **1984**, *766*, 126-140.

(65) Takahashi, E.; Wraight, C. A. *Biochim. Biophys. Acta* **1990**, *1020*, 107-111.

(66) Lancaster, R.; Michel, H. *Structure* **1997**, *5*, 1339-1359.

Chapter 2.

(1) Clayton, R. K.; Wang, R. T. *Methods Enzymol* **1971**, *23*, 696-704.

(2) Clayton, R. K.; Sistrom, W. R. *The Photosynthetic Bacteria*; Plenum Press: New York, 1978.

(3) Goldsmith, J. O.; Boxer, S. G. *Biochim Biophys Acta* **1996**, *1276*, 171-175.

(4) Okamura, M. Y.; Isaacson, R. A.; Feher, G. *Proc. Natl. Acad. Sci. USA* **1975**, *72*, 3492-3496.

(5) Woodbury, N. W.; Parson, W. W.; Gunner, M. R.; Prince, R. C.; Dutton, P. L. *Biochim. Biophys. Acta.* **1986**, *851*, 6-22.

Chapter 3.

(1) Feher, G.; Allen, J. P.; Okamura, M. Y.; Rees, D. C. *Nature* **1989**, *339*, 111-116.

(2) Gunner, M. R. *Current Topics in Bioenergetics* **1991**, *16*, 319-367.

(3) Blankenship, R. E.; Madigan, M. T.; Bauer, C. E. *Anoxygenic Photosynthetic Bacteria*; Kluwer Academic Publishers:, 1995; Vol. 2.

(4) Marcus, R. A.; Sutin, N. *Biochim. Biophys. Acta* **1985**, *811*, 265-322.

(5) DeVault, D. *Q. Rev. Biophys.* **1980**, *13*, 387-564.

(6) Gopher, A.; Blatt, Y.; Schonfeld, M.; Okamura, M. Y.; Feher, G.; Montal, M. *Biophys. J.* **1985**, *48*, 311-320.

(7) Lin, X.; Murchison, H. A.; Nagarajan, V.; Parson, W. W.; Allen, J. P.; Williams, J. C. *Proc. Natl. Acad. Sci. USA* **1994**, *91*, 10265-10269.

(8) Woodbury, N. W.; Allen, J. P. The pathway,kinetics and thermodynamics of electron transfer in wild type and mutant raction centers of purple nonsulfur bacteria. In *Anoxygenic Photosynthetic Bacteria*; Blankenship, R. E., Madigan, M. T., Bauer, C. E., Eds.; Kluwer: Dordrecht, 1995.

(9) Li, J.; Takahashi, E.; Gunner, M. R. *Biochemistry* **2000**, *39*, 7445-7454.

(10) Kleinfeld, D.; Okamura, M. Y.; Feher, G. *Biochemistry* **1984**, *23*, 5780-5786.

(11) Gunner, M. R.; Robertson, D. E.; Dutton, P. L. *J. Phys. Chem.* **1986**, *90*, 3783-3795.

(12) Gunner, M. R.; Dutton, P. L. *J. Am. Chem. Soc.* **1989**, *111*, 3400-3412.

(13) Franzen, S.; Boxer, S. G. *J. Phys. Chem.* **1993**, *97*, 6304-6318.

(14) McMahon, B. H.; Muller, J. D.; Wraight, C. A.; Nienhaus, G. U. *Biophysical Journal* **1998**, *74*, 2567-2587.

(15) Chidsey, C. E. D.; Takiff, L.; Slodstein, R. A.; Boxer, S. G. *Proc. Natl. Acad. Sci. USA* **1985**, *82*, 6850-6854.

(16) Polenova, T.; Mc Dermott, A. E. *J. Phys. Chem. B.* **1999**, *103*, 535-548.

(17) Arata, H.; Parson, W. W. *Biochim. Biophys. Acta* **1981**, *638*, 201-209.

(18) Woodbury, N. W.; Parson, W. W.; Gunner, M. R.; Prince, R. C.; Dutton, P. L. *Biochim. Biophys. Acta.* **1986**, *851*, 6-22.

(19) Arata, H.; Parson, W. W. *Biochim. Biophys. Acta* **1981**, *636*, 70-81.

(20) Puchenkov, O. V.; Kopf, Z.; Malkin, S. *Biochim. Biophys. Acta* **1995**, *1231*, 197-212.

(21) Edens, G. J.; Gunner, M. R.; Xu, Q.; Mauzerall, D. *J. Am. Chem. Soc.* **2000**, *122*, 1479-1485.

(22) Gunner, M. R.; Tiede, D. M.; Prince, R. C.; Dutton, P. L. Quinones as prosthetic groups in membrane electron-transfer proteins I: Systematic replacement of the primary ubiquinone of photochemical reaction centers with other quinones. In *Function of Quinones in Energy Conserving Systems*; Trumpower, B. L., Ed.; Academic Press: New York, 1982; pp 265-269.

(23) Shopes, R. J.; Wraight, C. A. *Biochim. Biophys. Acta* **1987**, *893*, 409-425.

(24) Page, C. C.; Moser, C. C.; Chen, X.; Dutton, P. L. *Nature* **1999**, *402*, 47-52.

(25) Takahashi, E.; Wells, T. A.; Wraight, C. A. Enviornmental control of the redox protential of Q_A in *Rb. sphaeroides* reaction centers: Polar replacement of Ile^{M260} causes marked change in Q_A and Q_B function. In *Proceedings of the XIth International Photosynthesis Congress*; Garab, G., Ed.; Kluwer: Dordrecht, 1998; Vol. II; pp 17-22.

(26) Warncke, K.; Dutton, P. L. *Biochemistry* **1993**, *32*, 4769-4779.

(27) Kleinfeld, D.; Okamura, M. Y.; Feher, G. *Biophys. J.* **1985**, *48*, 849-852.

(28) Sebban, P. *Biochim. Biophys. Acta* **1988**, *936*, 124-132.

(29) Kakitani, T.; Kanitani, H. *Biochim. Biophys. Acta* **1981**, *635*, 498-514.

(30) Sebban, P.; Wraight, C. A. *Biochimica et Biophysica Acta* **1989**, *974*, 54-65.

(31) Vitcup, D.; Ringe, D.; Petsko, G. A.; Karplus, M. *Nature structural biology* **2000**, *7*, 34-38.

(32) Daniel, R. M.; Smith, J. C.; Ferrand, M.; Héry, S.; Dunn, R.; Finney, J. L. *Biophys. J.* **1998**, *75*, 2504-2507.

(33) Hagen, S. J.; Hofrichter, J.; Eaton, W. A. *Science* **1995**, *269*, 959-962.

(34) Ortega, J. M.; Mathis, P.; Williams, J. C.; Allen, J. P. *Biochemistry* **1996**, *35*, 3354-3361.

(35) Clayton, R. K.; Wang, R. T. *Methods Enzymol* **1971**, *23*, 696-704.

(36) Okamura, M. Y.; Isaacson, R. A.; Feher, G. *Proc. Natl. Acad. Sci. USA* **1975**, *72*, 3492-3496.

(37) Chidsey, C. E. D.; Kirmaier, C.; Holten, D.; Boxer, S. G. *Biochim. Biophys. Acta* **1984**, *766*, 424-437.

(38) Franzen, S.; Goldstein, R. F.; Boxer, S. G. *J. Phys. Chem.* **1990**, *94*, 5135-5149.

(39) Lavalette, D.; Tetreau, C.; Brochon, J.; Livesey, A. *Eur. J. Biochem.* **1991**, *196*, 591-598.

(40) Schenck, C. C.; Blankenship, R. E.; Parson, W. W. *Biochim. Biophys. Acta* **1982**, *680*, 44-59.

(41) Gunner, M. R. The temperature and ΔG dependence of long range electron transfer in reaction center protein from *Rhodobacter sphaeroides*. Ph.D., University of Pennsylvania, 1988.

(42) Norris, J. R.; Bowman, M. K.; Budil, D. E.; Tang, J.; Wraight, C. A.; Closs, G. L. *Proc. Natl. Acad. Sci.* **1982**, *79*, 5532-5536.

(43) Holzwarth, A. R.; Muller, M. G. *Biochem.* **1996**, *35*, 11820-11831.

(44) Woodbury, N. W. T.; Parson, W. W. *Biochim. Biophys. Acta* **1984**, *767*, 345-361.

(45) Goldstein, R. A.; Takiff, L.; Boxer, S. G. *BBA 42789* **1988**, 1-11.

(46) Ogrodnik, A.; Volk, M.; Michel-Beyerle, M. E. *Biochim. Biophys. Acta* **1988**, *936*, 361-371.

(47) Ogronik, A.; Keupp, W.; Volk, M.; Aumeier, G.; Michele-Beyerle, M. E. *J. Phys. Cem.* **1994**, *98*, 3432-3439.

Chapter 4.

(1) Frauenfelder, H.; Sligar, S. G.; Wolynes, P. G. *Science* **1991**, *254*, 1598-1603.

(2) Zaccai, G. *Science* **2000**, *288*, 1604-7.

(3) Parak, F.; Knapp, E. W.; Kucheida, D. *J Mol Biol* **1982**, *161*, 177-94.

(4) Doster, W.; Cusack, S.; Petry, W. *Nature* **1989**, *337*, 754-756.

(5) Loncharich, R. J.; Brooks, B. R. *J Mol Biol* **1990**, *215*, 439-55.

(6) Di Pace, A.; Cupane, A.; Leone, M.; Vitrano, E.; Cordone, L. *Biophys J.* **1992**, *63*, 475-484.

(7) Ferrand, M.; Dianoux, A. J.; Petry, W.; Zaccai, G. *Proc Natl Acad Sci U S A* **1993**, *90*, 9668-72.

(8) Andreani, C.; Filabozzi, A.; Menzinger, F.; Desideri, A.; Deriu, A.; Di Cola, D. *Biophys. J.* **1995**, *68*, 2519-2523.

(9) Vitcup, D.; Ringe, D.; Petsko, G. A.; Karplus, M. *Nature structural biology* **2000**, *7*, 34-38.

(10) Reat, V.; Patzelt, H.; Ferrand, M.; Pfister, C.; Oesterhelt, D.; Zaccai, G. *Proc Natl Acad Sci U S A* **1998**, *95*, 4970-5.

(11) Frauenfelder, H.; McMahon, B. *Proc Natl Acad Sci U S A* **1998**, *95*, 4795-7.

(12) Kleinfeld, D.; Okamura, M. Y.; Feher, G. *Biochemistry* **1984**, *23*, 5780-5786.

(13) McMahon, B. H.; Muller, J. D.; Wraight, C. A.; Nienhaus, G. U. *Biophysical Journal* **1998**, *74*, 2567-2587.

(14) Xu, Q.; Gunner, M. R. *J.Phys.Chem. B* **2000**, *104*, 8035-8043.

(15) Feher, G.; Allen, J. P.; Okamura, M. Y.; Rees, D. C. *Nature* **1989**, *339*, 111-116.

(16) Gunner, M. R. *Current Topics in Bioenergetics* **1991**, *16*, 319-367.

(17) Blankenship, R. E.; Madigan, M. T.; Bauer, C. E. *Anoxygenic Photosynthetic Bacteria*; Kluwer Academic Publishers:, 1995; Vol. 2.

(18) Tiede, D. M.; Vazquez, J.; Cordova, J.; Marone, A. P. *Biochemistry* **1996**, *35*, 10763-10775.

(19) Li, J.; Gilroy, D.; Tiede, D. M.; Gunner, M. R. *Biochemistry* **1998**, *37*, 2818-2829.

(20) Graige, M. S.; Feher, G.; Okamura, M. Y. *Proc. Natl. Acad. Sci. USA* **1998**, *95*, 11679-11684.

(21) Li, J.; Takahashi, E.; Gunner, M. R. *Biochemistry* **2000**, *39*, 7445-7454.

(22) Utschig, L. M.; Ohigashi, Y.; Thurnauer, M. C.; Tiede, D. M. *Biochemistry* **1998**, *37*, 8278-8281.

(23) Paddock, M. L.; Graige, M. S.; Feher, G.; Okamura, M. Y. *Proc. Natl. Acad. Sci. USA* **1999**, *96*, 6183-6188.

(24) Schlichting, I.; Berendzen, J.; Chu, K.; Stock, A. M.; Maves, S. A.; Benson, D. E.; Sweet, R. M.; Ringe, D.; Petsko, G. A.; Sligar, S. G. *Science* **2000**, *287*, 1615-22.

(25) Edman, K.; Nollert, P.; Royant, A.; Belrhali, H.; Pebay-Peyroula, E.; Hajdu, J.; Neutze, R.; Landau, E. M. *Nature* **1999**, *401*, 822-6.

(26) Luecke, H.; Schobert, B.; Richter, H. T.; Cartailler, J. P.; Lanyi, J. K. *Science* **1999**, *286*, 255-261.

(27) Genick, U. K.; Borgstahl, G. E. O.; Ng, K.; Ren, Z.; Pradervand, C.; Burke, P. M.; Srajer, V.; Teng, T.; Schildkamp, W.; McRee, D. E.; Moffat, K.; Getzoff, E. D. *Science* **1997**, *275*, 1471-1475.

(28) Stowell, M. H. B.; McPhillips, T. M.; Rees, D. C.; Soltis, S. M.; Abresch, E.; Feher, G. *Science* **1997**, *276*, 812-816.

(29) Alexov, E.; Gunner, M. *Biochemistry* **1999**, *38*, 8253-8270.

(30) Grafton, A. K.; Wheeler, R. A. *J. Phys. Chem* **1999**, *103*, 5380-5387.

(31) Alexov, E.; Miksovska, J.; Baciou, L.; Schifer, M.; Hanson, D.; Sebban, P.; Gunner, M. R. *Biochemistry* **2000**, *39*, 5940-5952.

(32) Beroza, P.; Fredkin, D. R.; Okamura, M. Y.; Feher, R. *Biophys. J.* **1995**, *68*, 2233-2250.

(33) Paddock, M. L.; Rongey, S. H.; Feher, G.; Okamura, M. Y. *Proc. Natl. Acad. Sci. USA* **1989**, *86*, 6602-6606.

(34) Takahashi, E.; Wraight, C. A. *Biochemistry* **1992**, *31*, 855-866.

(35) Goldsmith, J. O.; Boxer, S. G. *Biochim Biophys Acta* **1996**, *1276*, 171-175.

(36) Clayton, R. K.; Wang, R. T. *Methods Enzymol* **1971**, *23*, 696-704.

(37) Okamura, M. Y.; Isaacson, R. A.; Feher, G. *Proc. Natl. Acad. Sci. USA* **1975**, *72*, 3492-3496.

(38) Woodbury, N. W.; Parson, W. W.; Gunner, M. R.; Prince, R. C.; Dutton, P. L. *Biochim. Biophys. Acta.* **1986**, *851*, 6-22.

(39) McComb, J. C.; Stein, R. R.; Wraight, C. A. *Biochim. Biophys. Acta* **1990**, *1015*, 156-171.

(40) Gunner, M. R.; Robertson, D. E.; Dutton, P. L. *J. Phys. Chem.* **1986**, *90*, 3783-3795.

(41) Steinbach, P. J.; Chu, K.; Frauenfelder, H.; Johnson, J. B.; Lamb, D. C.; Nienhaus, G. U.; Sauke, T. B.; Young, R. D. *Biophysical society* **1992**, *61*, 235-245.

(42) Tikhonov, A. N.; Arsenin, V. Y. *Solution of ill-posed problems*; Wiley: New York, 1977.

(43) Gunner, M. R.; Dutton, P. L. *J. Am. Chem. Soc.* **1989**, *111*, 3400-3412.

(44) Mancino, L. J.; Dean, D. P.; Blankenship, R. E. *Biochim. Biophys. Acta* **1984**, *764*, 46-54.

(45) McElroy, J. D.; Mauzerall, D. C.; Feher, G. *Biochim. Biophys. Acta* **1974**, *333*, 261-277.

(46) Breton, J. Low temperature linear dichroism study of the orientation of the pigments in reduced and oxidized reaction centers of *Rps. viridis* and *Rb. sphaeroides*. In *The photosynthetic bacterial reaction center: structure and dynamics.*; Breton, J., Vermeglio, A., Eds.; Plenum: New York and London, 1988; pp 59-69.

(47) Steffen, M. A.; Lao, K.; Boxer, S. G. *Science* **1994**, *264*, 810-816.

(48) Kleinfeld, D.; Okamura, M. Y.; Feher, G. *Biochim. Biophys. Acta* **1984**, *766*, 126-140.

(49) Labahn, A.; Paddock, M. L.; McPherson, P. H.; Okamura, M. Y.; Feher, G. *J. Phys. Chem.* **1994**, *98*, 3417-3423.

(50) Labahn, A.; Bruce, J. M.; Okamura, M. Y.; Feher, G. *Chem. Phys.* **1995**, *97*, 355-366.

(51) Allen, J. P.; Williams, J. C.; Graige, M.; Paddock, M. L.; Labahn, A.; Feher, G.; Okamura, M. Y. *Photosynth. Res.* **1998**, *55*, 227-233.

(52) Paddock, M. L.; Rongey, S. H.; McPherson, P. H.; Juth, A.; Feher, G.; Okamura, M. Y. *Biochemistry* **1994**, *33*, 734-745.

(53) Shopes, R. J.; Wraight, C. A. *Biochim. Biophys. Acta* **1987**, *893*, 409-425.

(54) Franzen, S.; Boxer, S. G. *J. Phys. Chem.* **1993**, *97*, 6304-6318.

(55) Sebban, P. *Biochim. Biophys. Acta* **1988**, *936*, 124-132.

(56) Ortega, J. M.; Mathis, P.; Williams, J. C.; Allen, J. P. *Biochemistry* **1996**, *35*, 3354-3361.

(57) Dutton, P. L.; Moser, C. C. *Proc. Natl. Acad. Sci.* **1994**, *91*, 10247-10250.

(58) Vermeglio, A.; Clayton, R. K. *Biochim. Biophys. Acta* **1977**, *461*, 159-165.

(59) Wraight, C. A. *Biochim. Biophys. Acta* **1979**, *548*, 309-327.

(60) Takahashi, E.; Maroti, P.; Wraight, C. A. Coupled proton and electron transfer pathways in the acceptor quinone complex of reaction centers from *Rhodobacter sphaeroides*. In *Electron and Proton Transfer in Chemistry and Biology*; Muller, A., Ed.; Elsevier:, 1992; Vol. Vol. 78; pp pgs. 219-236.

(61) Marcus, R. A.; Sutin, N. *Biochim. Biophys. Acta* **1985**, *811*, 265-322.

(62) DeVault, D. *Q. Rev. Biophys.* **1980**, *13*, 387-564.

(63) Brzezinski, P.; Andreasson, L. E. *Biochemistry* **1995**, *34 no.22*, 7498-7506.

(64) Kalman, L.; Sebban, P.; Hanson, D. K.; Schiffer, M.; Maroti, P. *Biochim Biophys Acta* **1998**, *1365*, 513-521.

(65) Balabin, I. A.; Onuchic, J. N. *Science* **2000**, *290*, 114-7.

Chapter 5.

(1) Frauenfelder, H.; Sligar, S. G.; Wolynes, P. G. *Science* **1991**, *254*, 1598-1603.

(2) Zaccai, G. *Science* **2000**, *288*, 1604-7.

(3) Parak, F.; Knapp, E. W.; Kucheida, D. *J Mol Biol* **1982**, *161*, 177-94.

(4) Doster, W.; Cusack, S.; Petry, W. *Nature* **1989**, *337*, 754-756.

(5) Loncharich, R. J.; Brooks, B. R. *J Mol Biol* **1990**, *215*, 439-55.

(6) Di Pace, A.; Cupane, A.; Leone, M.; Vitrano, E.; Cordone, L. *Biophys J.* **1992**, *63*, 475-484.

(7) Ferrand, M.; Dianoux, A. J.; Petry, W.; Zaccai, G. *Proc Natl Acad Sci U S A* **1993**, *90*, 9668-72.

(8) Andreani, C.; Filabozzi, A.; Menzinger, F.; Desideri, A.; Deriu, A.; Di Cola, D. *Biophys. J.* **1995**, *68*, 2519-2523.

(9) Vitcup, D.; Ringe, D.; Petsko, G. A.; Karplus, M. *Nature structural biology* **2000**, *7*, 34-38.

(10) Reat, V.; Patzelt, H.; Ferrand, M.; Pfister, C.; Oesterhelt, D.; Zaccai, G. *Proc Natl Acad Sci U S A* **1998**, *95*, 4970-5.

(11) Frauenfelder, H.; McMahon, B. *Proc Natl Acad Sci U S A* **1998**, *95*, 4795-7.

(12) Kleinfeld, D.; Okamura, M. Y.; Feher, G. *Biochemistry* **1984**, *23*, 5780-5786.

(13) McMahon, B. H.; Muller, J. D.; Wraight, C. A.; Nienhaus, G. U. *Biophysical Journal* **1998**, *74*, 2567-2587.

(14) Xu, Q.; Gunner, M. R. *J.Phys.Chem. B* **2000**, *104*, 8035-8043.

(15) Feher, G.; Allen, J. P.; Okamura, M. Y.; Rees, D. C. *Nature* **1989**, *339*, 111-116.

(16) Gunner, M. R. *Current Topics in Bioenergetics* **1991**, *16*, 319-367.

(17) Blankenship, R. E.; Madigan, M. T.; Bauer, C. E. *Anoxygenic Photosynthetic Bacteria*; Kluwer Academic Publishers:, 1995; Vol. 2.

(18) Tiede, D. M.; Vazquez, J.; Cordova, J.; Marone, A. P. *Biochemistry* **1996**, *35*, 10763-10775.

(19) Li, J.; Gilroy, D.; Tiede, D. M.; Gunner, M. R. *Biochemistry* **1998**, *37*, 2818-2829.

(20) Graige, M. S.; Feher, G.; Okamura, M. Y. *Proc. Natl. Acad. Sci. USA* **1998**, *95*, 11679-11684.

(21) Li, J.; Takahashi, E.; Gunner, M. R. *Biochemistry* **2000**, *39*, 7445-7454.

(22) Utschig, L. M.; Ohigashi, Y.; Thurnauer, M. C.; Tiede, D. M. *Biochemistry* **1998**, *37*, 8278-8281.

(23) Paddock, M. L.; Graige, M. S.; Feher, G.; Okamura, M. Y. *Proc. Natl. Acad. Sci. USA* **1999**, *96*, 6183-6188.

(24) Schlichting, I.; Berendzen, J.; Chu, K.; Stock, A. M.; Maves, S. A.; Benson, D. E.; Sweet, R. M.; Ringe, D.; Petsko, G. A.; Sligar, S. G. *Science* **2000**, *287*, 1615-22.

(25) Edman, K.; Nollert, P.; Royant, A.; Belrhali, H.; Pebay-Peyroula, E.; Hajdu, J.; Neutze, R.; Landau, E. M. *Nature* **1999**, *401*, 822-6.

(26) Luecke, H.; Schobert, B.; Richter, H. T.; Cartailler, J. P.; Lanyi, J. K. *Science* **1999**, *286*, 255-261.

(27) Genick, U. K.; Borgstahl, G. E. O.; Ng, K.; Ren, Z.; Pradervand, C.; Burke, P. M.; Srajer, V.; Teng, T.; Schildkamp, W.; McRee, D. E.; Moffat, K.; Getzoff, E. D. *Science* **1997**, *275*, 1471-1475.

(28) Stowell, M. H. B.; McPhillips, T. M.; Rees, D. C.; Soltis, S. M.; Abresch, E.; Feher, G. *Science* **1997**, *276*, 812-816.

(29) Alexov, E.; Gunner, M. *Biochemistry* **1999**, *38*, 8253-8270.

(30) Grafton, A. K.; Wheeler, R. A. *J. Phys. Chem* **1999**, *103*, 5380-5387.

(31) Alexov, E.; Miksovska, J.; Baciou, L.; Schifer, M.; Hanson, D.; Sebban, P.; Gunner, M. R. *Biochemistry* **2000**, *39*, 5940-5952.

(32) Beroza, P.; Fredkin, D. R.; Okamura, M. Y.; Feher, R. *Biophys. J.* **1995**, *68*, 2233-2250.

(33) Paddock, M. L.; Rongey, S. H.; Feher, G.; Okamura, M. Y. *Proc. Natl. Acad. Sci. USA* **1989**, *86*, 6602-6606.

(34) Takahashi, E.; Wraight, C. A. *Biochemistry* **1992**, *31*, 855-866.

(35) Goldsmith, J. O.; Boxer, S. G. *Biochim Biophys Acta* **1996**, *1276*, 171-175.

(36) Clayton, R. K.; Wang, R. T. *Methods Enzymol* **1971**, *23*, 696-704.

(37) Okamura, M. Y.; Isaacson, R. A.; Feher, G. *Proc. Natl. Acad. Sci. USA* **1975**, *72*, 3492-3496.

(38) Woodbury, N. W.; Parson, W. W.; Gunner, M. R.; Prince, R. C.; Dutton, P. L. *Biochim. Biophys. Acta.* **1986**, *851*, 6-22.

(39) McComb, J. C.; Stein, R. R.; Wraight, C. A. *Biochim. Biophys. Acta* **1990**, *1015*, 156-171.

(40) Gunner, M. R.; Robertson, D. E.; Dutton, P. L. *J. Phys. Chem.* **1986**, *90*, 3783-3795.

(41) Steinbach, P. J.; Chu, K.; Frauenfelder, H.; Johnson, J. B.; Lamb, D. C.; Nienhaus, G. U.; Sauke, T. B.; Young, R. D. *Biophysical society* **1992**, *61*, 235-245.

(42) Tikhonov, A. N.; Arsenin, V. Y. *Solution of ill-posed problems*; Wiley: New York, 1977.

(43) Gunner, M. R.; Dutton, P. L. *J. Am. Chem. Soc.* **1989**, *111*, 3400-3412.

(44) Mancino, L. J.; Dean, D. P.; Blankenship, R. E. *Biochim. Biophys. Acta* **1984**, *764*, 46-54.

(45) McElroy, J. D.; Mauzerall, D. C.; Feher, G. *Biochim. Biophys. Acta* **1974**, *333*, 261-277.

(46) Breton, J. Low temperature linear dichroism study of the orientation of the pigments in reduced and oxidized reaction centers of *Rps. viridis* and *Rb. sphaeroides*. In *The photosynthetic bacterial reaction center: structure and dynamics.*; Breton, J., Vermeglio, A., Eds.; Plenum: New York and London, 1988; pp 59-69.

(47) Steffen, M. A.; Lao, K.; Boxer, S. G. *Science* **1994**, *264*, 810-816.

(48) Kleinfeld, D.; Okamura, M. Y.; Feher, G. *Biochim. Biophys. Acta* **1984**, *766*, 126-140.

(49) Labahn, A.; Paddock, M. L.; McPherson, P. H.; Okamura, M. Y.; Feher, G. *J. Phys. Chem.* **1994**, *98*, 3417-3423.

(50) Labahn, A.; Bruce, J. M.; Okamura, M. Y.; Feher, G. *Chem. Phys.* **1995**, *97*, 355-366.

(51) Allen, J. P.; Williams, J. C.; Graige, M.; Paddock, M. L.; Labahn, A.; Feher, G.; Okamura, M. Y. *Photosynth. Res.* **1998**, *55*, 227-233.

(52) Paddock, M. L.; Rongey, S. H.; McPherson, P. H.; Juth, A.; Feher, G.; Okamura, M. Y. *Biochemistry* **1994**, *33*, 734-745.

(53) Shopes, R. J.; Wraight, C. A. *Biochim. Biophys. Acta* **1987**, *893*, 409-425.

(54) Franzen, S.; Boxer, S. G. *J. Phys. Chem.* **1993**, *97*, 6304-6318.

(55) Sebban, P. *Biochim. Biophys. Acta* **1988**, *936*, 124-132.

(56) Ortega, J. M.; Mathis, P.; Williams, J. C.; Allen, J. P. *Biochemistry* **1996**, *35*, 3354-3361.

(57) Dutton, P. L.; Moser, C. C. *Proc. Natl. Acad. Sci.* **1994**, *91*, 10247-10250.

(58) Vermeglio, A.; Clayton, R. K. *Biochim. Biophys. Acta* **1977**, *461*, 159-165.

(59) Wraight, C. A. *Biochim. Biophys. Acta* **1979**, *548*, 309-327.

(60) Takahashi, E.; Maroti, P.; Wraight, C. A. Coupled proton and electron transfer pathways in the acceptor quinone complex of reaction centers from *Rhodobacter sphaeroides*. In *Electron and Proton Transfer in Chemistry and Biology*; Muller, A., Ed.; Elsevier:, 1992; Vol. Vol. 78; pp pgs. 219-236.

(61) Marcus, R. A.; Sutin, N. *Biochim. Biophys. Acta* **1985**, *811*, 265-322.

(62) DeVault, D. *Q. Rev. Biophys.* **1980**, *13*, 387-564.

(63) Brzezinski, P.; Andreasson, L. E. *Biochemistry* **1995**, *34 no.22*, 7498-7506.

(64) Kalman, L.; Sebban, P.; Hanson, D. K.; Schiffer, M.; Maroti, P. *Biochim Biophys Acta* **1998**, *1365*, 513-521.

(65) Balabin, I. A.; Onuchic, J. N. *Science* **2000**, *290*, 114-7.

Chapter 6.

(1) Feher, G.; Allen, J. P.; Okamura, M. Y.; Rees, D. C. *Nature* **1989**, *339*, 111-116.

(2) Gunner, M. R. *Current Topics in Bioenergetics* **1991**, *16*, 319-367.

(3) Blankenship, R. E.; Madigan, M. T.; Bauer, C. E. *Anoxygenic Photosynthetic Bacteria*; Kluwer Academic Publishers:, 1995; Vol. 2.

(4) Graige, M. S.; Feher, G.; Okamura, M. Y. *Proc. Natl. Acad. Sci. USA* **1998**, *95*, 11679-11684.

(5) Kleinfeld, D.; Okamura, M. Y.; Feher, G. *Biochemistry* **1984**, *23*, 5780-5786.

(6) Xu, Q.; Gunner, M. R. *Biochemistry* **2001**, *40*, 3232-3241.

(7) Lancaster, R.; Michel, H. *Structure* **1997**, *5*, 1339-1359.

(8) Paddock, M. L.; Feher, G.; Okamura, M. Y. *Biochemistry* **1995**, *34*, 15742-15750.

(9) Paddock, M. L.; Feher, G.; Okamura, M. Y. *Proc. Natl. Acad. Sci.* **2000**, *97*, 1548-1553.

(10) Utschig, L. M.; Ohigashi, Y.; Thurnauer, M. C.; Tiede, D. M. *Biochemistry* **1998**, *37*, 8278-8281.

(11) Paddock, M. L.; Graige, M. S.; Feher, G.; Okamura, M. Y. *Proc. Natl. Acad. Sci. USA* **1999**, *96*, 6183-6188.

(12) Baciou, L.; Michel, H. *Biochemistry* **1995**, *34*, 7967-7972.

(13) Tandori, J.; Sebban, P.; Michel, H.; Baciou, L. *Biochemistry* **1999**, *38*, 13179-13187.

(14) Kuglstatter, A.; Miksovska, J.; Sebban, P.; Fritzsch, G. *FEBS Letts.* **2000**, *472*, 114-6.

(15) McComb, J. C.; Stein, R. R.; Wraight, C. A. *Biochim. Biophys. Acta* **1990**, *1015*, 156-171.

(16) Li, J.; Takahashi, E.; Gunner, M. R. *Biochemistry* **2000**, *39*, 7445-7454.

(17) Stowell, M. H. B.; McPhillips, T. M.; Rees, D. C.; Soltis, S. M.; Abresch, E.; Feher, G. *Science* **1997**, *276*, 812-816.

(18) Ermler, U.; Fritzsch, G.; Buchanan, S. K.; Michel, H. *Structure* **1994**, *2*, 925-936.

(19) Grafton, A. K.; Wheeler, R. A. *J. Phys. Chem* **1999**, *103*, 5380-5387.

(20) Zachariae, U.; Lancaster, C. R. *Biochim Biophys Acta* **2001**, *1505*, 280-90.

(21) Dunitz, J. D. *Chem Biol* **1995**, *2*, 709-12.